November 2017

Microbial Competition in Bioelectrochemical Systems

Varun Srinivasan

MICROBIAL COMPETITION IN BIOELECTROCHEMICAL SYSTEMS

A Dissertation Presented

by

VARUN N. SRINIVASAN

Submitted to the Graduate School of the

University of Massachusetts Amherst in partial fulfillment

of the requirements for the degree of

DOCTOR OF PHILOSOPHY

SEPTEMBER 2017

Department of Civil and Environmental Engineering

MICROBIAL COMPETITION IN BIOELECTROCHEMICAL SYSTEMS

A Dissertation Presented

By

VARUN N. SRINIVASAN

Approved as to style and content by:

_____

Caitlyn S. Butler, Chair

_____

John E. Tobiason, Member

_____

Klaus Nüsslein, Member

_____

Richard N. Palmer, Department Head

Civil and Environmental Engineering Department

DEDICATION

To my late grandfather, Dr. N.V. Parthasarathy who was an electrochemist. He was a constant inspiration to be curious and solve problems with ingenuity and logic. It is indeed fitting that my dissertation has an electrochemical component to it.

ACKNOWLEDGEMENTS

I would like to thank the University of Massachusetts-Amherst for funding this research. I would also like to thank the Edwin Sisson Doctoral Fellowship and the The Massachusetts Department of Transportation Highway Division under Interagency Service Agreement No. 87790 with the University of Massachusetts-Amherst for funding me during the course of my Ph.D.

I would also like to thank my dissertation advisor Caitlyn Butler. Caitlyn has supported me in all my endeavors and career goals. She has been instrumental in helping me conduct my research and has been an excellent advisor. Her trust and confidence in my abilities has made me a better researcher over the course of my Ph.D.

I would also like to thank Dr. Reckhow who advised me during my Masters thesis. He was a constant source of advice and support during the course of my Masters and Ph.D. He instilled in me the confidence to be the researcher I am today and for that I will be forever grateful. In that same vein, I would also like to thank Dr. Ostendorf for being a wonderful mentor to me.

I would also like to thank my committee members Dr. Tobiason and Dr. Nüsslein. Dr. Tobiason has always been supportive and I owe him for being critical about my writing when I wrote lab reports for the physical and chemical treatment processes course. I attribute my improvement as a scientific writer to him. Dr. Nusslein has been a great source of advice regarding microbiology. He has always been easily accessible and willing to help with all my issues and questions.

All the above-mentioned people have been great mentors to me and I am extremely lucky to have had their valuable input during the course of my research.

I would also like to thank all the class mates and colleagues who heave been part of this journey of mine. The camaraderie and friendships I have developed during my Masters and Ph.D. will be invaluable and always cherished. I would also like to specially thank Dr. Kaoru Ikuma for her useful suggestions and help with molecular tools.

I gratefully acknowledge the support and love from my parents and my sister who have always encouraged me to pursue whatever I wanted to do. Last, but not the least, I would like to thank my wife, Sneha Gupta, who has supported me throughout this process. During the last couple of years of my Ph.D. I went through the usual confusion and identity crisis of what I wanted to do after the Ph.D. and her faith and belief in me as a researcher has always guided me. I will forever be thankful to her for being a rock to lean on at moments of crisis and for showing me how to live life with passion. I am, indeed, very lucky to have found her!

ABSTRACT

MICROBIAL COMPETITION IN BIOELECTROCHEMICAL SYSTEMS

SEPTEMBER 2017

VARUN N. SRINIVASAN, B.TECH., ANNA UNIVERSITY

M.S., UNIVERSITY OF MASSACHUSETTS-AMHERST

Ph.D., UNIVERSITY OF MASSACHUSETTS-AMHERST

Directed by: Dr. Caitlyn S. Butler

Bioelectrochemical systems(BESs)/ microbial fuel fells (MFCs) are a well-studied potential technology for bioremediation and decentralized wastewater treatment. However, progress has been somewhat stalled at the bench-scale. In well controlled experiments electron recovery is high. In natural environments, wastewaters are complex and anode-respiring bacteria can be outcompeted in the presence of competing microorganisms, leading to a loss in electron-recovery and power production. Furthermore, the cathode of the MFC plays a vital role in providing flexibility for treatment options but is an understudied part of MFCs.

Modelling Intracellular Competition in a Denitrifying Biocathode:

One potential MFC configuration uses an organic-oxidizing anode biofilm and a denitrifying cathode biofilm. However nitrite, a denitrification intermediate with environmental and public health impacts, has been reported to accumulate. In this study,

before complete denitrification was achieved in a bench-scale, batch denitrifying cathode, nitrite concentrations reached 66.4 % ± 7.5 % of the initial nitrogen. Common environmental inhibitors such as insufficient electron donor, dissolved oxygen, insufficient carbon source, and pH, were considered as a cause of the accumulation. Improvement in these conditions did not mitigate nitrite accumulation. We present an activated sludge model with an integration of the Nernst-Monod model and indirect coupling of electrons (ASM-NICE) that effectively simulated the observed batch data, including nitrite-accumulation by coupling biocathodic electron transfer to intracellular electron mediators. The simulated half-saturation constants for mediated intracellular transfer of electrons during nitrate and nitrite reduction suggested a greater affinity for nitrate reduction when electrons are not limiting. The results imply that longer hydraulic retention times (HRTs) may be necessary for a denitrifying biocathode to ensure complete denitrification. These findings could play a role in designing full-scale MFC wastewater treatment systems to maximize total nitrogen removal.

Experimental Evaluation of Responses of Anode-Respiring Communities to Nitrate:

A poorly understood phenomenon with a potentially significant impact on electron recovery in MFCs is the role of competition between anode-respiring bacteria and microorganisms that use other electron acceptors. Nitrogen species are a major constituent of wastewater and nitrate can act as a competing electron acceptor in the anode. Studies investigating the impact of competition on population dynamics in mixed communities in the anode are lacking. Here, we investigated the impact of nitrate at different C/N ratios, 1.8, 3.7 and 7.4 mg-C/mg-N, on the electrochemical performance and the biofilm community in mixed-culture chemostat MFCs. The electrochemical performance of the

MFC was not affected under electron donor non-limiting conditions, 7.4 mg-C/mg-N. At lower C/N ratios, electron donor limiting, electron recovery was significantly lower. The electrochemical performance recovered upon removal of nitrate at 3.7 mg-C/mg-N. Microbial community analysis showed a decrease of *Deltaproteobacteria* accompanied by an increase in *Betaproteobacteria* in response to nitrate at low C/N ratios, and no significant changes at 7.4 mg-C/mg-N. Transcriptional analysis showed increased transcription of *nirK* and *nirS* genes during nitrate flux suggesting that denitrification to N_2 (and not facultative nitrate reduction by *Geobacter spp.*) might be the primary response to perturbation with nitrate.

Modelling Interspecies Competition in the Anode of a Microbial Fuel Cell:

MFCs offer great promise for simultaneous treatment of wastewater and energy recovery. Even though there have been extensive experimental studies of multi-species anode-respiring biofilms, models and process optimization studies have been scarce. The formulation and evaluation of models is a critical step in the application of MFCs to wastewater treatment and bioremediation. The purpose of this study was to formulate a model that could simulate the effect of influx of a competing electron acceptor such as nitrate on the anode biofilm community. A model was formulated considering two distinct communities of bacteria: an anode-respiring community (not capable of nitrate reduction) and a denitrifying community (not capable of anode-respiration). A competitive scenario involving the influx of acetate and nitrate at a C/N ratio of 1.8 mg-C/mg-N was used to calibrate the model using experimental data. Calibration results indicate that facultative reduction of nitrate by facultative anode-respiring bacteria could be an important factor playing a role in the robustness and resilience of the anode-

biofilms to fluxes of nitrate. Sensitivity analyses revealed that the biofilm retention coefficient (biofilm detachment rate) and species-specific growth kinetic parameters could play a significant role in the robustness of anode communities to influx of nitrate. Further investigation of change in detachment rate in response to the presence of nitrate in bulk solution is required.

TABLE OF CONTENTS

Page

LIST OF TABLES

Table Page

LIST OF FIGURES

Figure Page

CHAPTER 1

INTRODUCTION

1.1 Wastewater Treatment

Wastewater treatment is a necessity for public health and the environment. It serves to remove biological oxygen demand (BOD), total suspended solids and fecal coliform (Metcalf & Eddy, 2003) . But more recently, nutrient removal has become a recommended treatment requirement (EPA, 2001). This is due to the fact that 25 % of all water body impairments in the US are linked to nutrient-related causes (EPA, 2007). Even though the nutrient-related impairments could be due to both point and non-point source discharges, point source discharges are easier to manage and control. Hence an ever increasing number of point-source discharges, including wastewater treatment plants, have discharge effluent limits for nitrogen and phosphorus (EPA, 2007).

Wastewater treatment, as it is done today, is an energy intensive process and in most cases require external substrate addition for nutrient removal (Metcalf & Eddy, 2003). In addition to this, nutrient and energy recovery are also not accomplished (Shizas et al., 2005). It is estimated that wastewater treatment accounts for 2% of the total energy consumption in the United States (EPRI, 1994). Aeration for the activated sludge treatment process accounts for an average of 55.6% of the total energy consumption for wastewater treatment(Tchobanoglous et al., 2003). With increasing demand for higher quality effluents, the energy demand for wastewater treatment is likely to increase.

The energetic value of municipal wastewater has been estimated by different studies to be 6.3 kJ/L-7.8 kJ/L (Channiwala and Parikh, 2002; Heidrich et al., 2011;

Shizas et al., 2005). This translates to a theoretical energy of ~6000 kWh/MGal in wastewater. With increasing levels of energy-intensive treatment required, a cost effective and energy efficient process is required.

Anaerobic digestion can help recover energy from wastewater treatment facilities. This process is used for concentrated waste streams of greater than1000 mg-COD/L. The process is capable of handling high volumetric loading rates, minimizes the sludge produced and yields methane as an energy product. The temperature of the digester is often maintained above 30 °C. For these reasons, anaerobic digestion is used as a process for solids stabilization and reduction, rather than for municipal wastewater treatment. Anaerobic digestion has poor efficiency when treating dilute wastewater streams of 1000 mg COD/L or less. Also, the susceptibility of the process to changes in temperature and influx of toxic constituents make it an unstable process for municipal wastewater treatment. If used for wastewater secondary treatment, it needs to be followed up by an aerobic polishing step in order to ensure effluent quality. Thermodynamic limitations in a Carnot engine restrict the recovery of energy from methane, that is produced during anaerobic digestion, to only 35%. Considering that, only 70% of the gas produced in a digester is methane with the rest being carbon dioxide, hydrogen sulfide, nitrogen, hydrogen and water vapor, the extractable energy from the digester gas is limited. The gas also has to be scrubbed of these other constituents before energy can be extracted (Metcalf & Eddy., 2003). The digester gas can also be used for cogeneration which is a system for generating electricity and the jacket water from the internal combustion engine can be used for heating the digester.

Microbial fuel cells (MFC) convert energy, available in a biodegradable substrate, directly to electricity. This can be achieved using bacteria that can use an insoluble electron acceptor, such as the anode of a MFC, to transfer electrons. In a biocathode, bacteria are capable of accepting electrons from an external circuit (anode) and are capable of using an oxidized contaminant, such as nitrate, perchlorate, etc., as their electron acceptor. This decoupling of the electron donor and electron acceptor reactions is advantageous because it makes the MFC capable of treating a wide variety of reduced substrates in the anode and oxidized contaminants in the cathode. MFCs are capable of operating at temperatures below 20 °C and at low substrate concentrations (Aelterman et al., 2006; Pham et al., 2006).

1.2 Microbial Fuel Cells

The first observation of an electromotive force (EMF) generated through oxidation of a substrate through microbiological activity was made by Michael Potter in 1911 (Potter, 1911). He found that microorganisms were capable of producing a sustainable direct current using glucose as a substrate. But MFCs as an energy-efficient treatment process for organic waste emerged as a concept due to the drive for sustainable energy production and its potential as an application in remote areas without access to a grid such as developing countries and in space missions. Habermann and Pommer first explored the idea of using a MFC for treating domestic wastewater (Habermann and Pommer, 1991).

In a MFC, microorganisms oxidize reduced substrates at the anode and use the anode electrode as an electron acceptor. The electrons are then transported through an external load-bearing circuit to the cathode. Protons produced in the anode are

transported through an exchange membrane to the cathode where the protons and electrons react with a soluble electron acceptor (Figure 1.1). The substrate at the anode, which serves as an electron donor, is any substrate that the community in the anode can metabolize. This may include simple substrates such as acetate, glucose, etc. to complex organic matter in industrial, municipal and agricultural wastewaters (Chaudhuri and Lovley, 2003; Habermann and Pommer, 1991; He et al., 2005; Li et al., 2010; Liu et al., 2005a; Rabaey et al., 2003; Wen et al., 2010). Other substrates for microorganisms in the anode that have been shown to be suitable are sulfides, sea water organics and cellulose(Bass et al., 2007; Rezaei et al., 2008; Shantaram et al., 2005; Tender et al., 2002). Oxidized electron acceptors that have been used in the cathode are nitrate, nitrite, perchlorate, oxygen and manganese oxide and their reduction can be mediated wither biotically and abiotically (Butler et al., 2010; Butler and Nerenberg, 2010; Lovley and Phillips, 1988; Rhoads et al., 2005; Virdis et al., 2008).

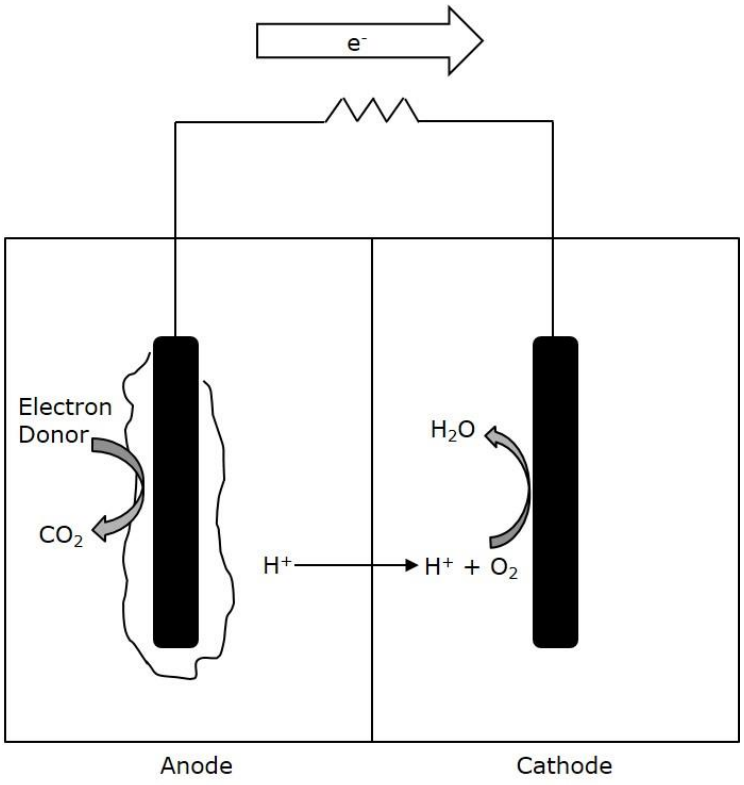

Figure 1.1: Schematic of a Microbial Fuel Cell

MFCs have a number of advantages for wastewater treatment. MFCs are an energy-producing treatment process with a low biomass yield (anaerobic growth). Voltage/ current produced also provides a good monitoring tool to track the performance of the MFC (Li et al., 2014; Logan and Regan, 2006a). Other advantages are capability for off-grid applications and direct electricity generation. (Figure 1.2).

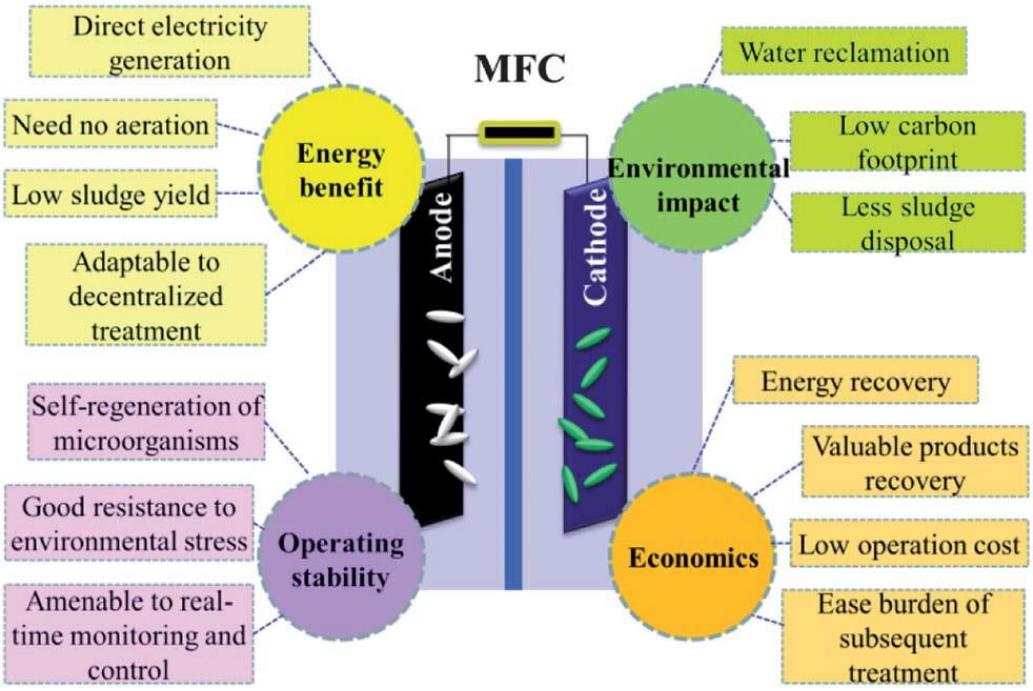

Figure 1.2: Advantages of a Microbial Fuel Cell for Wastewater Treatment (Li et al., 2014)

MFC research has advanced exponentially in the last decade (Figure 1.3). Power production has increased orders of magnitude from 0.1 mW/m^2 to 1500 mW/m^2 (Logan and Regan, 2006b). This has been largely due to improvements in MFC architecture, new electrode materials and design and catalysts, elucidation of causes of power losses, proton exchange membranes and understanding of microbial ecology and process in the anode and the cathode. The following sections place emphasis on these improvements and

research. Scaling-up MFCs and roadblocks to practical application of this technology are also discussed in the following sections.

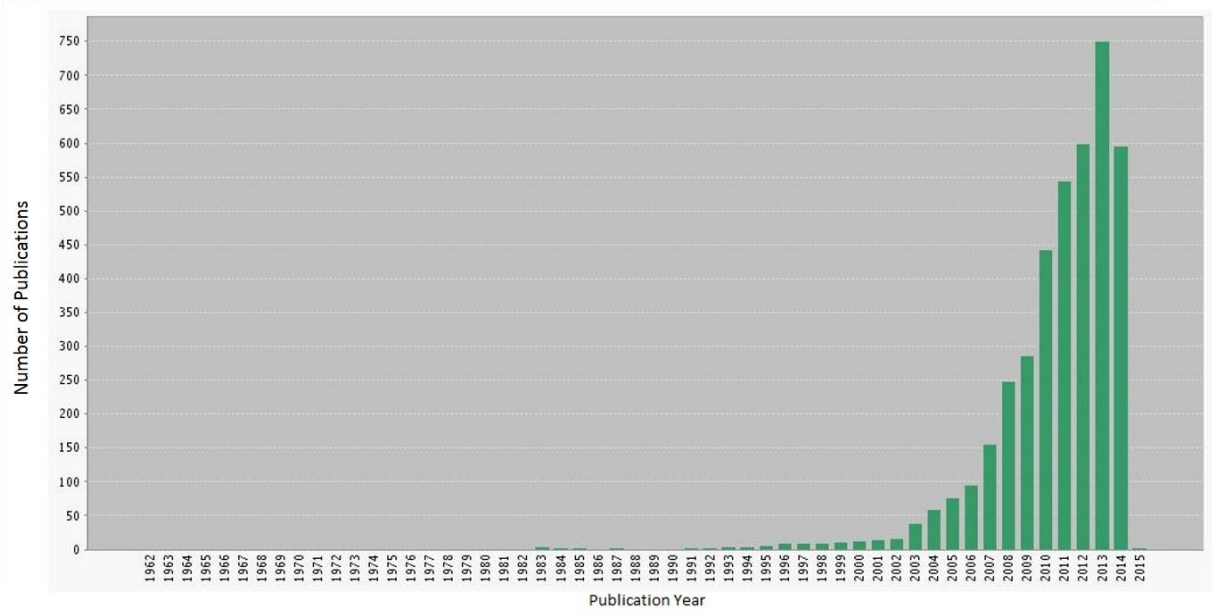

Figure 1.3: Number of Publications per year for subject work 'Microbial Fuel Cell' (ISI Web of Science)

1.2.1 MFC Design and Configuration

Several configurations and designs of MFCs have been tested and studied (Figure 1.4). The most -commonly used system is the two-chamber H-cell consisting of two bottles connected by a tube. The two bottles are separated by a cation exchange membrane (CEM) or a proton exchange membrane (PEM). This type of design separates the electrolytes of the two chambers but allows for proton transport from the anode to the cathode. The anode and the cathode are usually constructed using a graphite or carbon material. These could be in the form of plates, granules or cloth. The anolyte (anode media) is a phosphate-buffered growth media innoculaed with a bacterial consortia,

which is typically either a pure culture of a bacterial species/strain or a mixed culture of bacteria. The catholyte (cathode media) is aerated phosphate buffer or ferricyanide solution. Specific details about the anolyte and the catholyte are discussed in the following sections. Although this design has been used by many researchers to examine the effect of different substrates, different anode inoculum, electrode surface area and presence of electron shuttles (Bond and Lovley, 2003; Chaudhuri and Lovley, 2003; Liu and Logan, 2004), the design is not feasible as a scalable design.

Another design that is very commonly used is the single-chamber air cathode MFC (Liu et al., 2004; Liu and Logan, 2004). In this design, the cathode is placed in direct contact with air thus eliminating the need for constant input of a cathode electrolyte. The CEM/PEM is an expensive part of the MFC. Eliminating the membrane would help in making the implementation of a full-scale MFC more cost-efficient. Liu and Logan, 2004 found that eliminating the PEM increased the maximum power density of the MFC but decreased the columbic efficiency (CE). CE is the ratio of electrons conducted through the external circuit to the theoretical amount of electrons available in the substrate. This suggested that oxygen crossover from the cathode to the anode was occurring. Microorganisms in the anode could use the oxygen as an alternate electron acceptor thus competing for the electron donor and thus decreasing CE. A polytetrafluoroethylene (PTFE) coating was added, in a subsequent study, to limit oxygen crossover into the anode. This addition improved both the CE and the power density of the MFC (Cheng et al., 2006).

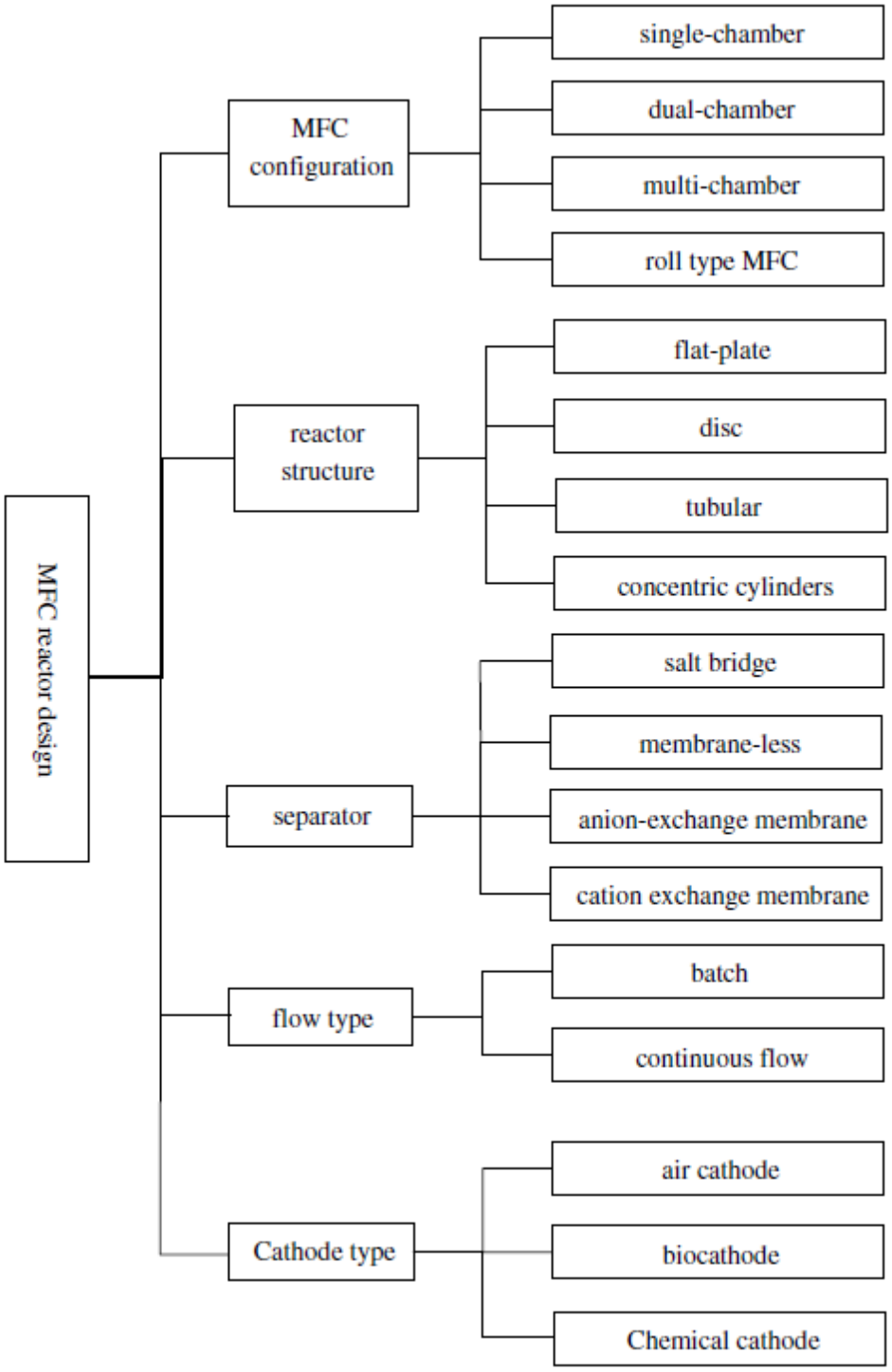

Figure 1.4: Design of MFCs by various Classification Criteria(Zhou et al., 2013).

The cell voltage in bioelectrochemical systems (BESs) is set by the open circuit voltage (OCV). The actual cell voltage is usually lower than the OCV due to losses that occur as

current is produced. These losses are due to electrode overpotentials and ohmic losses of the cell.

$$E = OCV - \Delta E_{\eta} - \Delta E_{\Omega} = OCV - (\Sigma\eta_{anode} - \Sigma\eta_{cathode}) - I\Sigma R_{\Omega} \qquad \textbf{Equation 1.1}$$

where E is the potential difference between the anode and the cathode, ΔE_{η} is overpotential losses, ΔE_{Ω} is ohmic losses, $\Sigma\eta_{anode}$ is the sum of overpotential losses at the anode, $\Sigma\eta_{cathode}$ is the sum of overpotential losses at the cathode, I is the current produced and ΣR_{Ω} is the total ohmic resistance.

Deviations from the ideal equilibrium potential are called overpotentials and these lead to a decrease in the useful cell voltage of the cell. Overpotential at the anode are caused by: activation, mass transport and bacterial metabolism losses (Logan, 2008). Activation losses are due to energy lost during oxidation and reduction reactions and due to electron transfer from the cell to the anode surface. Mass transport losses occur due to insufficient flux of reactants or products towards or away from the electrodes. At the anode, substrate flux to the anode has not been shown to cause losses.

Ohmic losses arise due to charge transfer resistance. Charge transfer resistance is caused by resistance to electron transfer through the electrodes and through conductive components of the circuitry and ion transfer through the electrolytes. The ohmic resistance can be determined by the current-interrupt method(Aelterman et al., 2006; Clauwaert et al., 2007b) or by electrochemical impedance spectroscopy (He and Mansfeld, 2009; Malvankar et al., 2012; Marsili et al., 2008). The ohmic loss across the membrane can be determined by using reference electrodes in the anode and the cathode

and measuring the voltage difference between the two reference electrodes(ter Heijne et al., 2006).

1.2.2 Anode

The anode of the MFC is the electron-generating chamber. The anode electrode is usually constructed of graphite or carbon materials since they are inexpensive, relatively non-reactive, durable and easily obtained. Bacteria in the anode oxidize substrates, which act as electron donors, and use the anode electrode as the electron acceptor.

1.2.2.1 Anode Potential

Anode potential (E_{an}) is defined as the potential difference between the anode and the surrounding electrolyte. E_{an} also refers to the electrode's affinity to electrons. It is determined by multiple factors such as electrode material, the electrolyte, the reactions at the electrode and the microorganisms reducing the anode. The anode potential can influence the community structure of the biofilm (Commault et al., 2013; Torres et al., 2009, 2007; Wagner et al., 2010). Determining optimal anode potentials is integral to optimizing the startup and performance of BESs. The maximum energy that a cell can capture from the oxidation of an electron donor coupled with the reduction of an electron acceptor is calculated from the Gibbs free energy using the following equation:

$$\Delta G^{0'} = -nF\Delta E_0^{'} \qquad \textbf{Equation 1.2}$$

where $\Delta G^{0'}$ is the Gibbs free energy at standard biological conditions (T=25 ^{0}C, pH=7), n is the number of electrons transferred, F is the Faraday's constant (96,485 C/mol e^-) and $\Delta E_0^{'}$ is the difference in the potentials between the electron donor and the electron

acceptor for a particular chemical reaction. In the case of ARB, the electron acceptor is the anode and the redox potential for the anode is the anode potential.

Optimizing the anode potential is necessary to get optimal biofilm growth and power production in the MFC. For electron transfer from the microbial cell to the electrode to be thermodynamically favorable, the anode should have a higher potential than the protein or mediator performing the electron transfer (Figure 1.5). Increasing the potential difference between the anode and the cathode optimizes the power output and increases electron transfer. This implies that the anode potential should be as negative as possible. On the contrary, more negative anode potentials (more reducing environment) may favor the growth of slow-growing microorganisms leading to a slow establishment of the anode communities. Bacterial metabolism losses occur because bacteria derive energy from substrate oxidation. This is an inherent limitation in the MFC technology. Bacterial growth is important for extracting usable energy from organic substrates using a MFC. However, bacteria need energy for their maintenance and growth needs. The greater the bacterial growth, greater is the amount of energy lost. In order to recover maximum energy through the external circuit, the anode potential needs to be as negative as possible.

Several studies have observed the effect of growing anode-respiring bacteria (ARB) at different anode potentials. Busalmen et al.(2008) showed that *Geobacter sulfurreducens* showed different electrochemical responses when adapted to two different anode potentials (0.1 or 0.4V vs SHE) which suggests the use of different respiratory mechanisms at different potentials. Finkelstein et al.(2006) acclimated a mixed culture benthic MFC at different anode potentials (-0.058 to 0.618 V vs Ag/AgCl). They

concluded that the current production was similar for the different anode potentials. However, they observed that the ARB communities regulated their respiratory pathways based on the anode potential to maximize energy efficiency. Another study (X. Wang et al., 2009) found that an anode poised at a more positive potential of 0.2 V vs Ag/AgCl resulted in a faster acclimation (with respect to current production) of the anodic community.

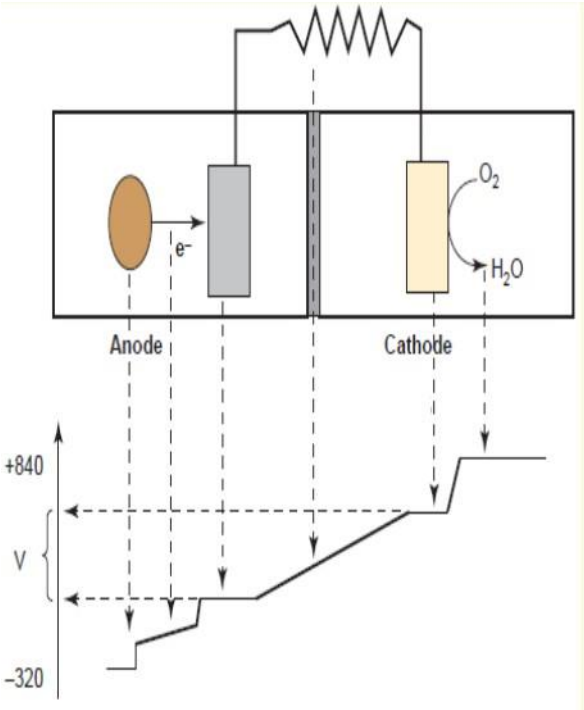

Redox reaction	E'_0 (mV)
$2H^+ + 2e^- \rightarrow H_2$	−420
$Ferredoxin(Fe^{3+}) + e^- \rightarrow Ferredoxin(Fe^{2+})$	−420
$NAD^+ + H^+ + 2e^- \rightarrow NADH$	−320
$S + 2H^+ + 2e^- \rightarrow H_2S$	−274
$SO_4^{2-} + 10H^+ + 8e^- \rightarrow H_2S + 4H_2O$	−220
$Pyruvate^{2-} + 2H^+ + 2e^- \rightarrow Lactate^{2-}$	−185
$FAD + 2H^+ + 2e^- \rightarrow FADH_2$	−180
$Fumarate^{2-} + 2H^+ + 2e^- \rightarrow Succinate^{2-}$	+31
$Cytochrome\ b(Fe^{3+}) + e^- \rightarrow Cytochrome\ b(Fe^{2+})$	+75
$Ubiquinone + 2H^+ + 2e^- \rightarrow UbiquinoneH_2$	+100
$Cytochrome\ c(Fe^{3+}) + e^- \rightarrow Cytochrome\ c(Fe^{2+})$	+254
$NO_3^- + 2H^+ + 2e^- \rightarrow NO_2^- + H_2O$	+421
$NO_2^- + 8H^+ + 6e^- \rightarrow NH_4^+ + 2H_2O$	+440
$Fe^{3+} + e^- \rightarrow Fe^{2+}$	+771
$O_2 + 4H^+ + 4e^- \rightarrow 2H_2O$	+840

Figure 1.5: Standard potentials of common electron donors and acceptors and the relationship between anode, cathode potentials and the voltage generated (Rabaey and Verstraete, 2005).

Torres et al. (2009) found that when the anodic community was adapted using different anode potentials (-0.15, -0.09, 0.02 and 0.37 V vs SHE), the electrodes poised at -0.15 and -0.09 V vs SHE showed faster biofilm growth and produced the highest current densities (> 8 A/m^2 for -0.15 V and > 6 A/m^2 for 0.09 V) compared to the electrodes

poised at 0.02 V (< 2 A/m^2) and 0.37 V (< 0.6 A/m^2). Cyclic voltammograms showed that the electrodes poised at the lowest anode potentials (-0.15 and -0.09 V vs SHE) showed evidence of extracellular electron transport. These electrodes also showed stronger selection for known ARB compared to the ones at more positive potentials which had more diverse communities. Even though several studies have attempted to determine ideal anode potentials for the acclimation and operation of an anode biofilm, there has been no agreement on the optimal anode potential. This could be due to the fact that the anode potential and the acclimation of an anode biofilm is influenced by not only the poised potential but also several other factors such as electrode and reactor configuration, electrolyte composition and the starting inoculum. For example, Wagner et al. (2010) argued that even though Torres et al. observed that the electrodes poised at -0.15 V and -0.09 V vs SHE showed larger current densities and faster startup times compared to electrodes poised at 0.02 and 0.37 V vs SHE, their reactor setup had four anode electrodes poised at different potentials in the same chamber. Biofilms growing on one electrode could produce mediators that affect the growth of the biofilm on another electrode and the electrodes also have different charges that could affect the growth of the biofilm on the different electrodes. This argument is supported by Parot et al. (2008) where they observed that the electrode poised at the lower potential (0.54 V vs SHE) showed the highest maximum current density in the multiple electrode/single chamber arrangement with contrasting results in the single electrode/multiple reactor arrangement. There, currently, is no agreement on the ideal anode potential for a MFC or other BESs(Wagner et al., 2010).

1.2.2.2 Proton Accumulation

Proton flux, produced at the anode, can also limit power production. Proton accumulation can lead to pH decrease locally inside the biofilm leading to suboptimal growth of bacteria. Franks et al. (2009) found that pH can be almost 0.9 units less near the anode surface compared to the bulk fluid and they also demonstrated that this drop in pH to 6.1 from 7 can limit the growth of *G.sulfurreducens*, a known ARB. Torres et al. (2008) observed that proton transport out of an anode biofilm could cause current density limitations in a MFC and proton accumulation increased with increasing current densities (Figure 1.6).

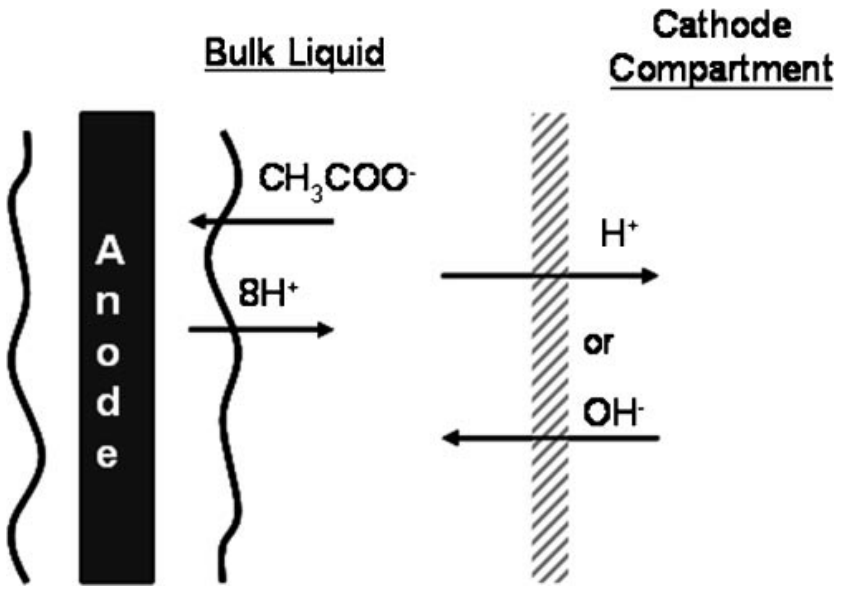

Figure 1.6: Proton Transport when Acetate is used as an Electron Donor in the Anode (Torres et al., 2008a).

1.2.2.3 Mechanisms of Electron Transfer

A critical limiting factor in the performance of BESs is electron transfer from the microorganisms to the electrodes. Electron transfer outside of the cell must lead to a redox active species that is capable of transferring an electron to the electrode. There are several mechanisms of electron transfer that have been documented in BESs. However, a classification can be made based on the type of species facilitating the electron transfer: direct electron transfer (DET) using a membrane bound species (Bond et al., 2002; Bond and Lovley, 2003; Nevin and Lovley, 2000) and mediated electron transfer (MET) using soluble mediators/shuttles (Hernandez and Newman, 2001; Newman and Kolter, 2000).

DET takes place through a direct physical contact of the bacterial cell. The first suggestion of an ability to transfer electrons directly to an electrode by *Shewenella putrefaciens* was shown by Kim et al., 1999. It was later shown that *S.putrefaciens* could produce electron shuttles which could account for the electron transfer to the electrode. This was supported by the observation that the optical density in the solution surrounding the electrode increased with increasing current suggesting a growth in the planktonic cells concentration rather than on the electrode (Lovley, 2006). DET can occur via two mechanisms: short-range and long-range electron transfer. One of the most extensively studied microorganisms capable of electron transfer to a solid electron acceptor is *Geobacter sulfurreducens.* This microorganism and *Geobacter spp.* as a whole have become a model genera of studying electron transfer mechanisms (Patrick D Kiely et al., 2011; Lovley, 2006; Sydow et al., 2014). Other microorganisms have also been shown to have anode respiring capabilities with different electron transfer mechanisms (Table 1.1).

1.3 Microbial Interactions:

The sociobiology of microorganisms is critical in almost all microbial communities and can influence the assembly and ecology of a microbial community and responses and outcome of disturbances to the community. These interactions can take the form of communication, cooperation, competition and cheating. Competition is the focus of this section since it is the focus of the dissertation.

1.3.1 Competition:

The advent of high throughput sequencing has revealed tremendous microbial diversity. Underlying the quantitatively dominant microbial populations is a highly diverse but low abundance population which has been termed as the rare biosphere (Sogin et al., 2006). This phenomenon has also been documented in bioelectrochemical systems.

Table 1.1: Some electrode-respiring bacteria and electron transfer mechanisms(Zhou et al., 2013)

Microbes	Mechanism
In anodic biofilm	
Aeromonas hydrophila	DET
Geobacter metallireducens	DET
Rhodoferax ferrireducens	DET
Shewanella putrefaciens	DET
Actinobacillus succinogenes	MET
Alcaligenes faecalis	MET
Enterococcus gallinarum	MET
Proteus vulgaris	MET
Shewanella oneidensis	MET
In cathodic biofilm	
G. sulfurreducens DL1	DET
Geobacter sulfurreducens	DET
Acidithiobacillus ferrooxidans	DET
Shewanella putrefaciens	DET
Desulfovibrio vulgaris	DET
D. vulgaris	DET
Clostridium beijerinckii	MET
Pseudomonas spp	MET
S. oneidensis	MET
Acinetobacter calcoaceticus	MET

Kiely et al (2010) observed that, in a mixed-culture MFC fed with formic acid, *Paracoccus* genera were revealed to be the most abundant (30%) in the community as revealed by 16S rRNA clone library construction and sequencing even though the power density produced by a *P.denitrificans* isolate from the anodic community was only half of what the mixed-culture MFC produced. A *S.putrefaciens* isolate produced even higher power than *P.denitrificans* even though the abundance of *Shewenella* was not detected by clone library sequencing. This suggested that there are diverse low-abundance communities existing in the anode biofilm of the MFC which could harbor anode

respiring species. It also suggests that these diverse communities could have microorganisms with various alternate metabolisms which could lead to competition for nutritional resources.

Nutritional resources are a focal point of microbial competition. The relationship between a limiting nutritional resource and bacterial growth was first demonstrated by Jacques Monod (Monod, 1949). Monod also developed equations describing this behavior

$$\mu = \mu_{max} \frac{S}{K_s + S} \qquad \textbf{Equation 1.3}$$

where μ is the specific growth rate of the microorganism ($time^{-1}$), μ_{max} is the maximum specific growth rate ($time^{-1}$) which is a characteristic of the particular species and the particular substrate, S is the substrate concentration (M) and K_s is the half-saturation constant (M) which is defined as the substrate concentration at which the specific growth rate is half of the maximum specific growth rate ($\mu=\mu_{max}/2$). Equation 1.3 considers only a single limiting substrate. For dual substrate limitation kinetics, the following modified version can be used to model the growth of a microorganism (Bae and Rittmann, 1996)

$$\mu = \mu_{max} \left(\frac{S_d}{K_{sd} + S_d}\right)\left(\frac{S_a}{K_{sa} + S_a}\right) \qquad \textbf{Equation 1.4}$$

where S_a and S_d are the electron acceptor and electron donor concentrations respectively, K_{sd} and K_{sa} are the half-saturation constants for the electron donor and the electron acceptor respectively.

The Monod microbial growth model does not explicitly provide a model for describing competition between cells, species or genera but provides a fundamental description of

the dependence of microbial growth on limiting resource concentrations. This was used by Tilman (Tilman, 1977) to examine the competition between two different algal populations as a function of shared limiting resources. This resource ratio competition model used the limiting resource growth kinetic model developed by Monod and developed a quantitative framework to determine the outcome of a competitive scenario between two species sharing a limiting resource. Consider species 1 and species 2 competing for a single limiting resource. For both species to coexist the following quantitative relationship was developed

$$\frac{K_s^1}{\mu_{max}^1 - D} = \frac{K_s^2}{\mu_{max}^2 - D} \qquad \textbf{Equation 1.5}$$

where K_s^1 and K_s^2 are the half-saturation constant for species 1 and species 2 for the common resource, μ_{max}^1 and μ_{max}^2 are the maximum specific growth rates for species 1 and species 2 and D is the dilution rate. Species 1 will outcompete species 2 when

$$\frac{K_s^1}{\mu_{max}^1 - D} < \frac{K_s^2}{\mu_{max}^2 - D} \qquad \textbf{Equation 1.6}$$

For competition to occur, the common resource or resources that the species are competing for should be in limiting concentrations. This framework developed for competition can be applied to BESs as shown in the next section.

1.3.2 Competition in BESs:

Bioelectrochemical systems utilize microorganisms that are capable of using electrodes as their electron acceptor (anode) or as their electron donor (cathode). This section is focused on anode-respiring bacteria (ARB). However, the same concepts can be applied to the cathode as shown in Chapter 2. In mixed-culture anode-biofilms, ARB compete

with other functional groups of bacteria such as fermenters, acetogens and methanogens in the absence of other electron acceptors in the anode. In the presence of competing electron acceptors such as nitrate, oxygen, sulfate, etc., microorganisms that can utilize these electron acceptors can also act as competitors. An understanding of competition in anode biofilms will aid in improving the performance of BESs.

The primary functional performers in BESs are ARB. Competition can occur for common resources such as for space (electrode surface area), electron donor, electron acceptor and other trace nutrients. When microorganisms, that are not capable of electrode respiration, compete with ERB, loss in power production and columbic efficiency can occur. The focus of this section is on competition in the anode.

The Monod model works well for dissolved substrates but in a BES, the ARB are limited by a dissolved substrate (electron donor) and/or a solid substrate (electron acceptor). In the anode of a MFC, the solid electrode is the electron acceptor. It serves as a solid conductor for electrons to pass through in response to the electrical-potential gradient. The ability of the electrode to act as an electron acceptor is determined by the anode potential. The above equation can be modified using the Nernst equation (Equation 1.7) as a starting point:

$$E = E^o + \frac{RT}{nF} lnQ \qquad \textbf{Equation 1.7}$$

$$\mu = \mu_{max} \left(\frac{S_d}{K_{sd} + S_d}\right)\left(\frac{1}{1 + \exp\left[-\frac{F}{RT}\eta\right]}\right) \qquad \textbf{Equation 1.8}$$

where E is the half-cell potential, E^o is the standard redox potential, n is the number of electrons, Q is the reaction quotient, F is the Faraday constant, R is the gas constant, T is the temperature (°C) and $\eta = (E_{anode} - E_{Ka})$, where E_{anode} is the anode potential and E_{Ka} is the anodic electron acceptor potential for the half-maximum rate (Marcus et al., 2007). The electron donor part of the equation remains the same while the electron acceptor part is modified using the Nernst equation. The Monod equation and hence the Nernst-Monod equation were developed for well-mixed suspended systems. BESs are biofilm systems and hence have diffusional limitations that a well-mixed suspended system might not have. Hence the equation has to be modified to include the diffusional limitations that biofilm have.

$$\mu = \mu_{max} X_f L_f \left(\frac{S_d}{K_{sd} + S_d}\right)\left(\frac{1}{1 + \exp\left[-\frac{F}{RT}\eta\right]}\right) \qquad \textbf{Equation 1.9}$$

where X_f is the biofilm cell density and L_f is the depth of the biofilm. For thin biofilms, an assumption can be made that there are no diffusional limitation and hence the system behaves like a suspended system. The thickness of the biofilms in BESs depend on a host of different factors such as the electrode material, flow rates, polarizing potential on the electrode, electron donor concentration, etc.

One of the most common forms of competition in BESs is from microorganisms capable of respiring on alternate electron acceptors such as oxygen, nitrate, nitrite, sulfate, etc. In this case, the resource the microorganisms are competing for is the electron donor. In a MFC, oxygen is commonly used in the cathode as an electron acceptor (air cathode). Since the anode and cathode are separated by a membrane, the diffusion of oxygen from

the cathode into the anode is controlled by the permeability of the membrane to oxygen. Chae et al. (2008) estimated the oxygen mass transfer coefficient and the oxygen diffusion coefficient for Nafion, which is one of the more commonly used PEMs, to be 2.80×10^{-4} cm/s and 5.35×10^{-6} cm^2/s when a 50 mM phosphate buffer solution was used as the catholyte. They also determined that the dissolved oxygen (DO) level in the anode of a two-chamber uninnoculated MFC increased from 0.3 to 1.5 mg/L in 700 minutes when oxygen was used in the cathode. It has been shown that the oxygen crossover can be lowered by adding a diffusion layer on the cathode of an air-cathode MFC, thus improving the performance of the MFC (Cheng et al., 2006). Butler and Nerenberg (2010) showed that the rate of diffusion of oxygen from the cathode to the anode was three times higher in MFCs that lacked diffusion-layers and the power density was also lower compared to MFCs with diffusion-layer cathodes. They also observed that the MFCs with diffusion-layer cathodes had higher abundance of bacteria of genus *Geobacter*, which are a known group of ARB. This suggests that the presence of oxygen, an alternate electron acceptor, can cause changes in microbial ecology leading to decreased performance due to decreased coulombic efficiency and lower relative abundance of ARB in the anode.

The effect of nitrate on bioelectrochemical biofilms is of particular interest because nitrogen is a key nutrient in the effluent of a wastewater treatment plant that is regulated by the EPA. Simultaneous nitrification and denitrification systems are key to removing nitrogen from wastewater and can lead to the presence of nitrate in the influent to the anode of a BES depending on the position of a BES in a wastewater treatment train (such as pre-denitrification). The effect of nitrate on microbial communities enriched for anode

respiration is of particular interest since BESs have been used for nitrogen removal for wastewater and groundwater. Denitrifying BESs have been implemented as single-chamber air cathode MFCs (Yan et al., 2012), denitrifying biocathode MFCs (Gregoire et al., 2014; He and Angenent, 2006; Nguyen et al., 2014) and in-situ groundwater denitrifying BESs (Tong and He, 2014; Zhang and Angelidaki, 2013). Nitrate is a competing electron acceptor in the anode and can lead to loss in coulombic efficiency and consequently power production. Factors such as crossover of nitrate from a biocathode into the anode, presence of nitrate in a single-chamber air cathode MFC, etc. can lead to nitrate being present in the anode and cause lower electrochemical performance in the anode of the MFC.

Several studies have observed production of methane in the anode of an MFC (Freguia et al., 2007; Jung and Regan, 2011; Lee et al., 2008; Torres et al., 2007). Even though methane production with acetate as the electron donor is low (Lee et al., 2008), the production of methane has been shown to be significant when fermentable substrates such as glucose (Freguia et al., 2008a; Lee et al., 2008) and ethanol (Parameswaran et al., 2009; Torres et al., 2007) are fed to the anode as the electron donor. Studies with more complex anode influents such as with digested anaerobic sludge and sludge from a primary clarifier have shown significant methane production with only little electricity generation suggesting that as the complexity of the anode influent increases, methane production increases (Ge et al., 2013). Similar results have been observed with microbial electrolysis cells (MECs) operated with swine wastewater and acetate (Wagner et al., 2009; A. Wang et al., 2009).

The presence of such competing microorganisms could lead to ARB being outcompeted from the microbial community and getting washed out. This could lead to a loss in electrochemical performance of BESs. A systematic assessment of the robustness and resilience of BES biofilms to perturbations and alternate electron acceptors (AEAs), that can act as a resource for competing metabolisms, is required.

1.4 Genetic/Evolutionary Algorithms

Single objective evolutionary algorithms (EA) are inspired by Darwin's theory of evolution. They are an attractive method for solving parametric estimation problems due to their non-specific nature. Furthermore, numerical methods (which are more commonly used) can get stuck in a local optimum and thus provide a sub-optimal solution. Thus, EAs are particularly useful for solving non-linear models.

In general, EAs start with a set of candidate solutions (population) that are randomly generated using a lower and upper limit for each of the parameters to be estimated. The members of the population are evaluated based on an objective function. This could be any objective that could be used to evaluate the performance of a mode such as root mean square error (RMSE) or sum of squares of residuals. In most cases, the objective will be to minimize this function. In each iteration (generation), the better solutions (parents) are selected based on the objective function and are used to generate a new set of solutions (offsprings). This means that if the fitness of a member of the population is great (for example, low RMSE) then that member has a higher probability of being selected as a parent for the next generation. The selection is made randomly, however the probability that a member will get selected as a parent is higher if its fitness is higher. This is the selection process for a single objective optimization. In the case where there is more than

one objective (eg: chemical dosing cost vs performance), a different method has to be employed to select the parents. The most commonly used method is non-dominated sorting. For multi-objective optimization, the basic assumption is that there is not a single best solution with respect to all objectives. Hence, in multi-objective optimization, there is a set of solutions that are superior to the rest of the solutions. These solutions are termed Pareto-optimal or non-dominated solutions. Once, the parents are selected, the members of the next generation (offsprings) are created using two genetic processes: crossover and mutation. Usually a certain proportion of the parents are selected for crossover while the rest of the parents are mutated. Crossover mixes two parents to create a new offspring. Mutation randomly changes the parameters to a new value and creates a new member of the next generation. An additional genetic process that can be incorporated is called elitism. Elitism involves copying a small proportion of the fittest members of the population, unchanged, into the next generation. This ensures that the fittest candidates at each generation are propagated to the next generation. These members are eligible for crossover and mutation if more fitter members of the population emerge at future generations. The new generation is thus created and all the steps are iteratively performed. The EA stops when a converging criterion is reached. This converging criterion can be a predetermined condition such as number of generations, when the value of the most fit objective function has not changed in a certain number of generations, etc. The general format outlined here is used for parametric estimation for the models that have been developed in this dissertation.

CHAPTER 2

MODELLING INTRACELLULAR COMPETITION IN A DENITRIFYING BIOCATHODE

Modified from originally published version (Srinivasan, V.; Weinrich, J.; Butler, C. Nitrite Accumulation in a Denitrifying Biocathode Microbial Fuel Cell. Environ. Sci. Water Res. Technol. 2016.)

2.1 Introduction

Microbial fuel cells (MFC) have emerged as a potentially energy-efficient treatment strategy with promising applications in wastewater (Clauwaert et al., 2008; Franks and Nevin, 2010; Logan, 2010; Logan et al., 2006), in-situ environmental remediation (Gregory et al., 2004; Gregory and Lovley, 2005; Strycharz et al., 2008) and decentralized treatment systems (Castro et al., 2014). A particular advantage of MFC application as a treatment strategy is the ability to decouple the electron donor from the electron acceptor in biological reactions, allowing the oxidation of natural or wastewater organics to facilitate the reduction of an oxidized contaminant at the cathode. A variety of oxidized contaminants have been reduced in this way including nitrate, perchlorate, uranium, trichloroethane and dichromate (Butler and Nerenberg, 2010; Clauwaert et al., 2007a; Gregory and Lovley, 2005; Guerrero-Rangel et al., 2010; Pandit et al., 2011; Strycharz et al., 2008; Virdis et al., 2010). Additionally, the electrons passed across an external load between the anode and cathode can offset energy requirements for treatment.

Nitrate is a contaminant of interest for drinking water systems with a maximum contaminant level (MCL) of 10 mg NO_3-N /L in the United States (Fan and Steinberg, 1996). Nitrate has also been regulated in wastewater effluents through total nitrogen discharge limits in an effort to curb eutrophication of surface waters and other environmental impacts. Biological nitrification-denitrification is one of the most common processes used for total nitrogen removal from wastewater (Ciudad et al., 2005). Nitrifying bacteria oxidize ammonia to nitrite and, then, nitrite to nitrate. Biological denitrification reduces nitrate to nitrogen gas. Denitrification is a dissimilatory microbiological process, which many heterotrophic and autotrophic organisms are capable of performing. It is a sequential reaction involving the reduction of nitrate to nitrite by a nitrate reductase enzyme. Nitrite is reduced to nitric oxide by a nitrite reductase enzyme. Nitric oxide is reduced to nitrous oxide by a nitric oxide reductase enzyme after which nitrous oxide is reduced to nitrogen gas by a nitrous oxide reductase (Rittmann and McCarty, 2001).

Though several studies have reported significant denitrification in microbial fuel cells (Clauwaert et al., 2009, 2007a; Virdis et al., 2010), some studies have reported accumulation of nitrite of up to 50-55% of the initial total nitrogen during autotrophic denitrification in cathodes (Desloover et al., 2011; Puig et al., 2011) and accumulation of nitrous oxide of up to 70% of the initial total nitrogen added as nitrate (Van Doan et al., 2013). Minimizing the accumulation of intermediates is critical to achieving maximum nitrogen removal. Denitrification intermediates have negative health and environmental effects. Nitrite can cause methemoglobinemia in aquatic life, small children and the

elderly (Bruning-Fann and Kaneene, 1993; Lewis and Morris, 1986) and nitrous oxide is a potent greenhouse gas (IPCC et al., 2001).

The accumulation of denitrification intermediates can occur due to differing metabolic rates of the denitrification steps. Additionally, several environmental factors could contribute to this accumulation. Denitrification enzyme production is repressed at DO concentrations above 2.5 mg-O_2/L (Körner and Zumft, 1989; Rittmann and McCarty, 2001). Incomplete denitrification can be due to limiting electron donor concentrations (Rittmann and McCarty, 2001) Inhibition of denitrification can occur outside the pH range of 7 to 8 leading to an accumulation of intermediates. pH below 7 can cause direct inhibition through the formation of free nitrous acid which is a protonated form of nitrite (Zhou et al., 2011). A pH above 8 can cause inhibition of general microbiological processes.

Mathematical modeling has played a very critical role in predicting nitrogen removal in wastewater treatment. The modeling of accumulation of intermediates has been achieved by modeling denitrification as a four-step denitrification process, using reaction-specific kinetic rate equations for each step. Broadly, two major models have been proposed in recent years: the “direct-coupling” approach used in Activated Sludge Model for Nitrogen (ASMN) (Hiatt and Grady, 2008) and the “indirect-coupling” approach used in the Activated Sludge Model for Indirect Coupling of Electrons (ASM-ICE) (Pan et al., 2013). The ASMN model directly couples carbon oxidation with each of the nitrogen oxide reduction steps. The ASM-ICE model indirectly couples carbon oxidation and nitrogen oxide reduction using intermediate electron carriers. A comparison of these models in predicting accumulation of nitrogen intermediates was made by Pan et al. (Pan

et al., 2015), concluding that the ASM-ICE model predicts the accumulation of nitrogen oxides better than the ASMN model.

The ASM-ICE model was formulated, assuming a dissolved carbon/electron source and using the dual-substrate limitation kinetics derived from the Monod model. The Monod model works well for dissolved substrates but in a denitrifying biocathode, the biofilm is limited by a solid electron donor. In this case, the ability of the cathode electrode to act as an electron donor is determined by the cathode potential according to the following equation, which has been adapted from a model prepared for a MFC anode by Marcus et al.(Marcus et al., 2007).

$$\mu = -\mu_{max} X_f L_f \left(\frac{S_a}{K_{sa} + S_a}\right)\left(\frac{1}{1 + \exp\left[-\frac{F}{RT}\eta\right]}\right) \qquad \textbf{Equation 2.1}$$

where F is the Faraday constant, R is the gas constant, T is the temperature (K), X_f is the biofilm cell density, L_f is the depth of the biofilm, $\eta = (E_{cathode} - E_{Kc})$, where $E_{cathode}$ is the cathode potential and E_{Kc} is the cathodic mid-point electron donor potential for the half-maximum rate (Marcus et al., 2007). The Nernst-Monod model for a biocathode can simulate electron transfer from a cathode to associated microorganisms assumed to be in a biofilm on the cathode surface (Gregoire et al., 2014; Ter Heijne et al., 2011). The ASM-ICE model can be used to simulate nitrite accumulation in denitrifying bioreactors (Pan et al., 2013). The incorporation of bioelectrochemical elements into an ASM model has not been previously described. An integration of the two models could help elucidate performance parameters in BESs designed for wastewater treatment.

Though complete denitrification has been demonstrated in MFCs using a cathode as an electron donor for autotrophic denitrification, more research is needed to understand the conditions that facilitate incomplete denitrification and the accumulation of intermediates. Additionally, the Monod kinetic parameters, that are crucial to the design of treatment processes, have not been determined for autotrophic denitrification in a MFC cathode. In this study, we investigated the mechanisms behind the accumulation of nitrite by performing experiments under different environmental conditions. We present an ASM with an integration of the Nernst-Monod model and Indirect Coupling of Electrons (ASM-NICE), for the simulation of nitrogen removal in a denitrifying biocathode. We used this model to estimate kinetic parameters for a denitrifying biocathode.

2.2 Materials and Methods

2.2.1 MFC Configuration and Operation

Duplicate flat-plate MFCs were constructed from rectangular Plexiglas frames (10 x 10 x 1.2 cm) and filled with graphite granules (porosity=0.55). The total volume and liquid volume of the electrode compartments were 120 mL and 54 mL respectively. Graphite rods were inserted into the anode and cathode chambers to act as electron collectors. The compartments were separated by a cation exchange membrane (CMI-7000, Membrane International, Glen Rock, NJ) which was activated using a 5% NaCl solution at 40 ˚C for 24 hours. Ag/AgCl reference electrodes (RE-6, BASi Inc. USA) were used to monitor the cathode potentials.

The MFC anodes were inoculated with a combination of anode effluent from a parent MFC (that was constructed and operated similarly to the experimental MFCs) and primary effluent from the Amherst Wastewater Treatment Plant (WWTP), Amherst, MA.

The cathodes were inoculated with a combination of cathode effluent from the denitrifying biocathode of the parent MFC, primary effluent from the Amherst WWTP and a pond sediment inoculum from the Campus Pond, University of Massachusetts-Amherst, MA. The reactors were initially operated in batch mode where the effluent of each electrode compartment was returned to the influent to allow the accumulation of biofilms on the anode and cathode. The end of a batch cycle was indicated by the voltage decreasing to less than 0.05 V measured across the anode and cathode. After 50 batch cycles, the anode chamber was switched to a continuous flow mode. The anode was operated in continuous flow to prevent electron donor limiting conditions occurring in the anode. The feed for the anode was supplied at a flow rate of 0.25 mL/min (hydraulic retention time=20.5 hours) resulting in a COD loading rate of 154 mg COD/L-day. The anode media during the course of experiments, unless otherwise stated, consisted of (per liter) 1.386 g Na_2HPO_4, 0.849 g KH_2PO_4, 0.05 g NH_4Cl, 0.05 g $MgCl_2$, and 0.710 g CH_3COOK (0.355 g COD). The cathode remained in batch operation during all experiments. In this configuration, a single batch cycle typically lasted three days and was marked by the voltage decreasing to less than 0.05 V measured across the anode and cathode. To promote complete mixing, the cathode feed was recycled at 30 mL/min between the cathode and a 1 L external sealed recycle bottle used for collection of gas and liquid samples. The cathode media during the course of experiments, unless otherwise stated, consisted of (per liter) 0.7098 g Na_2HPO_4, 1.4968 g KH_2PO_4, 0.05 g $MgSO_4$, and 0.1228 g $NaNO_3$. Additionally, trace minerals were added to each solution, including (per liter):1 mg $CaCl_2 \cdot 2H_2O$, 1 mg $FeSO_4 \cdot 7H_2O$, 100 µg $ZnSO_4 \cdot 7H_2O$, 30 µg $MnCl_2 \cdot 4H_2O$, 300 µg H_3BO_3, 200 µg $CoCl_2 \cdot 6H_2O$, 10 µg $CuCl_2 \cdot 2H_2O$, 10 µg

$NiCl_2 \cdot 6H_2O$, 30 µg $Na_2MoO_4 \cdot 2H_2O$, and 30 µg Na_2SeO_3. All the feed solutions were sparged with N_2 before the start of each batch cycle. The MFCs and feed bottles were covered with aluminium foil to ensure light did not inhibit denitrification or cause phototrophic growth. After the acclimation period and establishing steady state conditions, experiments were performed to obtain data for model fitting for the purpose of estimating denitrification kinetic parameters (Table 2.1, E2 &E3). Experiments were also performed to determine if environmental parameters such as dissolved oxygen concentration, pH and carbon limitation were responsible for the nitrite accumulation (Table 2.1, E4-E9).

2.2.2 Analyses and Calculations

Nitrate, nitrite, acetate, and sulfate were monitored in the influent and effluent of the anode and cathode compartments using a Metrohm 850 Professional Ion Chromatograph (IC) (Metrohm Inc., Switzerland) with a Metrosep A Supp 5-250 3.2 mM Na_2CO_3, 1.0 mM $NaHCO_3$ eluent was pumped at 2.6 mL/min, with a 100 mM HNO_3 suppressor solution and using a 20 µL sample loop. Ammonium was monitored using a Metrohm 850 Professional IC (Metrohm Inc., Switzerland) with a Metrosep C 2-250 cation column (Metrohm Inc., Switzerland). For cation analysis, an eluent consisting of 0.75 mM dipicolinic acid and 4 mM tartaric acid was pumped at 1 mL/min, using a 10 µL sample loop. Each sample was filtered through 0.1 µm syringe filters, stored at 4 ˚C and analyzed within 5 days of sampling.

Nitric oxide and nitrous oxide were measured using an Agilent 7890A Gas Chromatograph with a Thermal Conductivity Detector (Agilent, USA) with HP-PLOT Molesieve column (Agilent, USA). The inlet was heated to a temperature of 200°C, with

a total flow of 35.5 mL/min and the septum flow at 3 mL/min. A split inlet was used at a 4:1 ratio, or at 26 mL/min. The initial oven temperature at the beginning of each run was 35°C and held for 5 minutes, then ramped at 25°C/min to 200°C, where it was held for 4 minutes. The TCD filament was set at 250°C, with a 20 mL/min reference flow, and a 4.5 mL/min makeup flow. The makeup gas used was helium. Inorganic carbon was measured using a Shimadzu TOC-V_{CPH} Total Organic Carbon Analyzer (Shimadzu, Japan). pH was measured using a Fisher Science Education pH Meter (Fisher Scientific, USA).

2.2.3 Electrochemical Analyses

The MFCs were operated with a 100-Ω external resistance. The potential difference across the external resistances was monitored every 10 minutes using a Keithley Model 2700 Multimeter with a 7700 Switching Module (Keithley Instruments Inc., Cleveland, OH, USA). Low scan rate cyclic voltammetry (LSCV) was performed using a Gamry Series G750 Potentiostat/Galvanostat/ZRA (Gamry, USA). The cathode potential was swept from -0.4 V vs SHE to 0.4 V vs SHE at 1 mV/s and the current density was recorded. j_{max} and E_{Kc} were estimated by fitting the Nernst-Monod equation to the LSCV curve (Torres et al., 2008b).

2.2.4 Theory and Modeling

The model presented in this study was obtained through an integration of the Nernst-Monod model (Marcus et al., 2007) with the ASM-ICE model (Pan et al., 2013). The rate equations and the process matrix are presented in

Table 2.2. Briefly, the cathode oxidation and simultaneous reduction of the oxidized intracellular electron carrier (S_{Mox}) is represented by R1 which simulates electron transfer from the cathode to the biofilm. Nitrate and nitrite reduction are represented by R2 and R3 respectively. The transfer of electrons from cathode oxidation to the reduction of nitrate and nitrite is accomplished in the model through the reduction of the S_{Mox} to S_{Mred}, which is mathematically represented through a constant total concentration (C_{tot}) as R4. The parameters represented in the model are as follows: R_{NA} is the nitrate reduction rate (mmol/(g-VSS.L.h)), R_{NI} is the nitrite reduction rate (mmol/(g-VSS.L.h)), S_{NA} and S_{NI} are the nitrate and nitrite concentrations respectively (mmol/L), j is the current density (A/m^2), $\eta=E_{cat}-E_{KC}$ where E_{cat} is the cathode potential and E_{KC} is the cathodic electron donor potential for the half-maximum rate (V), j_{max} is the maximum current density (A/m^2), S_{Mox} and S_{Mred} are the concentrations (mmol/gVSS) of oxidized and the reduced form of the intermediate electron carrier, C_{tot} is the total concentration of the electron carrier (mmol/gVSS), K_{Mox} is the half saturation constant for S_{Mox} (mmol/gVSS), K_{MredNA} is the S_{Mred} affinity constant for nitrate reductase (mmol/gVSS) and K_{MredNI} is the S_{Mred} affinity constant for nitrite reductase (mmol/gVSS), r_{NA_max} and r_{NI_max} are maximum nitrate and nitrite reduction rates (mmol/(gVSS.h)) respectively.

Table 2.1: Experimental Design

Experiment	Media Change	Purpose
E1	No Change	Acclimation of biofilm to reach steady state conditions
E2	No Change	Data collection for model calibration
E3	20 mg NO_3^--N/L replaced with 30 mg NO_2^--N/L	Data collection for nitrite kinetic parameters
E4	Acetate concentration in the anode increased from 154 mg-COD/L to 770	Determine if electron donor was limiting
E5	Catholyte constantly sparged with N_2 in Recycle Bottle during Cycle	Eliminate potential DO diffusion in cathode
E6	Catholyte amended with 5 mg HCO_3^--C/L	Determine if inorganic carbon is limiting
E7	30 mg NO_2^--N/L, starting pH 6.6	Determine if pH lowers nitrite reduction rate
E8	30 mg NO_2^--N/L, starting pH 7.0	Determine if pH lowers nitrite reduction rate
E9	30 mg NO_2^--N/L, starting pH 7.4	Determine if pH lowers nitrite reduction rate

Table 2.2: Process Matrix for ASM-NICE

Process	S_{NA}	S_{NI}	S_{Mox}	S_{Mred}	Rate Expression
R1			-0.5	0.5	$j = -j_{max}(\frac{1}{1+exp(\frac{-F\eta}{RT})})(\frac{S_{Mox}}{S_{Mox}+K_{Mox}})$
R2	-1	1	1	-1	$R_{NA} = r_{NA\_max}X_f(\frac{S_{Mred}}{S_{Mred}+K_{MredNA}})(\frac{S_{NA}}{S_{NA}+K_{NA}})$
R3		-1	+0.5	-0.5	$R_{NI} = r_{NI\_max}X_f(\frac{S_{Mred}}{S_{Mred}+K_{MredNI}})(\frac{S_{NI}}{S_{NI}+K_{NI}})$
R4					$C_{tot} = S_{Mox} + S_{Mred}$

All kinetic parameters were estimated by solving the differential rate equations and fitting the modeled data to observed data. The following assumptions were made for the purpose of modeling: the biofilm on the cathode was at steady state, i.e., growth of the biofilms equals decay and detachment and for thin biofilms such as those observed in denitrifying cathodes, diffusional limitations are minimal. This assumption was confirmed with biofilm imaging (data not shown). The total electron carrier concentration, C_{tot} was assumed to be 0.01 (mmol/(gVSS)) as in Pan et al. (2013) (Pan et al., 2013). K_{Mox} was assumed to be 1% of the C_{tot} to ensure that the reduction of S_{Mox} was not rate limiting. K_{NA} was assumed to be 3.21 X 10^{-3} mmol/L (Claus and Kutzner, 1985). The biomass parameter (X_fL_f) was determined by dividing the amount of volatile suspended solids (VSS) by the projected surface area of the cathode. The amount of VSS was determined by using Standard Methods 2540 D and 2540 E at the end of operation of the MFCs. The

projected surface area of the cathode electrode was determined by performing a particle size distribution analysis and determining an average particle size for the graphite granules. The assumption was made that the particles were spherical. The d50 or 50 % particle size was used as the average particle size. The specific surface area (SSA) was calculated using the following equation

$$SSA = \frac{6 * (1 - \theta)}{d_{50}} \qquad \textbf{Equation 2.2}$$

where SSA is the specific surface area (m^2/m^3), θ is the packed bed porosity and d_{50} is the 50% passing particle size. All the modeling was done using R statistical software (R Core Team, 2015; Soetaert et al., 2010; Wickham, 2009). Parametric estimations was done by minimizing the sum of squares of the residuals and using a genetic algorithm, similar to the implementation by Pelletier et al. (Pelletier et al., 2006) .

2.2.5 Model Calibration and Validation

The nitrite parameters (K_{NI}, r_{NI_max}) were estimated by calibrating the model to the data for a representative batch from experiment E3 where nitrite was added to the media instead of nitrate. The rest of the parameters were estimated by calibrating the model to a typical batch data (Figure 2.1, replicate batches presented in Figure 2.2) using a genetic algorithm with multi-objective optimization which was implemented using a non-dominated sort method (Deb et al., 2002). The half-saturation constant for nitrate reduction (K_{NA}) was assumed from literature (Claus and Kutzner, 1985), since nitrate reduction has been extensively studied. The multi-objective optimization was performed using nitrate and nitrite model fits as the two objectives for data from E2. Model

validation was performed with two separate batches from experiment E1 from two different reactors to test and demonstrate applicability of the model to other reactors acclimated under the same conditions.

2.3 Results and Discussion

2.3.1 Denitrifying Biocathode Acclimation

During the initial acclimation period (~50 batch cycles), the denitrification rates gradually increased and became consistent, indicating the establishment of a steady-state biofilm. During a typical batch of the biocathode, the removal of nitrate with simultaneous accumulation of nitrite was observed (Figure 2.1A). Subsequent to the removal of nitrate, removal of accumulated nitrite was observed. Peak nitrite accumulation observed was 66.4 ± 7.5 % of the initial nitrogen concentration added as nitrate. This is consistent with previously reported nitrite peak accumulation values of 50-55 % of initial nitrogen added as nitrate (Desloover et al., 2011; Puig et al., 2011). The accumulation of nitrite was reproducible in different batches in the duplicate reactors (Figure 2.2). Nitrous oxide also accumulated in the recycle bottle headspace, with a peak accumulation of 1% of the initial nitrogen added as nitrate (Figure 2.1A). Previous studies have reported nitrous oxide accumulation of ~0.025 % to 70 % of the initial nitrogen added. (Desloover et al., 2011; Van Doan et al., 2013; Virdis et al., 2008) It should be noted that at the end of each batch cycle denitrification was complete and the average denitrification rate was 5.8 ± 0.4 g-N/(m^3-d). The cathode potential during the various stages of denitrification was also monitored. It decreased from -0.014 ±0.007 V vs SHE during nitrate reduction to -0.038 ± 0.004 V vs SHE during nitrite reduction.

Once nitrite was depleted, the cathode potential dropped to – 0.254 ± 0.007 V vs SHE (Figure 2.1B).

Volumetric power density (W/m^3) also followed a similar trend decreasing during the different stages of the denitrification. Polarization curves were performed at different stages of a single batch cycle. A curve was obtained when nitrate was the primary dissolved form of nitrogen and primary available acceptor (at 5 hours), when nitrite was the primary electron acceptor available (at 45 hours) and when nitrous oxide was the remaining available electron acceptor (at 70 hours) (Figure 2.3). The maximum power production during nitrite reduction (0.97 ± 0,21 W/m^3-total cathode volume (TCV)) only achieved 64% of the maximum power produced during nitrate reduction (1.51±0.29 W/m^3-TCV). Very little power production was observed during nitrous oxide reduction (0.03 ± 0.005 W/m^3-TCV). This suggests that the predominant reduction pathway in the cathode can dictate the power production in an MFC and influence the system's ability to achieve treatment goals. The electron equivalents recovered from the cathode during denitrification averaged 94.9 ± 3.9%.

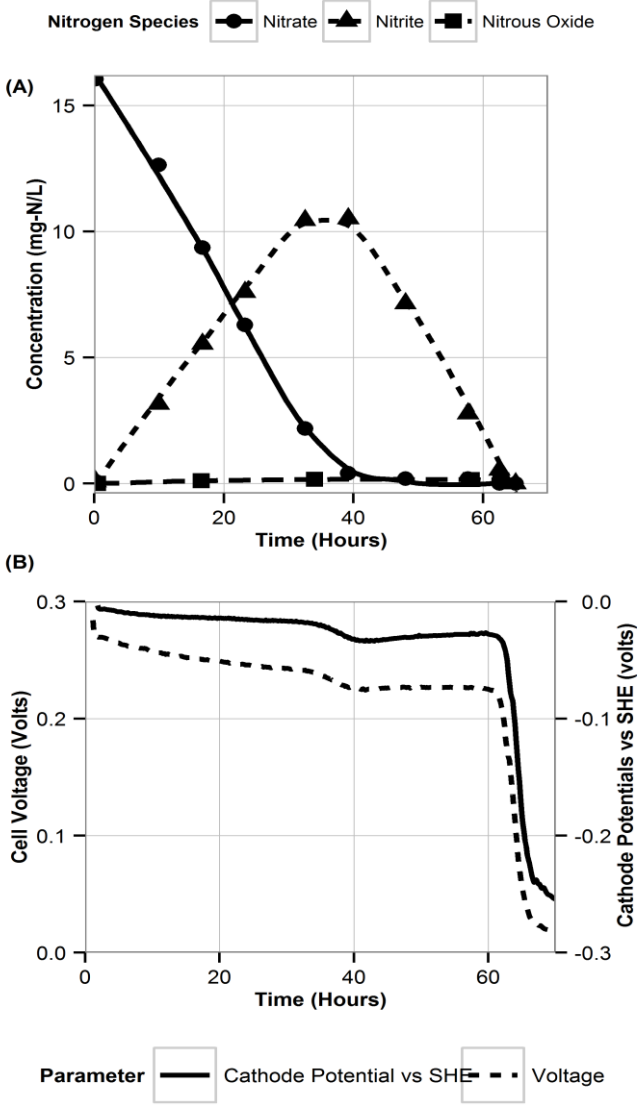

Figure 2.1: A typical batch cycle observation during denitrification. The lines are there only for highlighting trends and are not representative of model simulations.

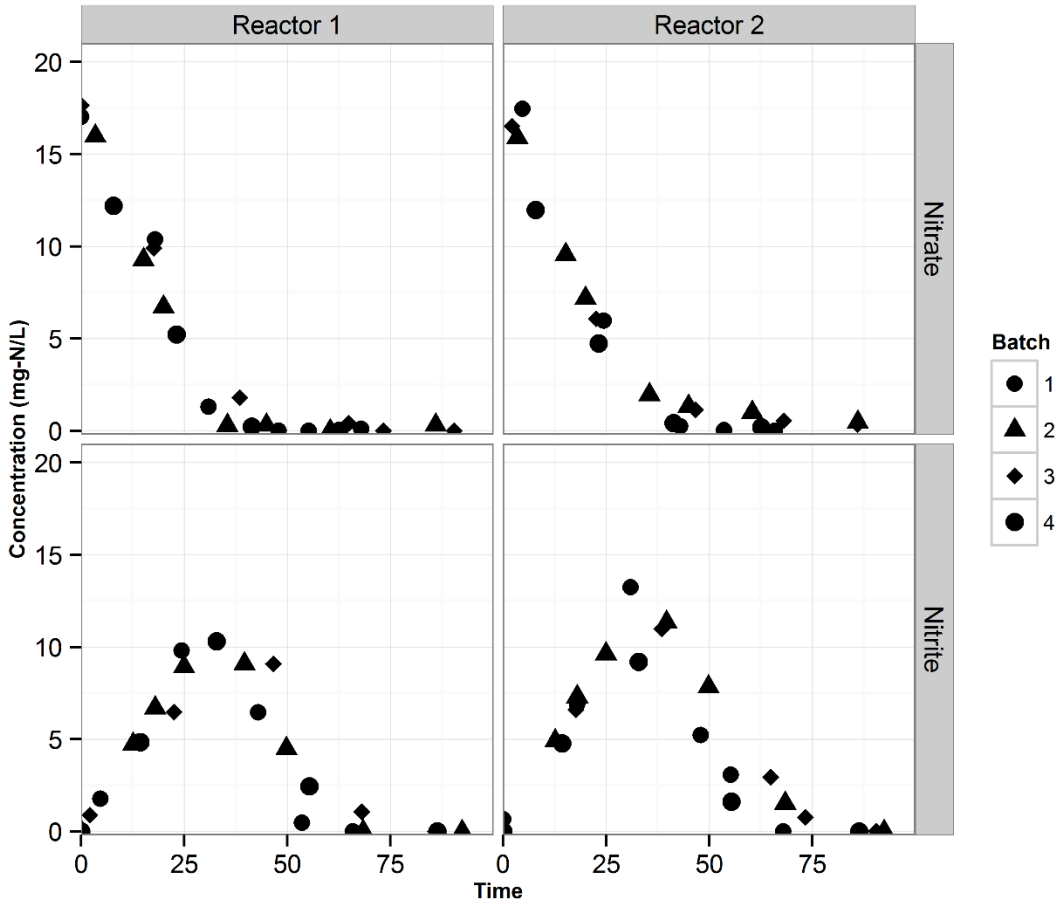

Figure 2.2: Batch Denitrification data during Steady State Operation for Reactor 1 and Reactor 2.

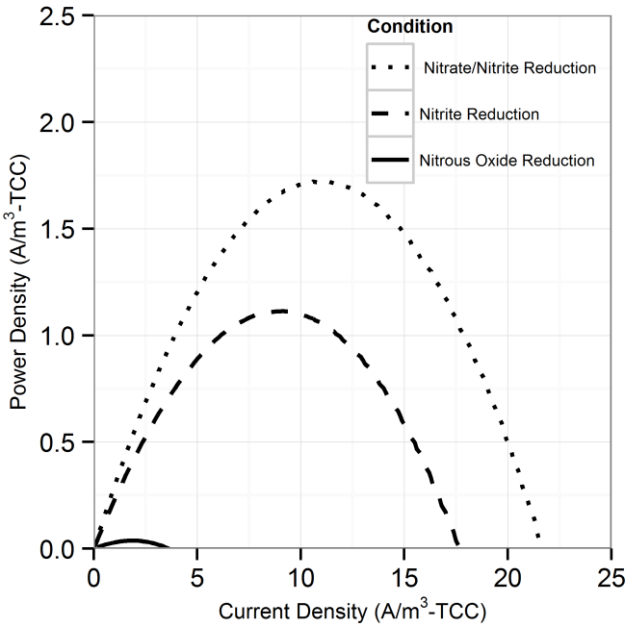

Figure 2.3: Polarization curves performed during different stages of denitrification

2.3.2 Inhibition of Nitrite Reduction by Environmental Factors

Inhibition of nitrite reduction can be caused by several factors such as insufficient electron donor, insufficient carbon source, presence of dissolved oxygen and high or low pH (Knowles, 1982; Körner and Zumft, 1989; Zhou et al., 2011). To determine if insufficient electron donor was a limiting factor causing accumulation of nitrite, the acetate feed in the anode was increased from 154 mg-COD/L.day to 770 mg-COD/L.day (Table 2.1, E4). Despite the increase in the electron donor loading rate, peak nitrite accumulation of 66.2 % of the total nitrogen added was observed.

Oxygen inhibition was also considered. Unanticipated oxygen diffusion occurring through the fittings or tubing could have compromised anoxic conditions. In addition to the initial N_2 purge, the feed was continuously sparged with nitrogen gas over the course of a batch cycle to maintain anoxic conditions (Table 2.1, E5). A peak nitrite

accumulation of 62.7 % of the total nitrogen added was observed, similar to cycles without a nitrogen-purge. Insufficient carbon source was considered as a possible cause of nitrite accumulation, so the cathode media was supplemented with bicarbonate (Table 2.1, E6). A peak nitrite accumulation of 77.5 % of the total nitrogen was measured. Cathode media with pHs of 6.6, 7.0, and 7.4 were fed to the cathode and the nitrite reduction rate was monitored (Table 2.1, E7-E9). No significant changes were observed. Changing the environmental conditions to overcome potential denitrification inhibition did not change nitrite accumulation in batch cycles of the cathode.

2.3.3 Modeling Denitrification

Modeling denitrification can improve our understanding of the microbial processes and yield kinetic parameters, which can be useful in designing denitrifying biocathode MFCs. When it was observed that various environmental factors did not significantly affect the accumulation of nitrite in the cathode, it was hypothesized that the accumulation of nitrite was caused due to intracellular electron competition between the enzymes involved in the different steps of denitrification. The ASM-ICE model has been used previously to simulate accumulation of nitrite in suspended cultures and bioreactors. For a denitrifying biocathode, we integrated the Nernst-Monod model, to simulate electron transfer from the electrode to the denitrifying biofilm, into the ASM-ICE (ASM-NICE). ASM-NICE (

Table 2.2) was used to simulate the accumulation of nitrite in the biocathode using a genetic algorithm for estimation of parameters. A Nernst-Monod current-potential dependency was observed with a mid-point potential (E_{kC}) of -0.13 V. A mid-point potential of -0.18 V has been previously reported for a denitrifying biocathode (Gregoire et al., 2014). It has been previously shown, for bioanodes, that a number of factors, including the source of the inoculum, can influence the value of the mid-point potential (Miceli et al., 2012).

The kinetic parameters were estimated by calibrating the model to two datasets: the typical batch data (Table 2.1, E2) and nitrite-only data (Table 2.1, E3). All the estimated parameter values (Table 2.3) are in the range of reported values in literature (Pan et al., 2015, 2013). It should be noted that since this is the first study to report kinetic rate constants using ASM-NICE, a direct comparison could not be made. K_{MredNA} and K_{MredNI} are affinity constants of the nitrate and nitrite reductase enzymes for the reduced mediator, M_{red}. The lower the value of these constants, the higher the affinity of the enzyme is to the reduced carrier. The value for K_{MredNI} for nitrite reduction is lower than that for K_{MredNA} for nitrate reduction, indicating that nitrite reduction has a higher capability to compete for electrons when the electron donor is limiting. Since current from the anode remained relatively constant and the concentration of nitrate was high during the initial stages of the batch, nitrate reduction consistently preceded nitrite reduction. Model fits from calibration (Figure 2.4 and Figure 2.6) for two different experimental scenarios (E2 and E3) show good agreement with observed data. Model validation was performed with duplicate batch data (E1) from duplicate reactors. The

results of the model validation (Figure 2.5) suggest that the ASM-NICE model for the biocathode is able to simulate the autotrophic denitrification process using the cathode as the electron donor reasonably well (Figure 2.7). By validating the model with data from two separate MFCs, the validity of the model and the estimated kinetic parameters are

demonstrated for different reactors acclimated under similar conditions. Denitrification using a biocathode has been widely used since nitrate has a relative metabolic potential close to that of oxygen ($E°_{NO3-}$=0.74 V vs SHE, $E°_{O2}$=0.9 V vs SHE). Using nitrate instead of oxygen eliminates oxygen diffusion across to the anode and thus a source of loss in coulombic efficiencies in MFCs (Butler and Nerenberg, 2010).

Table 2.3: Kinetic Parameters for Denitrification in a MFC Biocathode (a-this study, b- Experimentally measured, c- Assumed based on Pan et al. 2013, d- Assumed value from Claus and Kutzner (1985))

Parameter	Source	Value	Parameter	Source	Value
$\mathbf{r_{NA\_max}}$ (mg-N/gVSS•h)	a	1.68	j_{max} (A/m2)	b	-0.31
$\mathbf{K_{NI}}$ (mg-N/L)	a	0.56	E_{Kc} (V)	b	-0.13
$\mathbf{r_{NI\_max}}$ (mg-N/gVSS•h)	a	0.45	C_{tot} (mmol/gVSS)	c	0.01
$\mathbf{K_{mredNA}}$ (mmol/gVSS)	a	0.012	K_{Mox} (mmol/gVSS)	c	0.0001
$\mathbf{K_{mredNI}}$ (mmol/gVSS)	a	0.002	K_{NA} (mg-N/L)	d	0.0448

Xf (g-VSS)	b	0.641

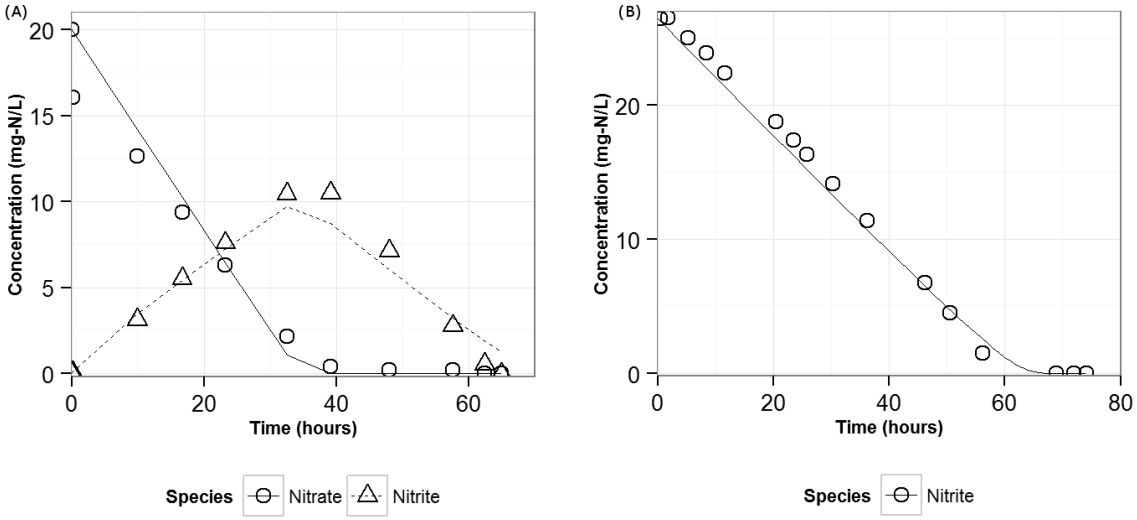

Figure 2.4: Measured (points) and Predicted (lines) Concentrations of Nitrate and Nitrite using ASM-NICE for the calibration Dataset- A) E2 B) E3.

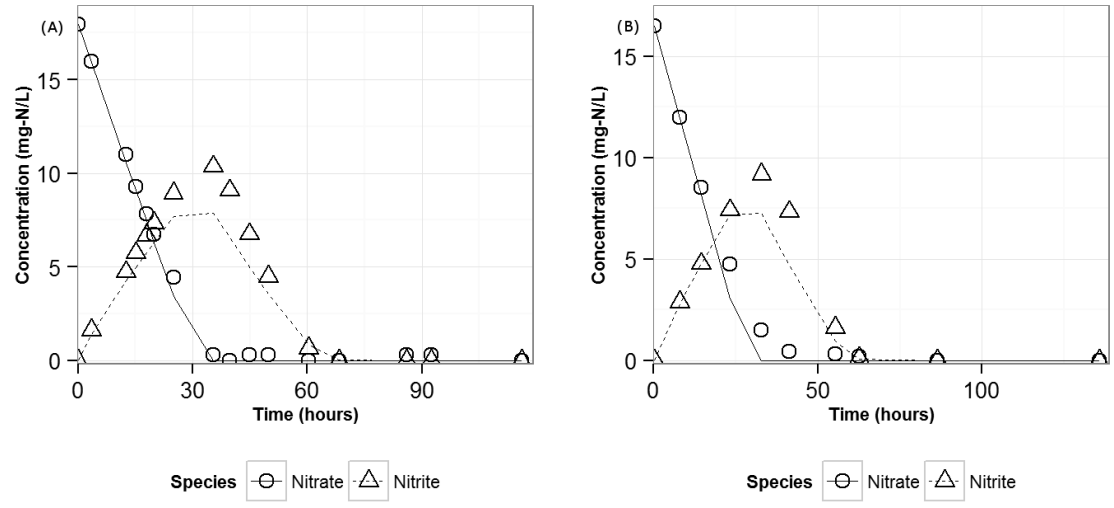

Figure 2.5: Measured (points) and Predicted (lines) Concentrations of Nitrate and Nitrite using ASM-NICE for the validation dataset (A) Reactor 1 (B) Reactor 2.

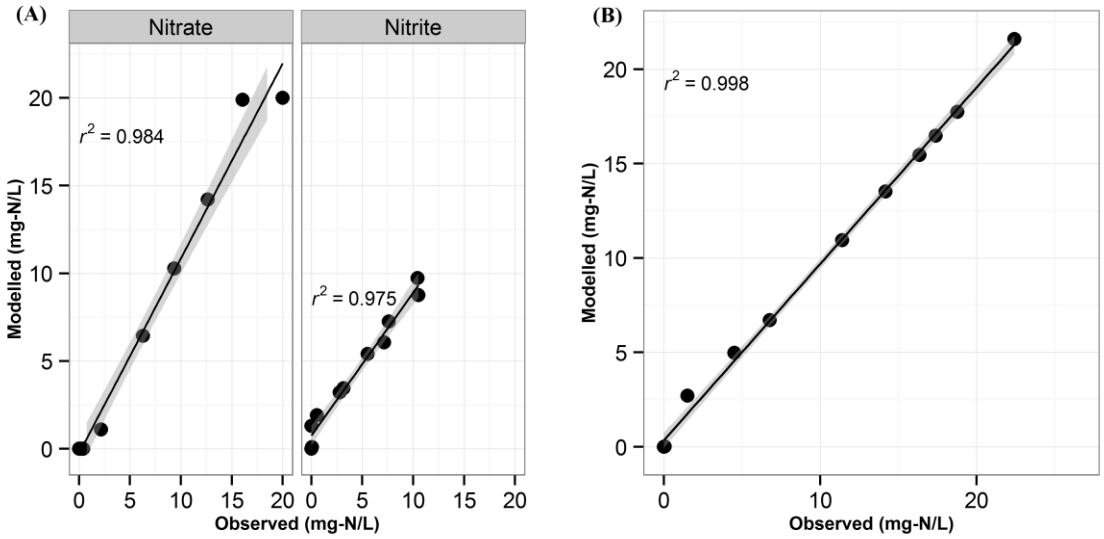

Figure 2.6: Modelled vs Observed Plots with R2 values for Calibration Datasets (A) Typical Batch- 20 mg NO3--N/L (E2) (B) Nitrite-Only 30 mg NO2--N/L (E3). The shaded areas represent confidence intervals for the trendline.

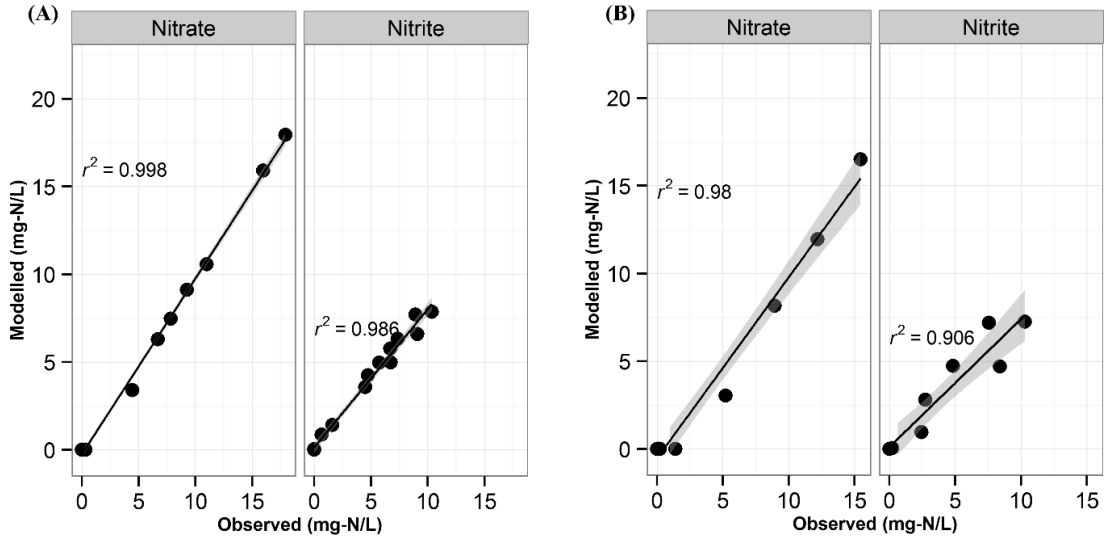

Figure 2.7: Modelled vs Observed Plots with R2 values for Validation Datasets (A) MFC Reactor-1 (b) MFC Reactor-2. The shaded areas represent confidence intervals for the trendline.

In this study, we calibrated and modeled denitrification in a biocathode using ASM-NICE. Such an integrated model has not been presented before to the best of our knowledge. The modeling suggested that when nitrate is at higher concentrations than nitrite, the reduction of nitrite is retarded by the competition for intracellular electron mediators. This would suggest that, when designing continuous-flow biocathodes for nitrate-nitrogen removal, longer hydraulic retention times (HRTs) could resolve the nitrite accumulation. A preliminary sensitivity analysis of the model to the kinetic parameters (K_{NI}, K_{Mox}, K_{NA}, E_{kC}, j_{max}) revealed that these parameters did not have a significant effect on the accumulation of nitrite (data not shown). However, the model showed significant sensitivity to K_{MredNI} and K_{MredNA} (Figure 2.8 and Figure 2.9). Briefly, an increase in K_{MredNI} caused the accumulation of nitrite to increase and vice versa. However, reduction of nitrate was not affected. A change in K_{MredNA} affected both nitrate

and nitrite reduction since nitrite is formed from the reduction of nitrate. K_{MredNA} and K_{MredNI} are properties of nitrate and nitrite reductase enzymes respectively. The developed model is also able to simulate nitrate and nitrite concentration profiles in a denitrifying biocathode, yielding kinetic parameters (K_{NI}, r_{NA_max}, r_{NI_max}, K_{MredNA}, K_{MredNI}) that can be used for process design.

2.4 Conclusions

This study focused on the dynamics of denitrification in a MFC biocathode, with respect to the accumulation of nitrite before complete denitrification was observed. It was also observed that the power production during nitrate-nitrite reduction was higher compared to that during nitrite reduction. Improvement or control of environmental parameters that affect denitrification pathways did not affect the amount of nitrite accumulation. Denitrification in the biocathode was modeled using ASM-NICE to simulate the use of the cathode electrode as the electron donor. Calibration of the model yielded kinetic parameters (K_{NI}, r_{NA_max}, r_{NI_max}, K_{MredNA}, K_{MredNI}), which could be used for prediction of the performance of a biocathode. The model will serve as a platform for future research into biocathodes and optimization of their performance. The use of this new model to simulate denitrifying biocathodes under various experimental conditions could yield important information for translating lab-scale studies to pilot scale and full-scale treatment systems. Furthermore, experimental work is needed to determine the specific microorganisms performing autotrophic denitrification in a biocathode and the influence of E_{Kc} on their performance.

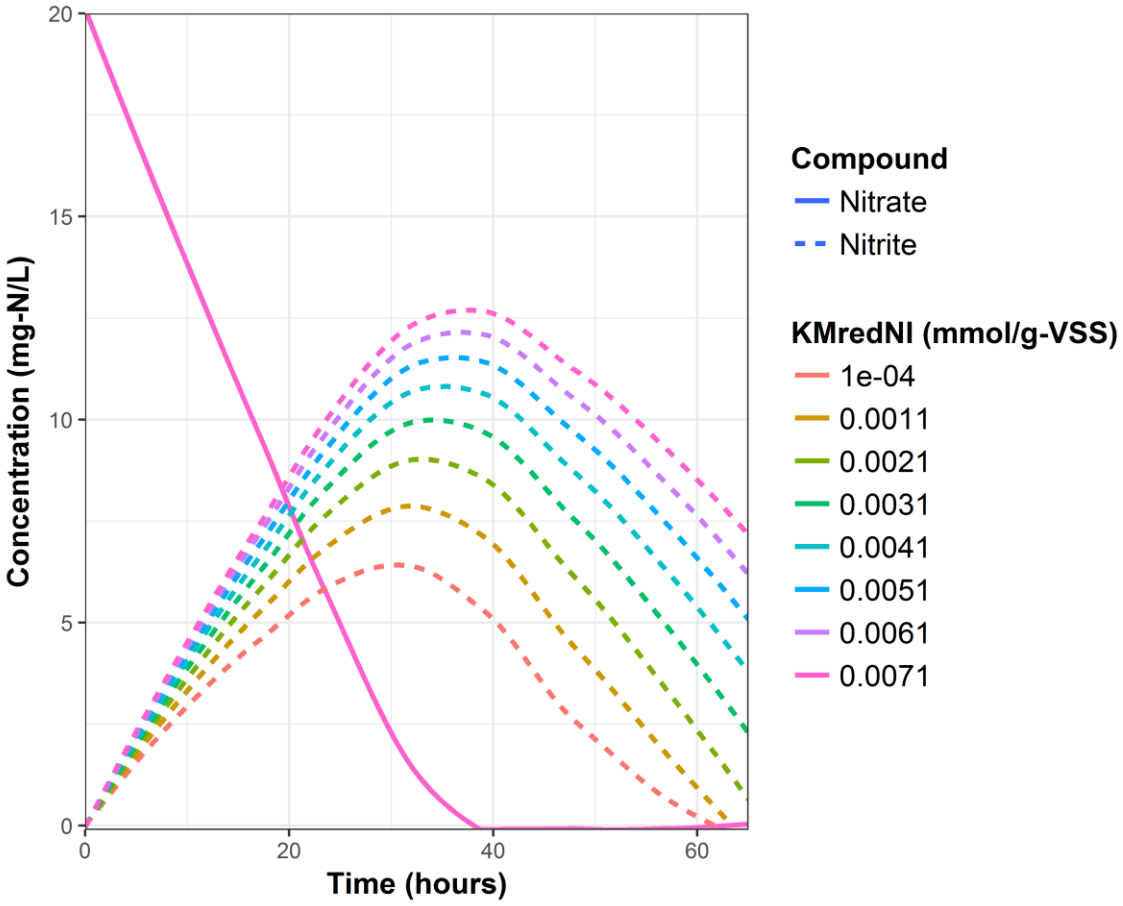

Figure 2.8: Sensitivity of the model to K_{mredNI}.

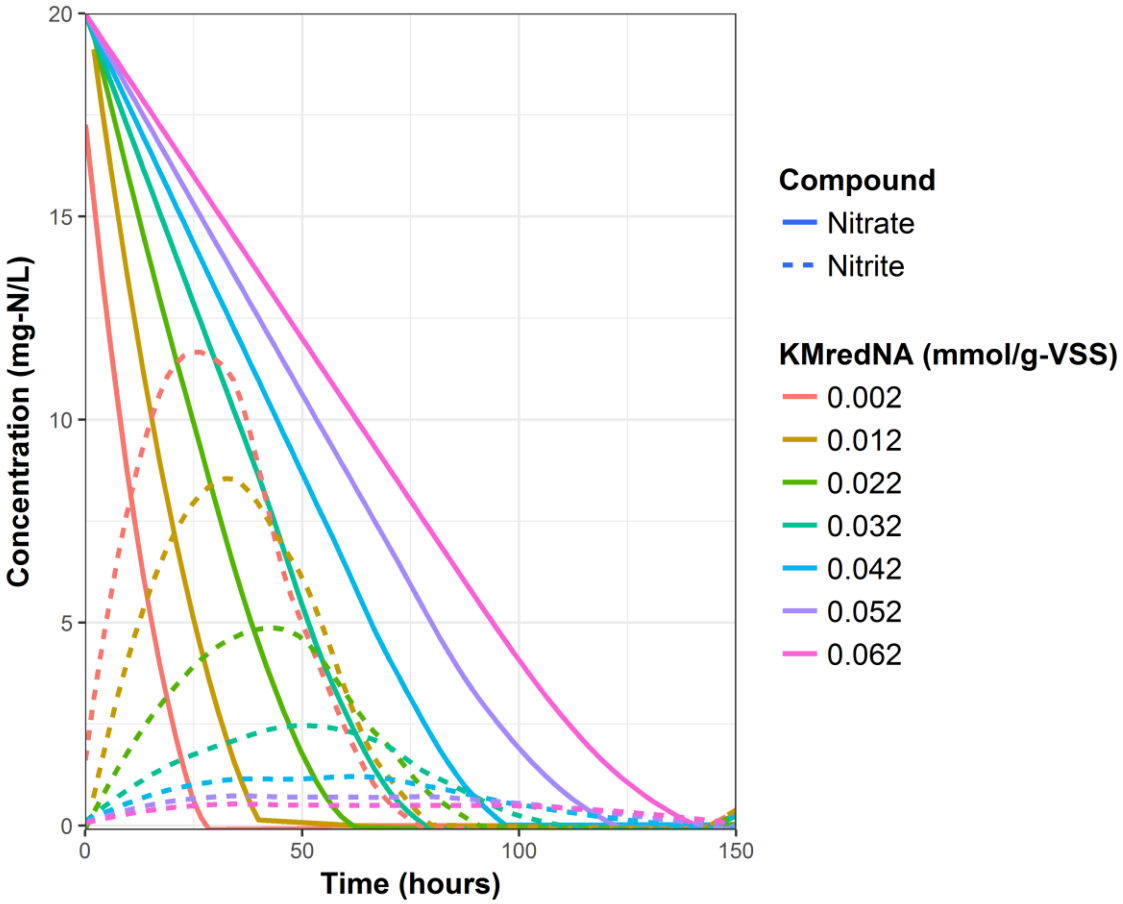

Figure 2.9: Sensitivity of the model to K_{mredNA}.

CHAPTER 3

ECOLOGICAL AND TRANSCRIPTIONAL RESPONSES OF ANODE-RESPIRING COMMUNITIES TO NITRATE IN A MICROBIAL FUEL CELL

Modified from originally submitted version (Srinivasan, V and Butler, C. Ecological and Transcriptional Responses of Anode-Respiring Communities to Nitrate in a Microbial Fuel Cell. Environmental Science & Technology. In Review)

3.1 Introduction

Bioelectrochemical systems (BESs) are a promising technology due to their ability to treat organic waste, decouple the electron donor and electron acceptor reactions and potential to produce an energetic product. BESs have great potential in applications as a mixed-culture bioprocess. However, before wide scale application, the robustness and resilience of anodic communities to environmental conditions have to be evaluated. In order to implement BESs in natural and engineering settings, there is a need for understanding the response of the anode-respiring communities to perturbations. Perturbations can have long term or short term effects which can adversely influence the performance of the biofilm and the technology.

For example, oxygen crossover from the cathode of a microbial fuel cell (MFC) to the anode can cause a decrease in coulombic efficiencies (CEs) and lead to the growth of aerobic microorganisms in the anode which can outcompete anode-respiring bacteria (ARB) (Butler and Nerenberg, 2010; Rinaldi et al., 2008). Similarly, the presence of methanogenic communities can lead to decrease in CEs in MFCs or hydrogen yield in

microbial electrolysis cells (MECs) (Jung and Regan, 2011; Lee et al., 2008; Parameswaran et al., 2009; Torres et al., 2007). ARB can also have alternate metabolisms such as nitrate, sulfate or ferric respiration capabilities that can serve as competing metabolisms (Aklujkar et al., 2009; Caccavo et al., 1994; Kashima and Regan, 2015). In a mixed community, where both non-ARB and ARB exist, the primary response to induction of competition is unknown. An understanding of the response of the biofilm community to these perturbations can lead to a better design and optimization of this technology for scale-up and implementation.

Nitrate is a regulated drinking water and wastewater contaminant. The common presence of nitrate in environments, in which MFCs can be potentially be used, makes it a co-contaminant of interest. The effect of nitrate on anode-respiring biofilms is of great interest since many bacteria harbor nitrate reduction capabilities including ARB such as *Geobacter spp.*(Kashima and Regan, 2015; Martínez Murillo et al., 1999; van den Berg et al., 2015) *and Shewenella spp.* (Cruz-García et al., 2007; Yoon et al., 2015). The effect of nitrate on mixed community anode respiring biofilms has been previously studied by Sukkasem et al. (Sukkasem et al., 2008). CE was affected by the presence of nitrate in the anode while the maximum voltage output was not affected. Sukkasem et al. performed some preliminary investigation into the effect of nitrate on the microbial community using polymerase chain reaction (PCR)- denaturing gradient gel electrophoresis (DGGE). They postulated the existence of two distinct groups of bacteria, obligate ARB and facultative ARB capable of nitrate reduction. However, more quantitative investigations are required to understand the effect of nitrate on the biofilm community. The existence of facultative ARB capable of nitrate reduction has been documented by other studies (Kiely et al., 2010).

The effect of nitrate on electrode-respiring *Geobacter metallireducens* was studied by Kashima and Regan (Kashima and Regan, 2015). They observed that *G.metallireducens* biofilms reduced nitrate at a range of anode potentials. The critical nitrate concentration, at which a significant decrease in BES performance was observed, depended on the biofilm thickness. The use of nitrate as a competing electron acceptor by facultative ARBs was controlled by diffusional limitations in thicker biofilms.

The above studies have investigated the effect of nitrate on anode-respiring biofilms using batch reactors. BESs when implemented in natural or engineered settings will benefit from a chemostat based study for more relevance to treatment purposes. In a chemostat, there is continuous addition of the perturbing component (nitrate) to the MFC which could cause significant changes in the community structure. On the other hand, when the chemostat is completely mixed (CSTR), the concentration of nitrate in the MFC will be lower than in the influent and hence the impact of the perturbation could be mitigated. An understanding of the effects of nitrate on the microbial community and the resiliency of the communities to recover from such perturbations could play an important role when MFCs are used for bioremediation/wastewater treatment.

This study is focused on understanding the effect of nitrate, at three stoichiometrically relevant C/N ratios (1.8, 3.7 and 7.4 mg-C/mg-N), on anode in mixed culture MFCs with an abiotic cathode. We hypothesize that at high C/N ratios (electron donor non-limiting), the presence of nitrate will not affect the electrochemical performance of the MFC and will enhance the removal of organic matter while electron-donor limiting conditions will negatively affect the electrochemical performance of the MFC. We also hypothesize that the presence of nitrate in the bulk solution at low C/N ratios will cause significant changes

in the biofilm community leading to decrease in the relative abundance of anode-respiring bacteria with time. We use a combination of 16S rRNA gene sequencing and transcriptional profiling using reverse transcription-quantitative PCR to study the community response over time to a continuous flux of nitrate.

3.2 Materials and Methods

3.2.1 MFC Design and Operation.

Dual chamber H-type MFCs with a cation exchange membrane (CMI-7000, Membrane International Inc., Glen Rock) were used for all the experiments. Graphite cloth coupons (2.2 x 11 x 0.32 cm) was used as electrodes with 5 electrode coupons in each chamber. Marine grade wire (Vertex Marine) was used to make all the electrical connections. An Ag/AgCl reference electrode (RE-6, BASi Inc. USA) was placed in each of the anode chambers to measure the anode potential.

The anode chambers were inoculated with primary effluent from the Amherst Wastewater Treatment Plant, Amherst MA and acclimated in recycle batch with an external resistance of 1500 Ω. The MFCs were inoculated with a 10:90 (by volume) mixture of inoculum and a phosphate-buffered minimal growth medium with acetate. The medium to the anode consisted of 1.66 g/L potassium acetate in 16 mM phosphate buffer (1.386 g/L Na_2HPO_4 and 0.849 g/L KH_2PO_4) with 0.05 g/L NH_4Cl, 0.08 g/L $MgCl_2$, 1 mL/L each of a trace mineral solution (per litre-100 µg $ZnSO_4 \cdot 7H_2O$, 30 µg $MnCl_2 \cdot 4H_2O$, 300 µg H_3BO_3, 200 µg $CoCl_2 \cdot 6H_2O$, 10 µg $CuCl_2 \cdot 2H_2O$, 10 µg $NiCl_2 \cdot 6H_2O$, 30 µg $Na_2MoO_4 \cdot 2H_2O$, and 30 µg Na_2SeO_3 and Ca-Fe solution (per litre-1 mg $CaCl_2 \cdot 2H_2O$, 1 mg $FeSO_4 \cdot 7H_2O$) and a calcium-iron solution (per litre-1 mg $CaCl_2 \cdot 2H_2O$, 1 mg $FeSO_4 \cdot 7H_2O$). The feed was sparged with filter-sterilized N_2 gas for at least 45 minutes

prior to addition to the reactor. The feed solution was replaced when the voltage dropped below 0.05 V during the acclimation phase. The MFCs were operated in batch mode until reproducible maximum voltages were obtained for two successive batches. The MFCs were then switched to chemostat-mode at a flow rate of 0.21 mL/min (HRT=20 hours). The anode chamber was sparged continuously with filter-sterilized N_2 gas to prevent oxygen diffusion into the anode and 2-bromoethanosulfonic acid (BES) was added at 3 mM to inhibit acetoclastic methanogenesis (Parameswaran et al., 2009; Zinder et al., 1984). All media was autoclaved. The anode chamber was continuously stirred throughout the experiment. The cathode contained 70 mM potassium ferricyanide in 80 mM phosphate buffer solution. All experiments were performed in duplicate.

3.2.2 Experimental Design.

The acetate concentration in the influent of the anode was decreased consecutively to determine $S_{critical}$ of acetate required for maximum coulombic efficiency (analogous to minimum substrate concentration required for growth) in each reactor. The $S_{cricitcal}$ for the anode of an MFC is defined (in this study) as the minimum acetate concentration that would produce the maximum voltage obtained during the end of the acclimation phase. The $S_{critical}$ has been shown to be important in other competition studies (Füchslin et al., 2012). The MFCs were run at each successively decreasing acetate concentration for >3 HRTs. Once $S_{critical}$ was determined (Table 3.1) and steady state conditions were achieved (Phase I), nitrate (as sodium nitrate) was introduced into the anode of the MFC at different C/N ratios with one of the reactors serving as a control (no nitrate). The C/N ratios used in this experiment were 1.8, 3.7 and

7.4 mg-C/mg-N (1.4, 2.8 and 5.7 meq e^--donor/meq e^- -NO_3^-). The different C/N ratios were tested in different MFC chemostats to avoid gradual adaptation of the community to nitrate (Figure 3.1). Nitrate was fed to the anode continuously for 43 days to study the long-term effect of nitrate on the anode-respiring biofilm (Phase II). Sodium chloride was added to normalize the conductivity of the media across different conditions. After 43 days, nitrate was removed from the influent to the anode and the MFC was operated without nitrate (Phase III) to test the resilience of the anode biofilms (Figure 3.2).

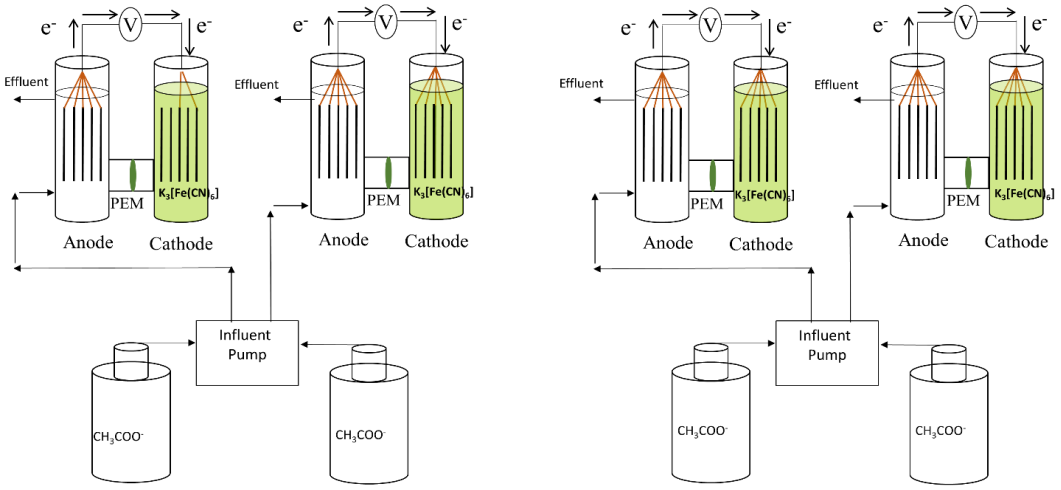

Figure 3.1: Reactor Schematics

Table 3.1:Acetate and Nitrate Concentrations in each Reactor

Reactor	Influent Concentration				C/N Ratio (mg-C/mg-N)	e^- eq-donor/e^- eq-NO_3^-
	Acetate		Nitrate			
	mM	mM e^-	mM	mM e^-		
Control	0.59	4.75	0	0	No nitrate	No nitrate
R1.84	0.59	4.75	0.66	3.32	1.8	1.42
R3.7	0.59	4.75	0.33	1.66	3.7	2.85
R7.4	0.59	4.75	0.17	0.83	7.4	5.69

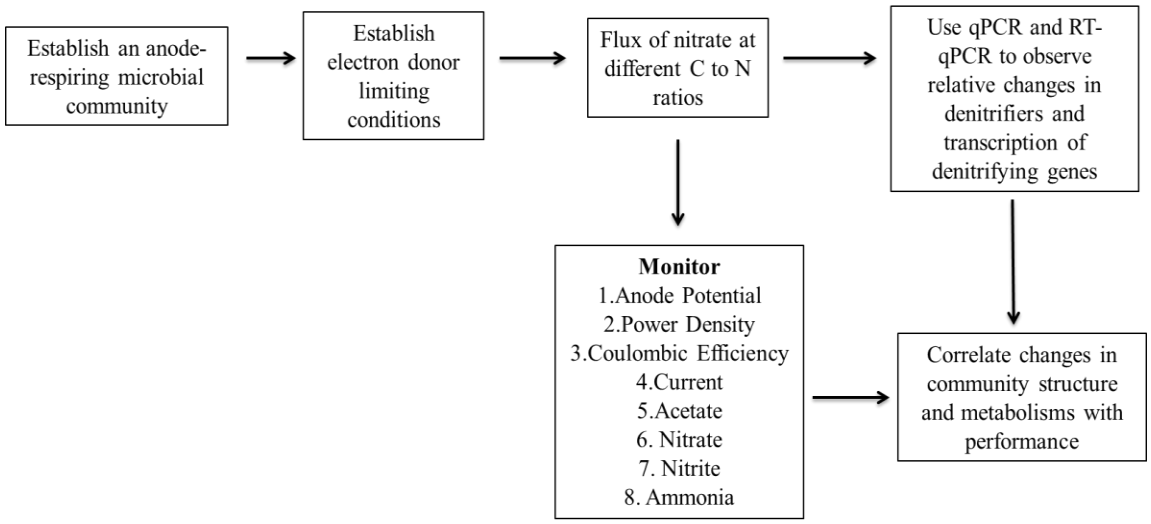

Figure 3.2 : Experimental Design

3.2.3 Measurements and Analyses.

Acetate was monitored in the influent and effluent of the anode using a Metrohm 850 Professional Ion Chromatograph (Metrohm Inc., Switzerland) with a Metrosep A Supp 5-250 Anion Column (Metrohm Inc., Switzerland) using an eluent consisting of 3.2 mM Na_2CO_3, 1.0 mM $NaHCO_3$. Samples were filtered using a 0.45 µm syringe filters and

stored at 4 °C before analysis. Nitrate, nitrite and ammonium were measured using HACH kits.

The voltage across an external resistance of 1500 Ω was monitored every 15 minutes using a Keithley Model 2700 Multimeter with a 7700 Switching Module (Keithley Instruments Inc., Cleveland, OH, USA). Current and power was calculated using Ohm's law (P=IV) and normalized by the anode surface area or the anode liquid volume (280 mL). Polarization curves were performed using a Gamry Series G750 Potentionstat/Galvanostat/ZRA (Gamry, USA). The voltage sweep was applied at a rate of 1 mV/s. Coulombic efficiency (CE) was calculated using the following equation:

$$CE = \frac{M_{ac} * I}{b_{ac} F q \Delta c} \qquad \textbf{Equation 3.1}$$

where I is the current (ampere or C/s), F is the Faraday's constant (96500 C/mol), q is the flow rate at which the influent is delivered, Δc is the difference in concentration in the influent and the effluent, b_{ac} is the moles of electrons/ mole of acetate (8 mol of electrons/mol of acetate) and M_{ac} is the molecular weight of acetate (59 g/mole).

3.2.4 Biofilm Sampling and DNA Extraction.

Anode electrode samples were collected at various stages of the experiment. A total of six electrode samples were collected with one before the nitrate flux (Day 0), two during the nitrate flux (Day 20 and 43) and one at the end of the study after the nitrate flux was removed (Day 56). For the sampling, one piece of each electrode (0.44 x 2.2 x 0.32 cm, total 5 pieces) was cut under sterile conditions using a sterile razor and preserved using LifeGuard™ Soil Preservation Solution (Mo Bio Laboratories Inc.) and stored at -20 °C

until extraction. Each piece was cut from each electrode (Total 5 electrode-5 pieces) to account for spatial variation in microbial community structure.

RNA and DNA were extracted from the electrode samples using the RNA Power Soil Cut (Mo Bio Laboratories Inc.) with a DNA Elution Accessory Kit (Mo Bio Laboratories Inc.). The extracted RNA was then treated with DNase Max Kit (Mo Bio Laboratories Inc.) to remove DNA contamination. The extracted DNA and RNA were then quantified with a spectrophotometer (NanoDrop, ND-100, NanoDrop Technologies, Wilmington, DE). mRNA was then converted into cDNA using the High Capacity cDNA Reverse Transcription Kit (Life Technologies) and stored at -20 °C.

3.2.5 Quantitative PCR.

The activity of denitrifying genes was assessed using nitrite-reductase specific primers for *nirK* and *nirS*. The *nirK* activity was assessed using nirK876 and nirK1040 (Henry et al., 2004). *nirS* activitiy was assessed using nirSCd3af and nirSR3cd (Kandeler et al., 2006; Throbäck et al., 2004). Bioelectrochemical activity was assessed using *Geobacter spp.* as model ARBs. The activity of *Geobacter spp.* was measured using *Geobacter* specific primers Geo564F and Geo840R (Himmelheber et al., 2009). For performing relative quantification, 16SrRNA gene was used as the reference transcript. The primer pair used for 16SrRNA gene quantification was 1114f and 1275r (Table 3.2) (Christophersen et al., 2011). Amplification of cDNA templates was carried out using a StepOne™ Real-Time PCR System (Applied Biosystems) using SYBR Green as a detection system. Reaction mixture consisted of 25 µL containing: 0.2 µM of each primer, 12.5 µL of SYBR Green PCR master mix including Hot-Start iTaq DNA Polymerase, dNTPs, $MgCl_2$, SYBR® Green I dye and ROX (Life Technologies), 5 µL of the template cDNA corresponding to

10 ng of total DNA and RNase-free water to make up to 25 µL volume. The real-time PCR conditions for the amplification of nirK and nirS genes were 600 s at 95 °C, 6 touchdown cycles: 15 s at 95 °C for denaturation, 30 s at 63 °C for annealing, 30 s at 72 °C for extension and 15 s at 80 °C for a final data acquisition step. The annealing temperature was progressively decreased by 1 °C down to 58 °C. Finally, a last cycle with an annealing temperature of 58 °C was repeated 40 times. One last step from 60 to 95 °C with an increase of 0.3 °C/s was added to obtain a melt curve. The real-time PCR conditions for the amplification of 16SrDNA gene was 600 s at 95 °C followed by 40 cycles: 15 s at 95 °C for denaturation, 60 s at 60 °C for annealing. One last step from 60 to 95 °C with an increase of 0.3 °C/s was added to obtain a melt curve. The reactions for each target were performed separately. Triplicate wells were run for each sample for each gene target. Standard curves, melting curves and negative controls were run for each qPCR run.

Table 3.2: Primer Sequences

Primer	Sequence
nirK 876	5’-ATYGGCGGVAYGGCGA-3’
nirK 1040	5’-GCCTCGATCAGRTTRTGGTT-3’
nirSR3cd	5’-GASTTCGGRTGSGTCTTSAYGAA-3’
nirSCd3af	5’-AACGYSAAGGARACSGG-3’
Geo564F	5’-CAAGTCGTACGAGAAACATATC-3’
Geo840R	5’-GAAGAGGATCGTCTTTCCACGA-3’
1114f	5’-CGGCAACGAGCGCAACCC-3’
1275r	5’-CCATTGTAGCACGTGTGTAGCC-3’

3.2.6 Illumina MiSeq Sequencing and Analysis.

The extracted DNA was sent to Research and Testing Facility (Lubbock, TX) for PCR amplification and sequencing targeting the V3-V4 region using the primers 338aF (5'-ACTCCTACGGGAGGCAGCAG-3') and 785R (5'-GACTACHVGGGTATCTAATCC-3') and the amplicons were sequenced on the Illumina MiSeq platform using V3 chemistry. The raw Fastq files were cleaned using Sickle 1.33 (Joshi and Fass, 2011) with a minimum window quality score of 20. The quality-controlled sequences were analyzed using mothur(Schloss et al., 2009) using the protocol described in Kozich et al (Kozich et al., 2013). The sequences were trimmed to remove primers and barcodes, quality filtered using sickle v1.33 (Joshi and Fass, 2011) with a minimum quality score of 20, assembled in mothur and aligned to SILVA 123 database. The alignment was screened to remove poorly aligned sequences using vertical = T and trump = . options in mothur. Chimeras were remove using the UCHIME algorithm available through mothur and clustered into OTUs at sequence similarity cutoff of 97% using the average neighbor clustering algorithm. The sequences were classified using the Naïve Bayesian Classifier (80% confidence threshold) using the RDP training set and consensus taxonomy of OTUs was determined using the 80% cutoff.

3.2.7 Statistical Analyses.

The anode potential, coulombic efficiency and acetate removal data were split into three phases: before nitrate flux, during nitrate flux (Day 0 to Day 43) and nitrate removed (days 44 to 60). Statistical analysis comparing the three phases within each treatment was performed using 1-way analysis of variance (ANOVA) followed by a Tukey's Honestly

Significant Difference (HSD). The HSD results are reported only if the 1-way ANOVA showed a significant effect.

The normalized (using 16S rRNA transcripts as reference) relative quantities of gene transcripts (Rq_{target}) were calculated for each target transcript and logarithmic (base 2) fold change values between sampling day (t) and the start of nitrate flux (Day 0) as follows:

$$\log_2(\text{Fold Change}) = \frac{Rq^{t}_{target}}{Rq^{0}_{target}} \qquad \textbf{Equation 3.2}$$

Statistical analysis of the fold change values within each C/N ratio treatment condition was performed using 1-way ANOVA using sampling day as the main effect. Significant interaction effects were further determined with Tukey's HSD test. All sequencing data was rarefied (8038 sequences which is equal to the minimum number of sequences across all samples) to ensure equal number of sequences in each sample prior to all analyses. Mothur was used to construct phylogenetic trees and calculate UniFrac (Lozupone and Knight, 2005) weighted metrics for the different samples. Non-metric multidimensional scaling (NMDS) analysis using the UniFrac weighted metric was performed in R (R Core Team, 2015) using the phyloseq (McMurdie and Holmes, 2013) package. Other R packages used in the analysis and plotting were ggplot2 (Wickham, 2009), vegan (Oksanen et al., 2016), dplyr (Wickham and Francois, 2016) and ampvis (Albertsen et al., 2015).

3.3 Results and Discussion

3.3.1 The electrochemical performance of the MFCs is adversely affected by nitrate at low C/N ratios

The MFCs were acclimated under optimal operating conditions with respect to power production and $S_{critical}$ for each reactor (0.59 mM) were determined (Phase I). Acetate removal was not complete during this period. When nitrate was introduced into the anode, complete removal of nitrate was observed in the effluent of the anode (based on no detection of nitrate in the effluent samples) across all the C/N ratios (data not shown). Neither nitrite nor ammonium were detected in the effluent during the period of nitrate flux. Acetate removal (Figure 3.3) increased significantly from 41.7 ± 9.4 % to 85.9 ± 10.6 % ($p<0.001$, 7.4 mg-C/mg-N), 64.9 ± 20.2 % to 98.9 ± 4.4 % ($p<0.001$, 3.7 mg-C/ mg-N) and 56.2 ± 9.4 % to 100 ± 0 % ($p<0.001$, 1.8 mg-C/mg-N). The increase in acetate removal efficiency suggests that the presence of nitrate is helpful in improving treatment efficiency which is a common issue with anaerobic wastewater treatment. Several anaerobic wastewater treatment technologies, including MFCs, require a post-treatment polishing step (usually aerobic) to improve effluent quality (Van Haandel et al., 2006; Zhang et al., 2013). In this case, the presence of nitrate in the anode of the MFC served as an inherent polishing step. Though not the emphasis of this study, if a sustainable balance between anode respiration and denitrification could be achieved, both carbon and nitrogen removal could be achieved along with ensuring complete chemical oxygen demand (COD) removal. The disadvantage of this type of a polishing step is that it could lead to loss in coulombic efficiency and hence loss in power production in an MFC due to loss of the electrons to nitrate reduction.

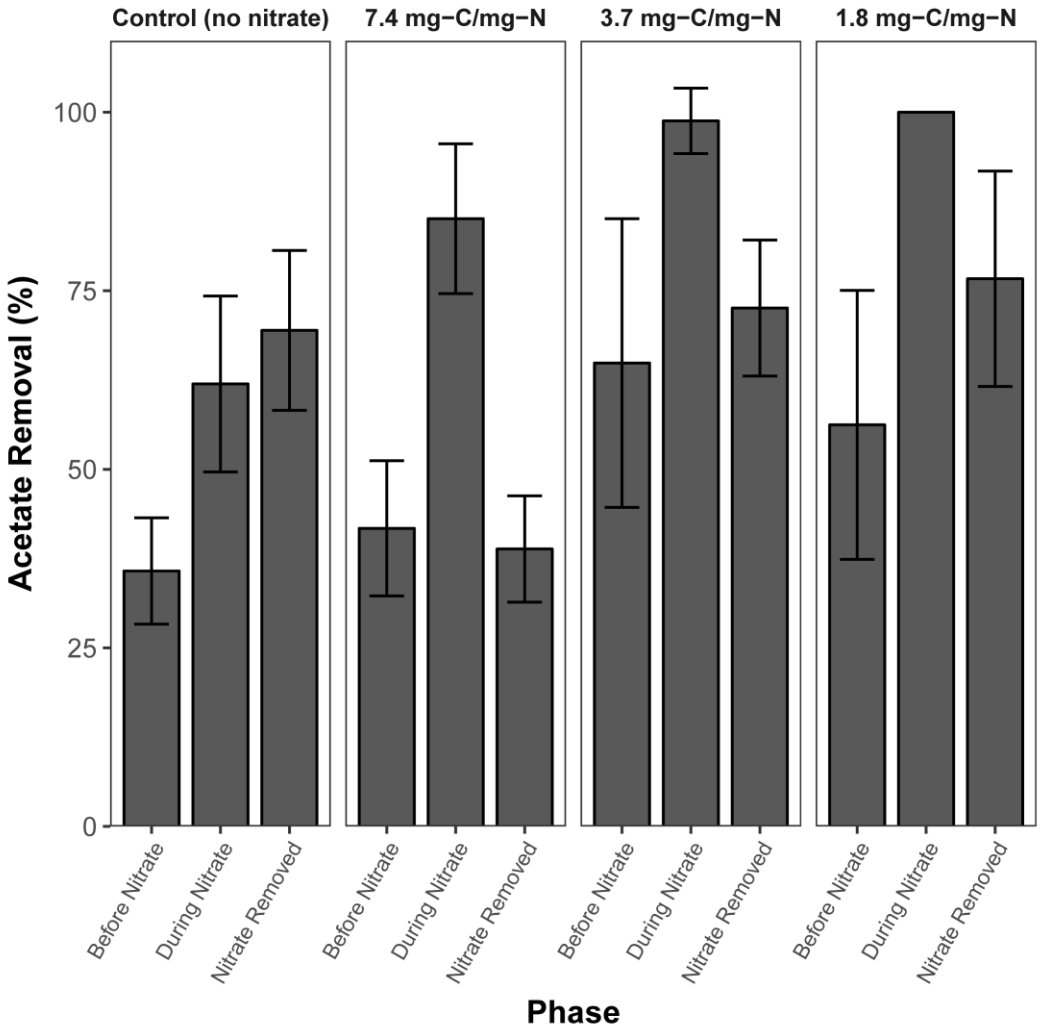

Figure 3.3: Mean Acetate removal during the different phases. Error bars represent standard deviations.

The electrochemical performance of the MFCs was assessed by calculating the coulombic efficiency (CE) which is the percentage of electrons recovered as current. The CE before the introduction of nitrate was 39.9 ± 2.4 % (Figure 3.4 & Figure 3.5). The CE did not change significantly when the electron donor was not limiting in the presence of nitrate at 7.4 mg-C/mg-N ($p= 0.09$). This would suggest that even though nitrate was present in the anode, there was no significant decrease in coulombic efficiency while a significant increase in treatment efficiency was observed as discussed above. The CE

decreased significantly when nitrate was introduced at 3.7 mg-C/mg-N ($p<0.001$) and 1.8 mg-C/mg-N ($p < 0.001$). The CE decreased to 10.9 % (3.7 mg-C/mg-N) and 0.5 % (1.8 mg-C/mg-N) after 43 days of nitrate flux. Nitrate in the influent accounted for 3.32 mM e^- (1.8 mg-C/mg-N) and 1.66 mM e^- (3.7 mg-C/mg-N). This is 69% and 35% of the electrons respectively that were in the influent in the form of acetate. Hence, when the electron donor was limiting, the competition for acetate resulted in a decrease in coulombic efficiency due to loss of electrons to denitrification. Stable anode performance was observed in the control (amended with sodium chloride) indicating that the decrease in CE was not due to factors such as change in solution conductivity or introduction of oxygen during biofilm sampling. When nitrate was removed from the influent after 43 days of nitrate flux, the CE of the reactors increased compared to that during nitrate flux across all experimental conditions. The CE was not significantly different between phase I and phase III for the reactor where nitrate was introduced at 7.4 mg-C/mg-N ($p=0.093$) and at 3.7 mg-C/mg-N ($p=0.35$). However, the CE for the reactor where nitrate was introduced at 1.8 mg-C/mg-N was significantly lower at 12.1 ± 11.1 % ($p<0.001$) in phase III compared to phase I. This suggests that the performance of the MFCs were resilient to nitrate fluxes when the anode was perturbed with nitrate at C/N ratios equal to or greater than 3.7 mg-C/mg-N while at lower C/N ratios, the performance might take longer to recover or not recover. When electron donor was extremely limiting in the presence of nitrate, the community structure of the anode-respiring biofilm could have been irreversibly affected and hence the coulombic efficiency did not recover in the short-term.

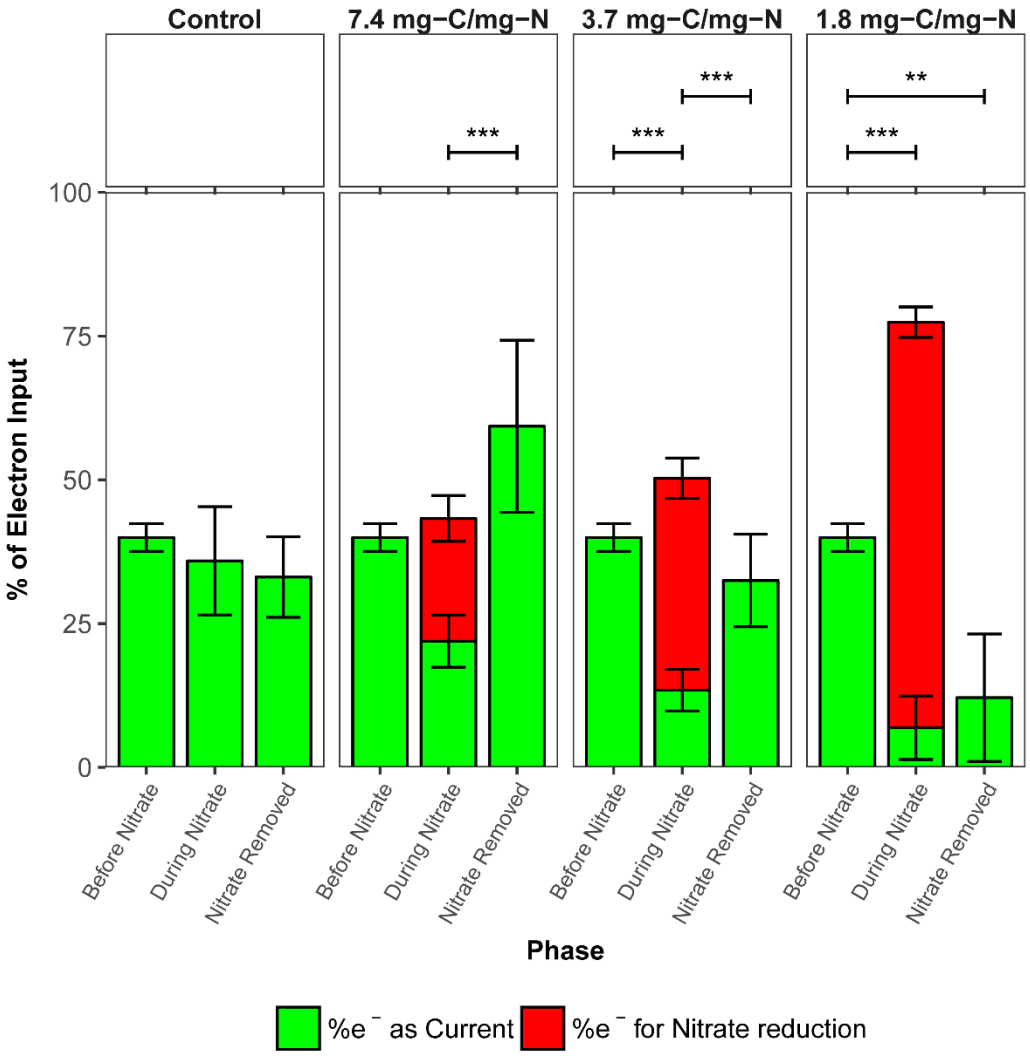

Figure 3.4: Electron Sinks in the Anode presented as average percentage of electron input (acetate removed) for each Phase. Error bars represent standard deviations. The %e- for nitrate reduction was calculated assuming complete denitrification and 5 e-/mole of nitrate reduced. The top panel indicate significance level of comparisons based on based on 1-Way ANOVA with a Two-Tailed post-hoc Tukey's HSD test. Asterisks indicate statistical significance (p<0.001-*, p<0.01-**, p<0.05-*)**

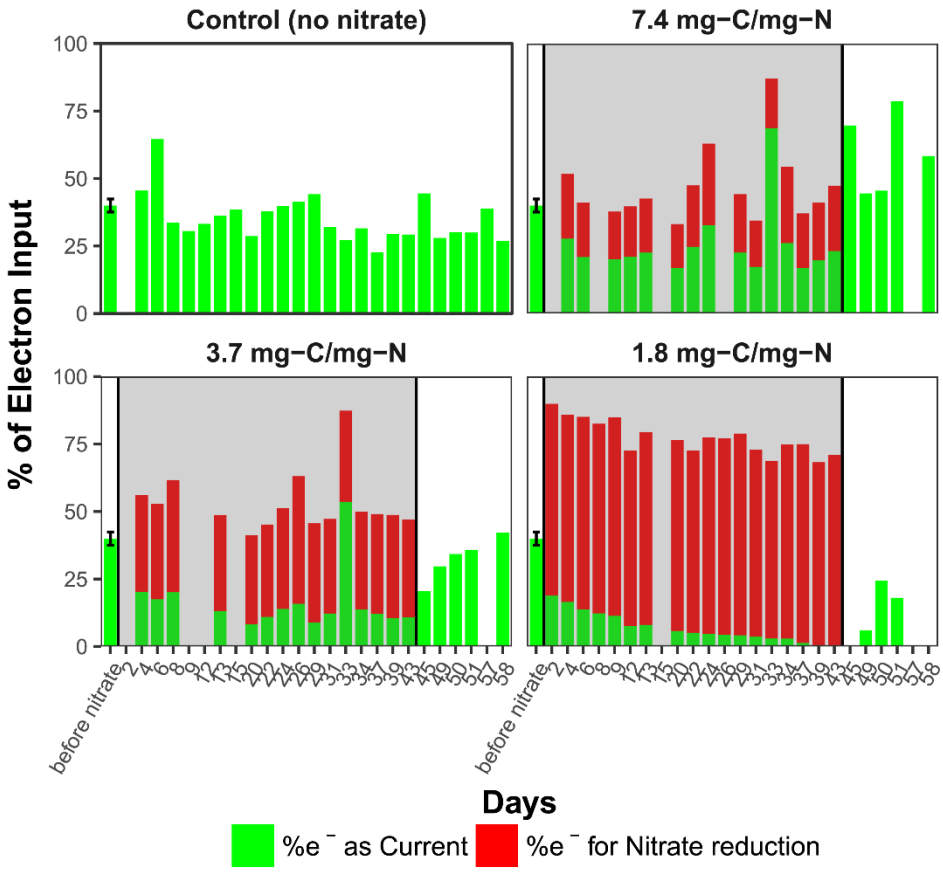

Figure 3.5: Electron Sinks in the Anode over time in each reactor. Periods of nitrate flux are represented by shaded areas.

3.3.2 Performance of the anode is resilient to nitrate fluxes at high C/N ratios.

To further elucidate the effect of nitrate on the anode of the MFC, the anode potential of the MFCs at different C/N ratios was examined. The average anode potential (±SD) before nitrate flux was introduced was -0.31 ± 0.01 V (vs SHE). When nitrate was added at a high C/N ratio of 7.4 mg-C/mg-N in the influent, there was no observable effect on the anode potential. However, when nitrate was added at 3.7 and 1.8 mg-C/mg-N, the anode potential increased to different steady state values (Figure 3.6). At 3.7 mg-C/mg-N, the anode potential increased to a final value of -0.06 ± 0.004 V (vs SHE) while it

increased to 0.28 ± 0.005 V (vs SHE) when nitrate was introduced at 1.8 mg-C/mg-N. Steady state values were defined as a constant anode potential for greater than 3 HRTs. When nitrate was removed from the influent of the treatment group, the anode potential returned to the original values before the nitrate flux. The anode potential influences both the metabolic pathway used for electron transfer and from a thermodynamic point of view, the theoretical energy gain from the electron transfer reaction (Torres et al., 2010). An increase in the anode potential can be indicative of electrons being deposited on alternative electron acceptors (AEAs), such as nitrate, and the increase is dependent on the concentration of the AEA as determined by the Nernst equation (Marcus et al., 2007; Torres et al., 2010). This is because the anode potential is essentially the redox potential in the anode environment and is dependent on the identity and concentration of the electron acceptor being used. Maximum power density (W/m^2), as measured using polarization curves, showed similar trends (Figure 3.7). The maximum power density decreased over time when nitrate was introduced at 3.7 and 1.8 mg-C/mg-N while it did not change when nitrate was introduced at 7.4 mg-C/mg-N.

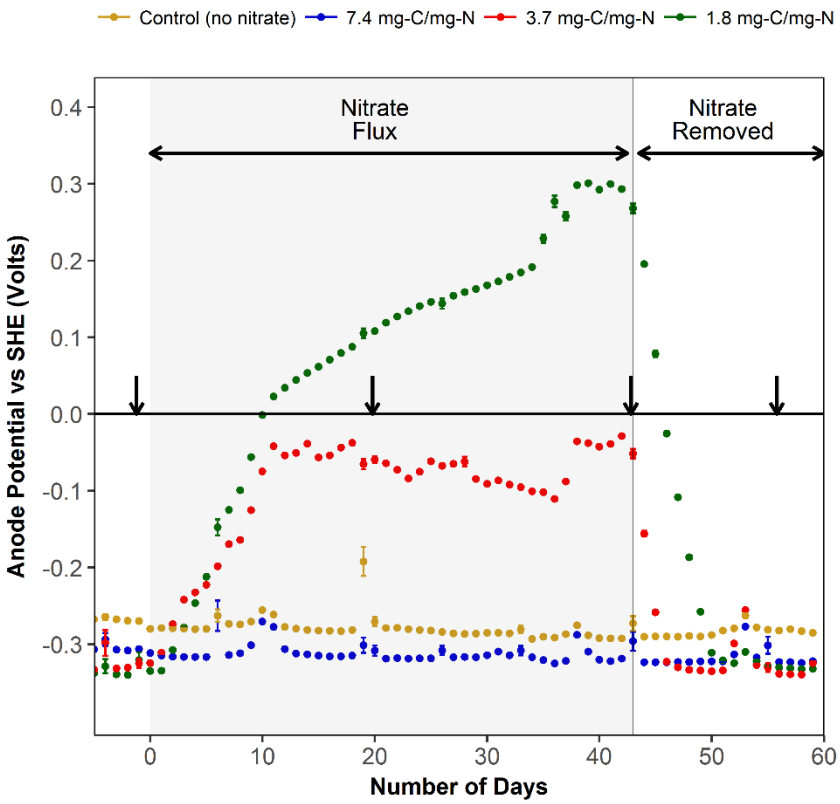

Figure 3.6: Anode Potential (Volts) through the course of the experiment. The arrows indicate when biofilm samples were taken.

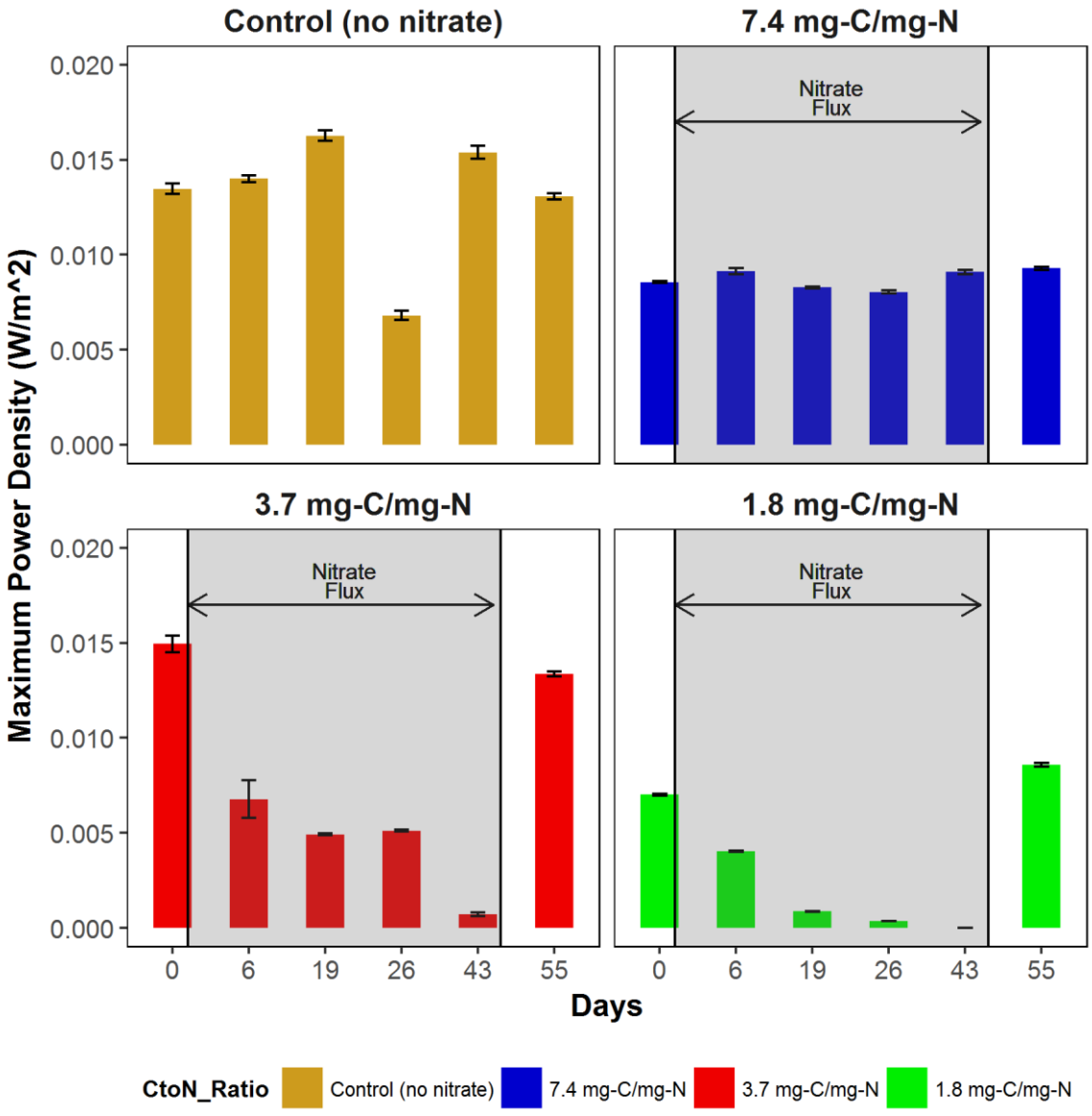

Figure 3.7: Mean Maximum Power Density (W/m^2) as measured using Polarization Curves. Error bars represent the standard deviation of three curves performed consecutively.

3.3.3 Emerging Denitrifiers are Primarily responsible for Nitrate Reduction in Nitrate-perturbed Anodes.

The microbial community, in the anode, was capable of reducing nitrate as soon as nitrate was introduced despite the biofilm in the MFCs having been acclimated over a long period of time with the anode serving as the sole electron acceptor. This suggests either facultative nitrate reduction by microorganisms capable of both anode respiration and nitrate reduction and use the anode as the electron acceptor in the absence of nitrate or the existence of a diverse microbial community harboring microorganisms capable of nitrate reduction and not anode respiration.

Sequencing of the 16S rRNA gene V3-V4 region was used to understand the effect of nitrate on the biofilm community. Samples of the biofilm were taken before nitrate was introduced (Day 0), during nitrate flux (Days 20 and 43) and after nitrate was removed from the influent (Day 56). A total of 734,652 high quality reads were obtained from sequencing after filtering and trimming. In the initial anode biofilm community, *Deltaproteobacteria* were predominantly present (70.6 ± 16.2 %). In these samples, most of the *Deltaproteobacteria* were putatively classified as *Geobacter spp.* (69.2 ± 16.5 %, Figure 3.9). Previous studies have shown the dominance of *Geobacter spp.* in anodic communities fed with acetate (Commault et al., 2013; Miceli et al., 2012; Torres et al., 2009; White et al., 2009). *Betaproteobacteria* were the next most abundant group composing 19.7 ± 12.6 % of the community. Most of the *Betaproteobacteria* were putatively classified as *Zoogloea spp.* (13.5 ± 10.7 %, Figure 3.9). *Zoogloea spp.* have been previously found in anode-respiring biofilms (Gao et al., 2014; Phung et al., 2004) and are usually implicated in the formation of a gelatinous matrix (Dugan et al., 1992) that could

aid in biofilm formation. To our knowledge, there have been no studies implicating *Zoogloea spp.* in anode respiration. However, *Zoogloea spp.* harbor the nitrite reductase gene and are capable of nitrate reduction (Strand et al., 1988). This suggests that there is inherent capacity in these anode-respiring biofilms for complete nitrate removal even when the anode community was acclimated with the anode serving as the sole electron acceptor. When nitrate was introduced into the anode, there was a decrease in the relative abundance of *Deltaproteobacteria* (Figure 3.8). Under electron donor non-limiting conditions (7.4 mg-C/mg-N), the relative abundance of *Deltaproteobacteria* decreased from 88.8 % (day 0) to 72.7 % (day 20) and 70.1 % (day 43). This was accompanied by an increase in *Betaproteobacteria* (mostly classified as *Zoogloea spp.*) from 7 % on day 0 to 21.3 % on day 20 and 20.6 % on day 43. When electron donor was most limiting (1.8 mg-C/mg-N), the relative abundance of *Deltaproteobacteria* decreased from 53.8 % (day 0) to 30.0 % (day 20) and 8.8 % (day 43). Concurrently, the relative abundance of *Betaproteobacteria* increased from 36.4 % (day 0) to 55.1 % (day 20) and 58.1 % (day 43). *Zooglea spp.* which were dominant members of *Betaproteobacteria* (Figure S3) are known denitrifiers (Bellini et al., 2013; Strand et al., 1988) and hence the increase in relative abundance of this genus could indicate denitrifying activity. This suggests that even though *Geobacter spp.* are capable of facultatively reducing nitrate to ammonium, this might not be the predominant mechanisms of nitrate reduction in nitrate-perturbed anode biofilm communities. When nitrate was introduced at 3.7 mg-C/mg-N, the change in the biofilm community was less straightforward. The relative abundance of *Deltaproteobacteria* initially decreased from 61.4 % (day 0) to 22.2 % (day 20) and then increased to 57.0 % (day 43). Concurrently, the relative abundance of *Betaproteobacteria* increased from 16.7

% (day 0) to 45.6 % (day 20) and then decreased to 23.0 % (day 43). This oscillation of community composition could be due to kinetics of acetate and nitrate utilization by members of the *Geobacter spp.* and *Zoogloea spp.* (Strand et al., 1988; van den Berg et al., 2016, 2015) but is beyond the scope of this study.

NMDS analysis of the UniFrac weighted metrics (Figure 3.10) showed that the difference in communities between sampling days within each C/N ratio increased at lower C/N ratios. Changes in the community due to nitrate are primarily along the NMDS axis 1. This further confirms that the communities are changing with time in the presence of nitrate. Additionally, it should be noted that the community after 43 days of nitrate flux is different from the community at day 0 when the C/N ratio is low.

3.3.4 The anodic community was resilient to nitrate perturbation.

When nitrate was removed from the influent after 43 days of nitrate flux, the relative abundance of the *Deltaproteobacteria* increased from 70.1 % (day 43) to 75.8 % (day 56) while *Betaproteobacteria* decreased from 20.6 % (day 43) to 13.5 % (day 56) in the reactor which was perturbed with nitrate at 7.4 mg-C/mg-N. Similarly, in the reactor perturbed at 1.8 mg-C/mg-N, *Deltaproteobacteria* increased from 8.8 % (day 43) to 31.2 % (day 56) while *Betaproteobacteria* decreased from 58.1 % (day 43) to 28.7 % (day 56). Interestingly, in this reactor, the relative abundance of *Gammaproteobacteria* increased from 3.7 % (day 43) to 24.2 % (day 56). A majority of the *Gammaproteobacteria* were putatively classified as *Pseudomonas spp.* (16.7 %, Figure 3.9) which have been identified in other MFC studies (Park et al., 2014; Rabaey et al., 2004; Read et al., 2010; Sun et al., 2010). Even though *Pseudomonas spp.* have only been implicated in electron transfer through soluble mediators, it is possible that there are syntrophic interactions between

Pseudomonas spp. and other bacteria through metabolites produced by *Pseudomonas spp.* and their presence in the biofilm could be due to the competitive advantage the biofilm offers in a chemostat where soluble mediators produced could be washed out (Pham et al., 2008; Venkataraman et al., 2011). *Pseudomonas spp.* are also known denitrifiers and hence the perturbation with nitrate could have lent them a competitive advantage (Barak et al., 1998; Körner and Zumft, 1989; van Rijn et al., 1996). At 3.7 mg-C/mg-N, even though recovery of the community towards the community at day 0 is observed, NMDS analysis (Figure 3.10) of the communities showed that the community at day 56 is different from day 0. It is possible that with longer recovery times, the community could have recovered or it attained a new steady state composition. At 1.8 mg-C/ mg-N, NMDS analysis of the UniFrac weighted metric (Figure 3.10) confirms that the community at day 56 (after nitrate flux has been removed) is different from the community at day 0. Most of this change is along the NMDS axis 2 which is different from the change due to nitrate flux.

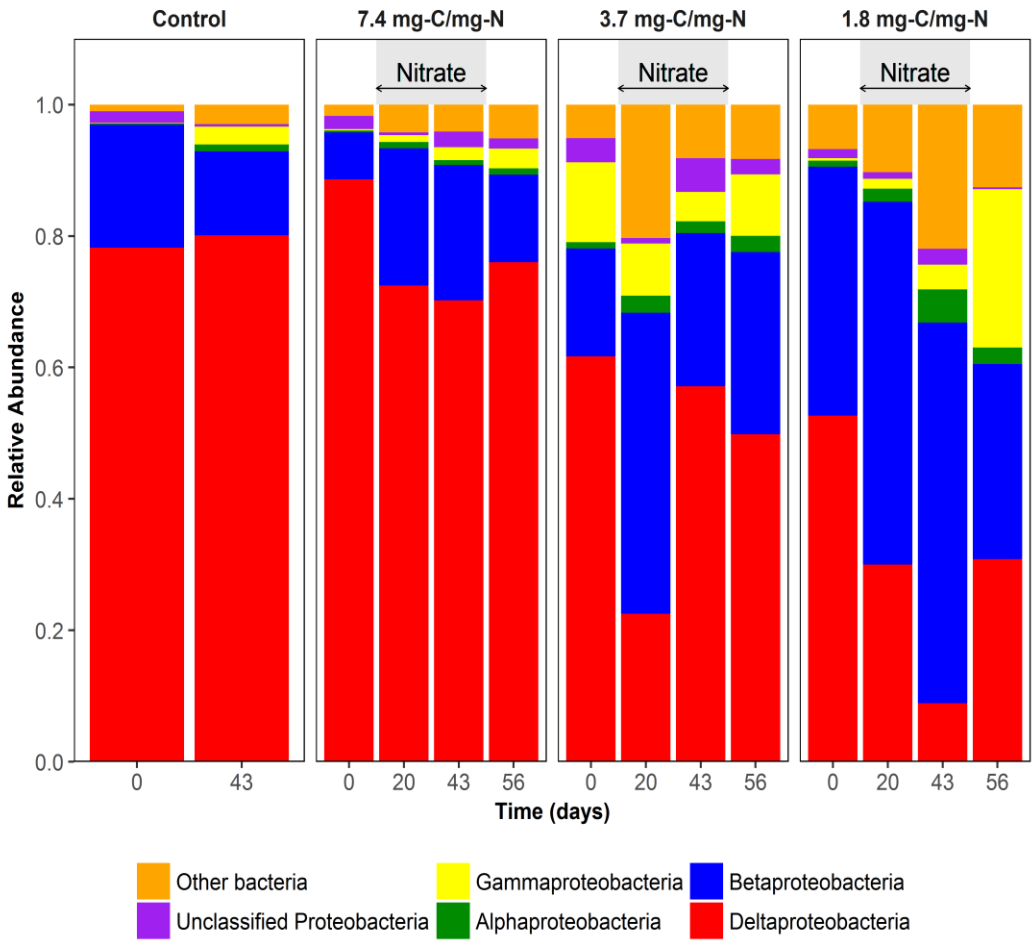

Figure 3.8: Relative abundance of bacterial classes at different C/N ratios during different stages of the experiment. The most abundant phylum Proteobacteria has been shown as its classes with the other phyla grouped as Other bacteria. Shaded areas represent period of nitrate flux.

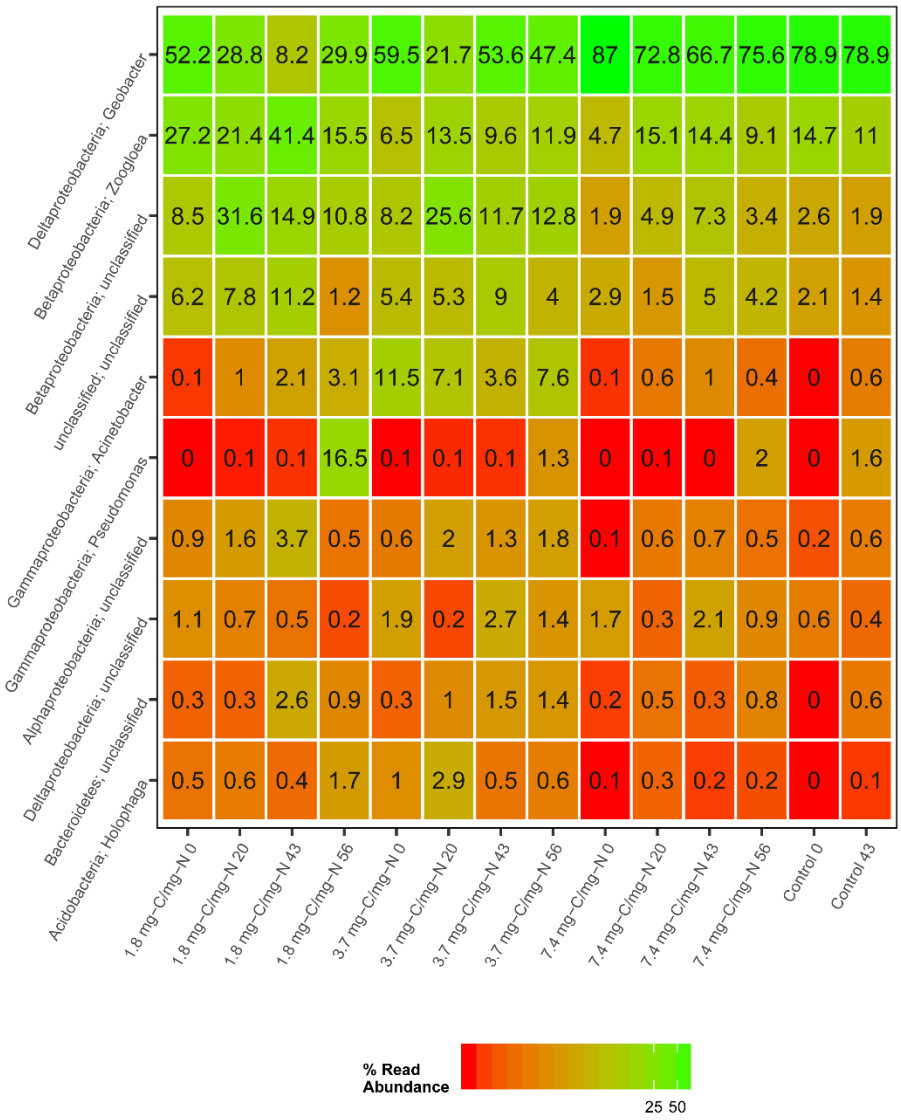

Figure 3.9: Relative abundances of the top 10 OTUs represented as a heatmap for each sample. The y-axis contains the class and genus information for each OTU while the x-axis contains the sample name represented as C/N Ratio:Sampling Day.

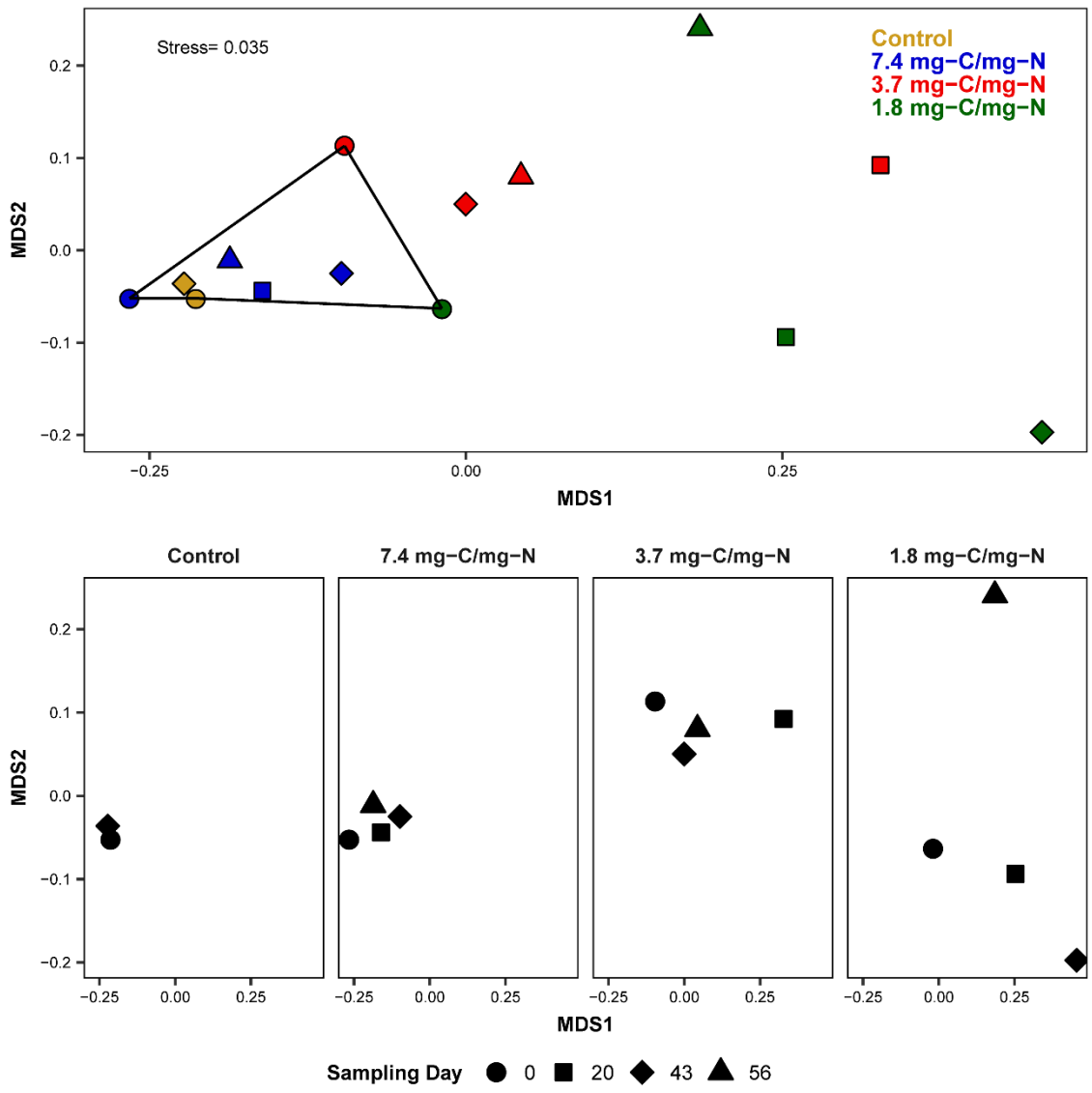

Figure 3.10: NMDS results of 16S rRNA gene sequencing data using distance matrix generated using UniFrac weighted metric for all C/N Ratios are shown in the top plot. Communities at day 0 are connected by lines. The results separated by C/N ratios are shown in the bottom plot.

3.3.5 Denitrification is upregulated in nitrate perturbed MFCs.

The effect of nitrate introduction on denitrifying genes was studied by quantifying the amount of nitrite reductase gene (*nirK* and *nirS*) transcripts using RT-qPCR. *Geobacter* specific primers were used to quantify the change in activity of *Geobacter spp*. The total

quantity of *Geobacter spp.* specific transcripts were on the order of 10^8 copy numbers which was on par with the 16S rRNA reference gene transcripts (Figure 3.11). This would be expected since *Deltaproteobacteria* (putatively classified as *Geobacter spp.*) were predominant in the community (Figure 3.8). *nirS* transcripts were an order of magnitude greater than *nirK* transcripts. Growth of *Zooglea spp.,* which was found to be a major response to the introduction of nitrate are known nitrite-utilizing organisms and possess the nitrite reductase gene-*nirS*. The higher quantity of *nirS* compared to *nirK* could be attributed to their predominance in nitrate perturbed reactors. No significant changes in *Geobacter spp.* activity was observed (Figure 3.12) in the reactor with nitrate at 7.4 mg-C/mg-N during nitrate flux. However, a significant increase in *nirS* transcipts from day 0 was observed at day 20 corresponding to denitrification activity in response to the introduction of nitrate. However, no significant changes were observed in *nirS* tanscripts at day 43 (compared to day 0). At 1.8 mg-C/mg-N, the activity of *Geobacter spp.* decreased significantly over time during nitrate flux and remained lower than at day 0 even after nitrate was removed from the influent. There was no significant change from day 43 to day 56 in *Geobacter* activity ($p = 0.54$). There was a corresponding upregulation of *nirS* during nitrate flux which was statistically significant (Day 0-Day 20 & Day 0-Day43, $p<0.001$) followed by a downregulation after nitrate was removed (Day 43-Day 56, $p<0.001$). It is interesting to note that even though there was a significant downregulation of *nirS* from day 43 to day 56, it was not accompanied by a significant upregulation of *Geobacter spp.* activity from day 43 to day 56. This could be due to the emergence of *Gammaproteobacteria* as an abundant group in the biofilm community at day 56 in the reactor perturbed at 1.8 mg-C/mg-N. When nitrate was introduced at 3.7 mg-C/mg-N, there

were no significant changes in *Geobacter spp.* activity or any significant up or downregulation of *nirS* activity. *nirK* showed significant changes in transcription (All comparisons, $p<0.01$). However, when nitrate was removed from the influent, *Geobacter spp.* showed increased activity. It is possible that, at this intermediate C/N ratio, the nitrate concentration was high enough with the acetate concentration not being extremely limiting, the kinetics of DNRA and nitrate reduction by bacteria containing the *nirK* genes was favorable. Further investigation into the competition between DNRA and denitrification with co-culture studies of *Geobacter spp.* and *Zoogloea spp.* is warranted before this can be confirmed.

Even though previous studies, investigating the effect of nitrate on the performance of the anode of an MFC, have implicated both denitrification and *Geobacter*-mediated DNRA as potential responses to the introduction of nitrate into the anode, either quantitative evidence was lacking or the study was performed in a pure culture system. Here we show that, even though *Geobacter spp.* are capable of nitrate reduction through the DNRA pathway, in mixed-culture systems, the primary response to the introduction of nitrate is mainly the emergence of heterorophic denitrifiers and that there is inherent capacity in these communities for denitrification. Furthermore, at intermediate and high C/N ratios, the relative abundance and activity of ARB either recovers or does not change significantly (respectively) suggesting that the communities are robust and resilient to fluxes of nitrate.

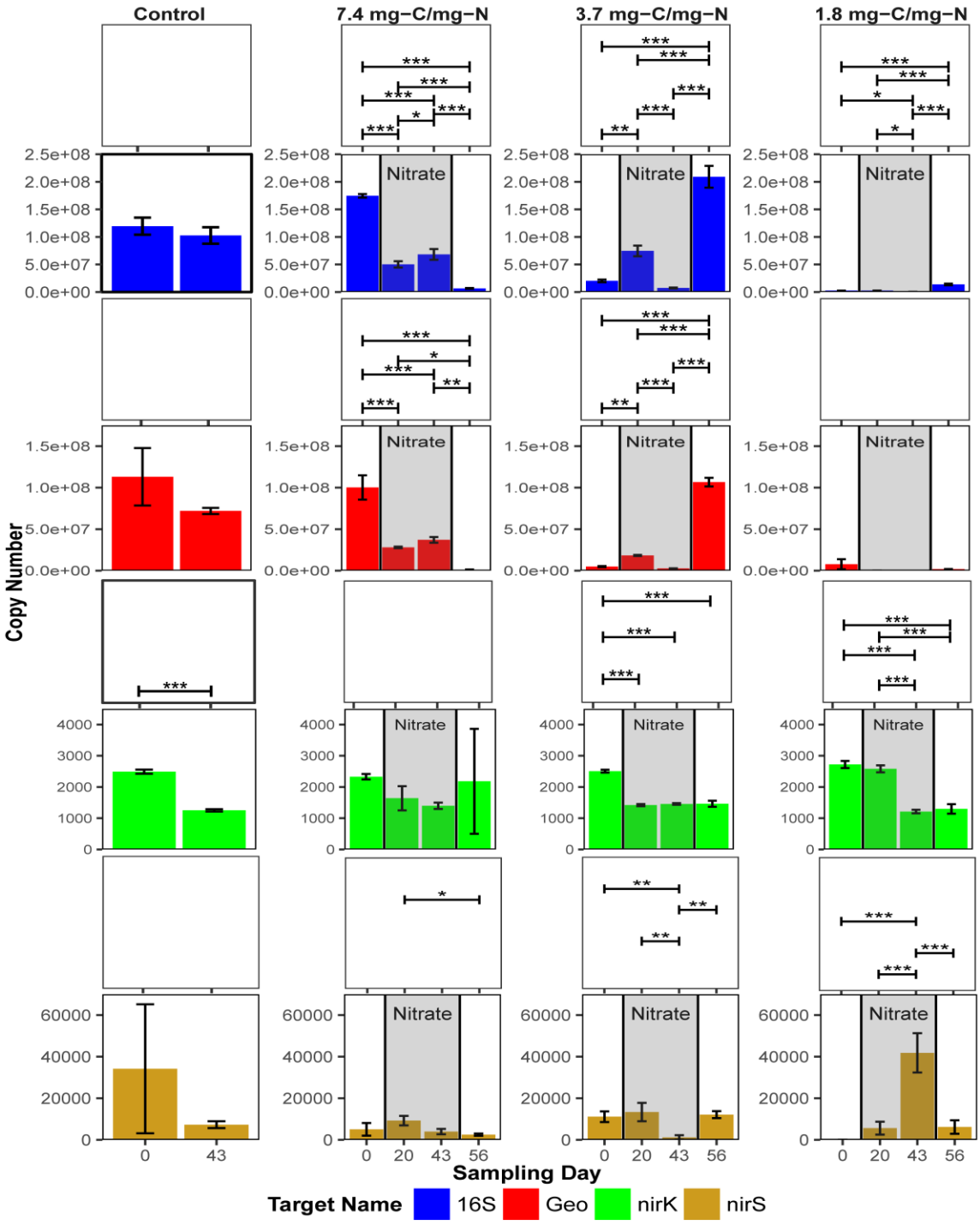

Figure 3.11: Absolute copy numbers (as determined from standard curves) in 16S, Geo, nirK and nirS transcripts due to the nitrate induction at different C/N ratios. Error bars represent standard deviation from three replicates. Asterisks indicate statistical significance (p<0.001-*, p<0.01-**, p<0.05-*) based on 1-Way ANOVA with a Two-Tailed post-hoc Tukey's HSD test.**

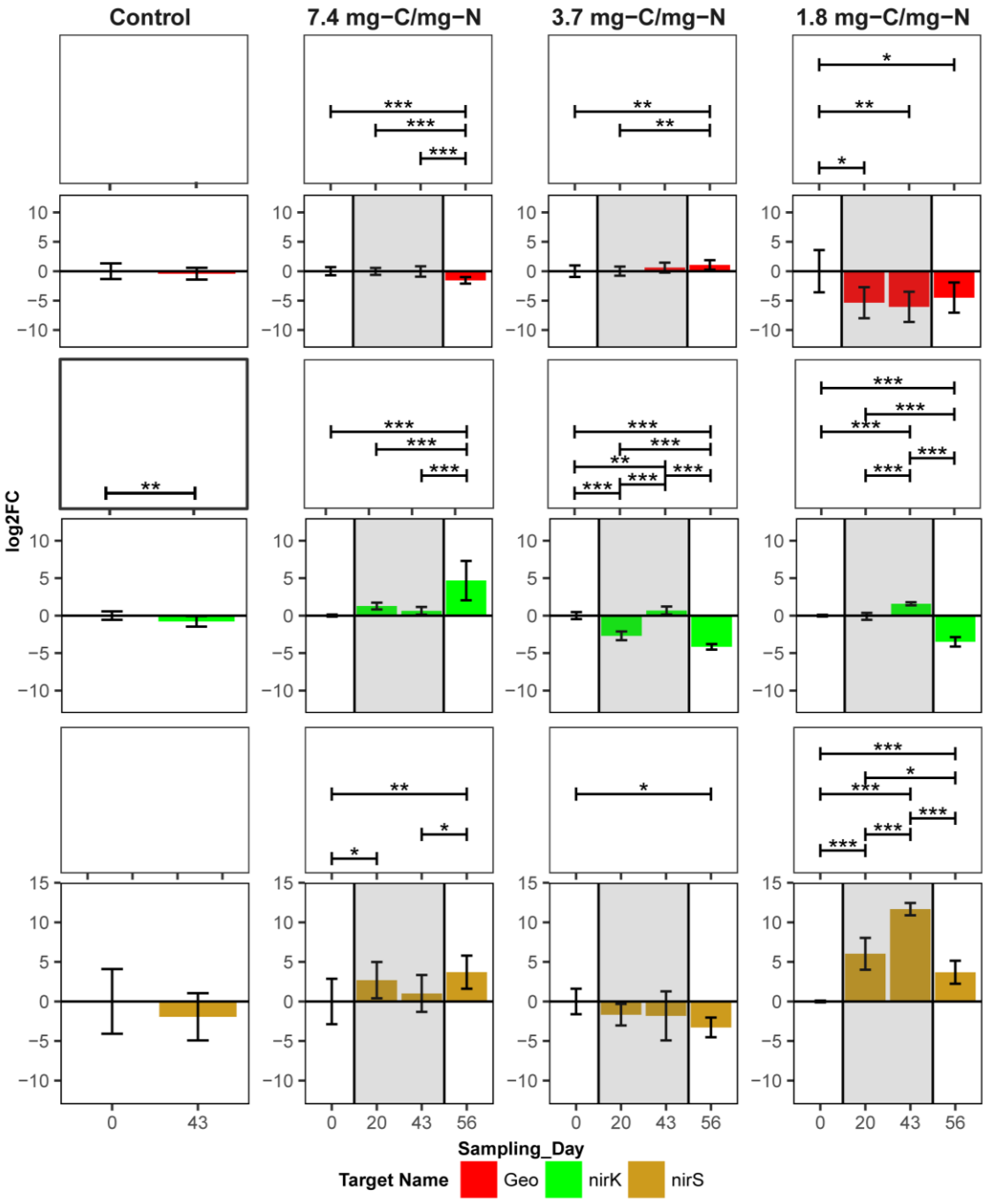

Figure 3.12: Fold Changes in Geo, *nirK* and *nirS* expression due to the nitrate induction (shaded area) at different C/N ratios represented as the log2 transformed value. Relative transcript ratios comparing target transcripts with 16SrRNA for each sample within each C/N Ratio was calculated and used to determine fold changes as compared to Day 0 sample. Error bars represent standard deviation. Asterisks indicate statistical significance (p<0.001-*, p<0.01-**, p<0.05-*) based on 1-Way ANOVA with a Two-Tailed post-hoc Tukey's HSD test with each Sampling Day compared to the respective Day 0 data.**

CHAPTER 4

MODELLING INTERSPECIES COMPETITION AND COMMUNITY DYNAMICS IN THE ANODE OF A MICROBIAL FUEL CELL

4.1 Introduction

A major challenge in the research on microbial fuel cells (MFCs) and its application in wastewater treatment, groundwater treatment and bioremediation is the complex web of biological, biochemical and electrochemical interactions that affect its electrochemical and treatment performance. Some of the different phenomena are bacterial kinetics (Marcus et al., 2007; Torres et al., 2008b), identity of the bacteria/archaea in the anode (Kim et al., 1999; Rotaru et al., 2014; Snider et al., 2012), electron transfer rate (Bonanni et al., 2013; Matsuda et al., 2012; Okamoto et al., 2014; Schröder, 2007), composition of the biofilm EPS (Malvankar et al., 2012, 2011; Marcus et al., 2007) (which contributes to its conductivity), thickness of the biofilm (Bond et al., 2012), substrate diffusion into the anode biofilm (Lee et al., 2009), electrochemical losses (Clauwaert et al., 2008), external resistance (Aelterman et al., 2008; Jung and Regan, 2011; Pinto et al., 2011; Rismani-Yazdi et al., 2011), cathodic reactions (Cheng and Logan, 2011; Dewan et al., 2008), electrode material (Logan, 2010; Logan et al., 2006; Pocaznoi et al., 2012) and configuration of the MFC (Du et al., 2007; Freguia et al., 2008b; Liu et al., 2005b). A primary requirement for widescale application of the technology is the ability to model the performance of the technology and being able to predict changes in performance due

to environmental factors. This model has to incorporate all the afore-mentioned factors to be able to predict the performance of a MFC accurately under changing conditions.

Despite the importance of models in process optimization, very few studies incorporating models to understand the effect of operating conditions have been published. Marcus et al. (Marcus et al., 2007) developed a one-dimensional model with electron donor oxidation by dual substrate-limited kinetics represented by the Nernst-Monod equation (Equation 4.9). Picioreanu et al. (Picioreanu et al., 2008) integrated IWA's anaerobic digestion model (ADM1) within a computational model of a microbial fuel cell. This model incorporated competing methanogenic archaea and anode-respiring bacteria in both the suspension and in the biofilm. They determined that a smaller electrical resistance enabled selection of anode-respiring bacteria and higher electrical resistance enabled the growth of methanogenic archaea. Similar results were obtained by a model developed by Pinto et al. (Pinto et al., 2010). A study by Merkey and Chopp (Merkey and Chopp, 2014) modelled interspecies competition between two different communities of bacteria using the anode as the electron acceptor implying two different mechanisms of electron transfer- direct electron transfer through a conductive biofilm and electron transfer through soluble electron mediators. They found that bacteria that use direct electron transfer are competitively favored due to the faster rates of electron transfer. Except for Picioreanu et al. (Picioreanu et al., 2008), all published models have focused on the anode-respiring bacteria (ARB) and their behavior under various operating conditions. More attention is needed incorporating non-ARB into these models and understanding community dynamics in the presence of competing electron acceptors in the anode.

The community in the anode of a MFC has been observed to be diverse (Ki et al., 2008; Patrick D. Kiely et al., 2011; Kim et al., 2006; Miran et al., 2015). It is highly likely that these diverse communities are composed of obligate ARB, facultative ARB (capable of both anode-respiration and an alternate metabolism) and/or non-ARB. The presence of active or dormant communities of facultative ARB and/or non-ARB creates a vulnerability in the performance of the system when an alternate electron acceptor is introduced. The most fundamental interaction, in the presence of a competing electron acceptor, is the competition for the electron donor. This competition can be modeled by using resource competition models such that used by Tilman (Tilman, 1977). Even though more complex agent-based modeling approaches can yield information about spatial organization of the community and specific cellular growth patterns (Picioreanu et al., 2008, 2004), lumped-system models such as the one developed here, can yield information about important phenomena and parameters that can further be focused on in future experimental and modeling studies.

We focus on using nitrate as a model competing electron acceptor. Choosing nitrate as the competitor has some important advantages from the perspective of modelling: the availability of nitrate as a competing electron acceptor is mainly influenced by the flow rate into the anode and thickness of the biofilm. It does not involve complex gas transfer kinetics that would be the case with electron acceptors such as oxygen. Another important advantage is its relevance to wastewater treatment and bioremediation due to its ubiquitous presence in the environment and requirement for nitrogen removal from waste streams.

4.2 Model Formulation

The specific experimental simulated is as follows: nitrate is introduced into the anode of an acclimated MFC. The anode is assumed to be performing at steady state and the microbial community is composed by anode-respiring bacteria (such as *Geobacter spp.*) with a small fraction of non-ARB. This was evaluated experimentally (Figure 4.9). The anode is also assumed to be fed with acetate (electron donor) at the minimum concentration required to sustain stable power production. The application of this multi-species lumped-system model is evaluated by its ability to simulate community dynamics in a nitrate-perturbed anodic community. The model is also used to understand important parameters that the influence community dynamics in the anode to gain a better understanding of the operating and system properties that influence the robustness of the community.

The following assumptions were made to formulate the model:

1. There are no diffusional limitations in the biofilm, i.e., the anode biofilm is a thin biofilm. This implies a biofilm that is less than 50 μm in thickness (Ter Heijne et al., 2011). This was confirmed by microscopic observation using DAPI staining (Figure A. 3).
2. The anode chamber is completely mixed and hence behaves like a continuous stirred-tank reactor (CSTR).
3. There are two main metabolisms in the anode in the presence of nitrate: anode respiration and denitrification. The two metabolisms are performed by different communities of bacteria: *Geobacter spp.* are used as the model organism performing anode respiration and *Zoogloea spp.* as the model organism

performing denitrification. This assumption has been validated through community analysis of anode biofilms perturbed with nitrate (Figure 0.9).

4. The microbial growth and substrate utilization kinetics can be modelled based on dual-substrate limited Monod kinetics or modification of the equation. Both electron donor and electron acceptor are limiting for both organisms.
5. In order to simplify the model, anode respiration is only performed through direct electron transfer by *Geobacter spp.* in the biofilm. This is a reasonable assumption due to different studies showing that microorganisms performing mediated electron transfer will likely be out-competed/washed out in a chemostat MFC (Merkey and Chopp, 2014). Also, since we assumed a thin biofilm, most cells in the biofilm have direct contact with the electrode. Anode respiration/electron transfer stops when a cell detaches from the biofilm. The same assumption is also made for denitrifying microorganisms (*Zoogloea spp.*). Even though denitrification can still be performed in the bulk solution, it is likely that in a chemostat the cells that are in suspension are likely to be washed out at nitrate-limiting concentrations. The competition in the biofilm community is of most interest since if ARB in the biofilm is completely out-competed, it lowers the ability of the MFC to recover the electrochemical performance when the competing electron acceptor is removed. We can incorporate more elements into the model once a better understanding of the competition in the biofilm is gained. Dissimilatory reduction to ammonium (DNRA) by *Geobacter spp.* has not been incorporated since no evidence of this metabolism was observed experimentally.

6. A maximum biofilm carrying capacity for the electrode (X_{cap} – g-VS/m^2) is assumed. This means that the total mass of cells on the electrode cannot exceed this quantity. This imposes a constraint on cell growth and imposes competition for space on the electrode. X_{cap} of 1 g/m^2 was assumed.
7. Temperature was assumed to be 25 ˚C (298.15 K).
8. Lastly, it is assumed that there is no time delay in the growth of denitrifiers and nitrate utilization after nitrate is introduced into the anode. This is a reasonable assumption since *Zoogloea spp.* were found in the anode biofilm community even after acclimation of the anode (no nitrate) for an extended period of time.

The biomass mass balances are as follows

$$\frac{dX_{geo}}{dt} = \{\mu_{geo} - \alpha D\}X_{geo} \qquad \textbf{Equation 4.1}$$

$$\frac{dX_{denit}}{dt} = \{\mu_{denit} - \alpha D\}X_{denit} \qquad \textbf{Equation 4.2}$$

where X_{geo} and X_{denit} are biomass density of anode-respiring and denitrifying bacteria (g-VS/m^2), μ_{geo} and μ_{denit} are the specific growth rates of anode-respiring and denitrifying bacteria (min^{-1}), D is the dilution rate (min^{-1}) and α is the biomass retention coefficient (Pinto et al., 2010). The dilution rate in this case is 0.00084 min^{-1} which is equal to an HRT of 19.8 hours. α is a dimensionless coefficient which is a property of microorganism. It can be viewed as a retardation of dilution and a measure of the detachment rate of the microorganism. Lower values of α imply higher biofilm retention and vice versa. Here we have made the simplifying assumption that it is the same for both groups of organism.

The substrate mass balances are as follows:

$$\frac{dS_{ac}}{dt} = \{S_{ac}^{in} - S_{ac}\} * D - q_{ac}^{geo} * X_{geo} - q_{ac}^{denit} * X_{denit} \qquad \textbf{Equation 4.3}$$

$$\frac{dS_{nit}}{dt} = \{S_{nit}^{in} - S_{nit}\} * D - q_{nit}^{denit} * X_{denit} \qquad \textbf{Equation 4.4}$$

where S_{ac}^{in} and S_{ac} are acetate concentrations (g/L) in the influent and in the reactor (equal to effluent concentration), $S_{nit}^{in}$and S_{nit} are nitrate concentrations (g/L) in the influent and in the reactor (equal to effluent concentration), q_{ac}^{geo} and q_{ac}^{denit} are acetate utilization rates for anode respiring and denitrifying bacteria respectively (g-Ac/(g-VS.min)), q_{nit}^{denit}nitrate utilization rate for denitrifying bacteria (g-nitrate/(g-VS.min)).

The growth kinetics for the anode-respiring and denitrifying bacteria are given by:

$$\mu_{geo} = \mu_{geo}^{max}\left(\frac{S_{ac}}{S_{ac} + K_{s-geo}^{ac}}\right)\left(\frac{1}{1 + \exp\left[-\frac{F}{RT}(E_a - E_{Ka}\right]}\right) \qquad \textbf{Equation 4.5}$$

$$\mu_{denit} = \mu_{denit}^{max}\left(\frac{S_{ac}}{S_{ac} + K_{s-denit}^{ac}}\right)\left(\frac{S_{nit}}{S_{nit} + K_{s-denit}^{nit}}\right) \qquad \textbf{Equation 4.6}$$

where K_{s-geo}^{ac} and $K_{s-denit}^{ac}$ are half-saturation constants (g/L) for acetate utilization by anode-respiring and denitrifying bacteria respectively, μ_{geo}^{max} and μ_{denit}^{max} are maximum specific growth rates (min^{-1}) of anode-respiring and denitrifying bacteria respectively, E_a is the anode potential (volts), E_{Ka} is the anodic acceptor potential for the half-maximum-

rate (volts), F is the Faraday's constant (96500 C/mol), R is the ideal gas law constant (8.314 J mol^{-1} K^{-1}) and T is the temperature (298 K).

The current density is given by

$$j = j_{max}\left(\frac{S_{ac}}{S_{ac} + K_{s-geo}^{ac}}\right)\left(\frac{1}{1 + \exp\left[-\frac{F}{RT}(E_a - E_{Ka}\right]}\right) \qquad \textbf{Equation 4.7}$$

where j_{max} is the maximum current density.

The mass balance on the biomass is governed by the maximum biomass carrying capacity (X_{cap} – g/m^2).

$$X_{geo} + X_{denit} = X_{cap} \qquad \textbf{Equation 4.8}$$

4.3 Methods

4.3.1 Parameter Estimation

The system of ordinary differential equations was solved by using the ode solver from the deSolve (Soetaert et al., 2010) package in R. The differential equations were solved using LSODA method which has the ability to select between stiff and non-stiff solutions by dynamically monitoring the data as it is solved. Several parameters were obtained from literature and some others were assumed (Table 4.1). E_{ka}, j_{max} and α were estimated in this study using a genetic algorithm with a single-objective optimization method (Deb et al., 2002; Pelletier et al., 2006) as outlined in Section 1.4. Model parameters were estimated by minimizing the following objective function

$$F(obj) = \sum_{i=1}^{n} \left[\sum_{t=0}^{t} \left(y_{i,t}^{exp} - y_{i,t}^{pred} \right)^2 \right] \qquad \textbf{Equation 4.9}$$

where $y_{i,t}^{exp}$ and $y_{i,t}^{pred}$ are the experimentally determined and predicted values respectively at each time point t for the i^{th} state variable. The model outputs that were used for the optimization (estimation of E_{ka}, j_{max} and α) were X_{geo}, X_{denit} and current.

4.4 Results and Discussion

The main purpose of this modeling effort was to model the change in relative biomass abundance of anode-respiring and denitrifying bacteria when nitrate is introduced into the reactor as a competing electron acceptor. Even though the model was calibrated using a genetic algorithm, a sufficient calibration was not achieved (Figure 4.1). The model predicts a community structure that quickly shifts to predominantly denitrifying bacteria even though experimental data shows that this shift is a much slower process and ARB do not get completely out-competed in the community. This could be due to ARB that are facultatively able to reduce nitrate to ammonium (DNRA) (Kashima and Regan, 2015; van den Berg et al., 2016, 2015) which are not represented in the model or incomplete reduction of nitrate to nitrite by ARB (Aklujkar et al., 2009). Nitrite was not detected in the effluent of the MFC nor was ammonium. However, it is possible that ammonium produced through DNRA might have been used for assimilation and hence not detected in the effluent. The same scenario is possible for nitrite. Future studies should focus on understanding the kinetics of nitrate reduction by ARB such as *Geobacter spp.* as quantitative information on kinetic parameters is currently unavailable. This information could then be incorporated into the model. Generally, the model predicts that ARB are

out-competed by denitrifying bacteria in the presence of nitrate when ARB do not possess the capability to use nitrate as an electron acceptor.

Table 4.1: Model Parameters

Parameter	Value	Units	Source
q_{ac}^{geo}	0.005408	g-Ac/(g-VS.min)	(Marcus et al., 2007)
$K_{s-denit}^{ac}$	0.00062	g/L	(van den Berg et al., 2016)
q_{ac}^{denit}	0.007489	g-Ac/(g-VS.min)	(van Niekerk et al., 1987)
D	0.00084	min^{-1}	Measured
S_{ac}^{in}	0.035	g/L	Measured
S_{nit}^{in}	0.041	g/L	Measured
SA	0.00242	m^2	Measured
F	96500	C/mol	Constant
R	8.3145	J/(mol.K)	Constant
T	298.15	K	Assumed
$K_{s-denit}^{nit}$	0.00062	g/L	(van den Berg et al., 2016)
μ_{geo}^{max}	0.0021	min^{-1}	(Esteve-Núñez et al., 2005)
μ_{denit}^{max}	0.00254	min^{-1}	16
Xa	1	g/m^2	Assumed
K_{s-geo}^{ac}	0.00177	g/L	(Marcus et al., 2007)

j_{max}	1.7	A/m^2	Estimated in this study
E_{ka}	0.1	volts	Estimated in this study
α	0.02	dimensionless	Estimated in this study
Influent nitrate	0.041	g/L	Measured
Influent acetate	0.035	g/L	Measured
C/N Ratio	1.8	g-C/g-N	Calculated

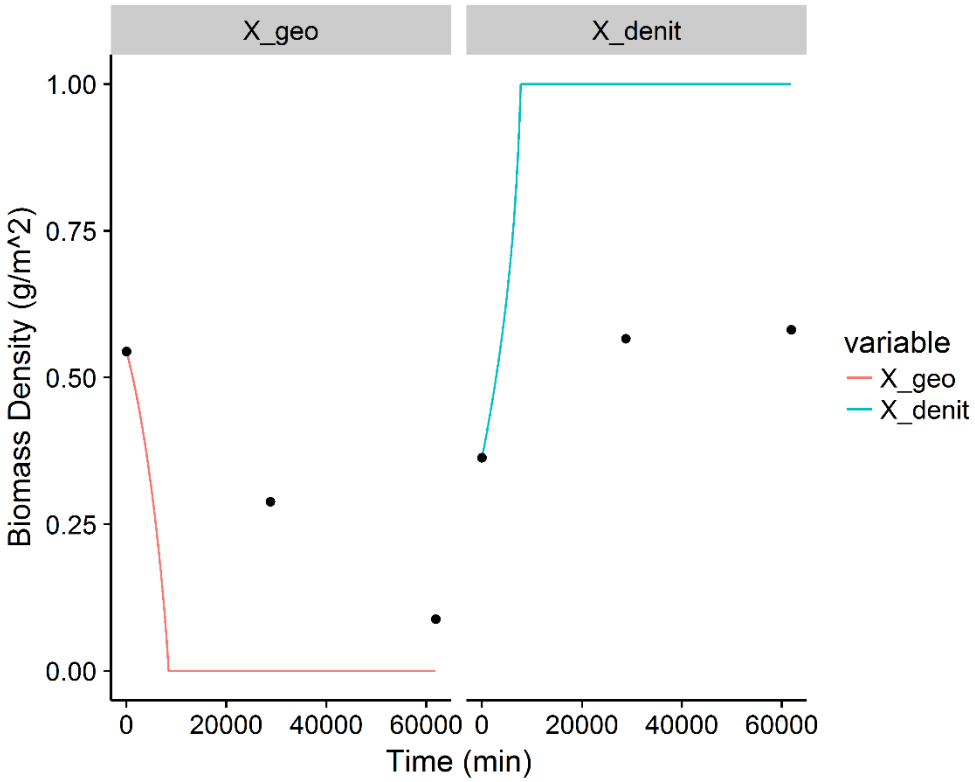

Figure 4.1: Predicted and observed biomass densities of anode-respiring and denitrifying bacteria. Points represent observed data and lines represent predicted data.

A useful exercise is to perform sensitivity analysis on the different parameters that influence the change in community structure. E_{ka} and j_{max} showed no effect on the trends predicted. However, the biofilm retention coefficient (α) showed significant effects on the change in community structure (Figure 4.2). Lower biofilm retention factors showed higher retention of anode-respiring bacteria in the community. This suggests that the detachment rate of microorganisms plays a key role. This retention factor might be influenced by the surface properties of the electrode, type of electrode material and species of microorganism. In this case, the model assumed that the biofilm retention coefficient was the same for both groups of bacteria. However, this is unlikely and in the presence of nitrate, it is likely that denitrifying bacteria will have a higher α due to detachment into the suspension due to the presence of nitrate in the bulk solution (Kashima and Regan, 2015) and hence subject to more washout. The dependence of α on nitrate will have to be experimentally determined before being incorporated into the model. Furthermore, there is likely to be an equilibrium established where there are denitrifying bacteria in the suspension and in the biofilm performing denitrification independently and competing. This is not currently captured by our model and warrants investigation since the biomass density of denitrifying bacteria in the biofilm reaches a plateau value of 0.66 g/m^2 (experimental) while the model predicts the biomass density reaching X_{cap}.

The maximum specific growth rate of denitrifying bacteria did not show an effect. However, the model was sensitive to the maximum specific growth rate of anode-respiring bacteria. Higher μ_{geo}^{max} values improved retention of anode-respiring bacteria in the community. Since μ_{geo}^{max} is a characteristic of the species of anode-respiring bacteria

active in the community, acclimation regimes targeting specific species of bacteria with high μ_{geo}^{max} might be useful in improving the robustness and resilience of anode-respiring communities to influx of competing electron acceptors. Detailed kinetic information for different anode-respiring bacteria for growth on the anode electrode is currently lacking. Most studies have been done using soluble electron acceptors such as fumarate and might not mimic growth using a solid electron acceptor well.

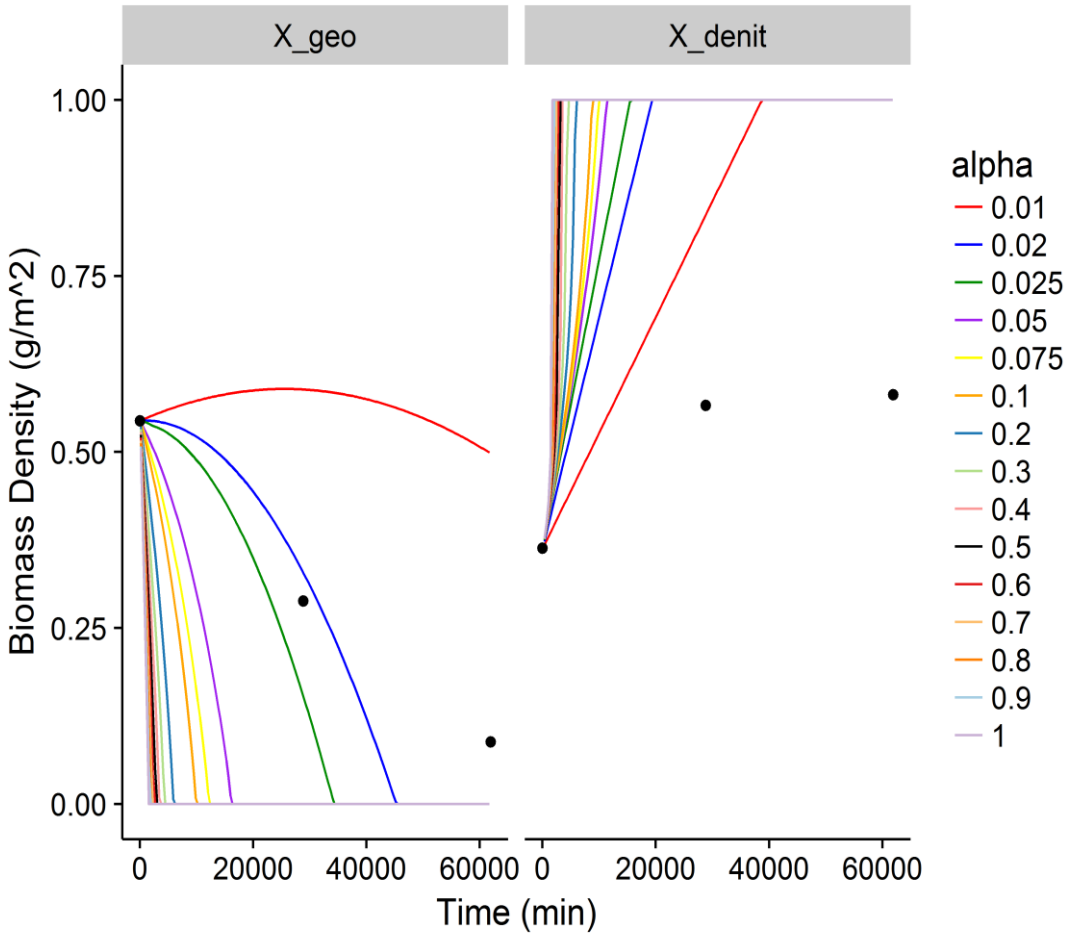

Figure 4.2: Effect of biofilm retention coefficient on the community structure in the presence of nitrate. Points represent observed data.

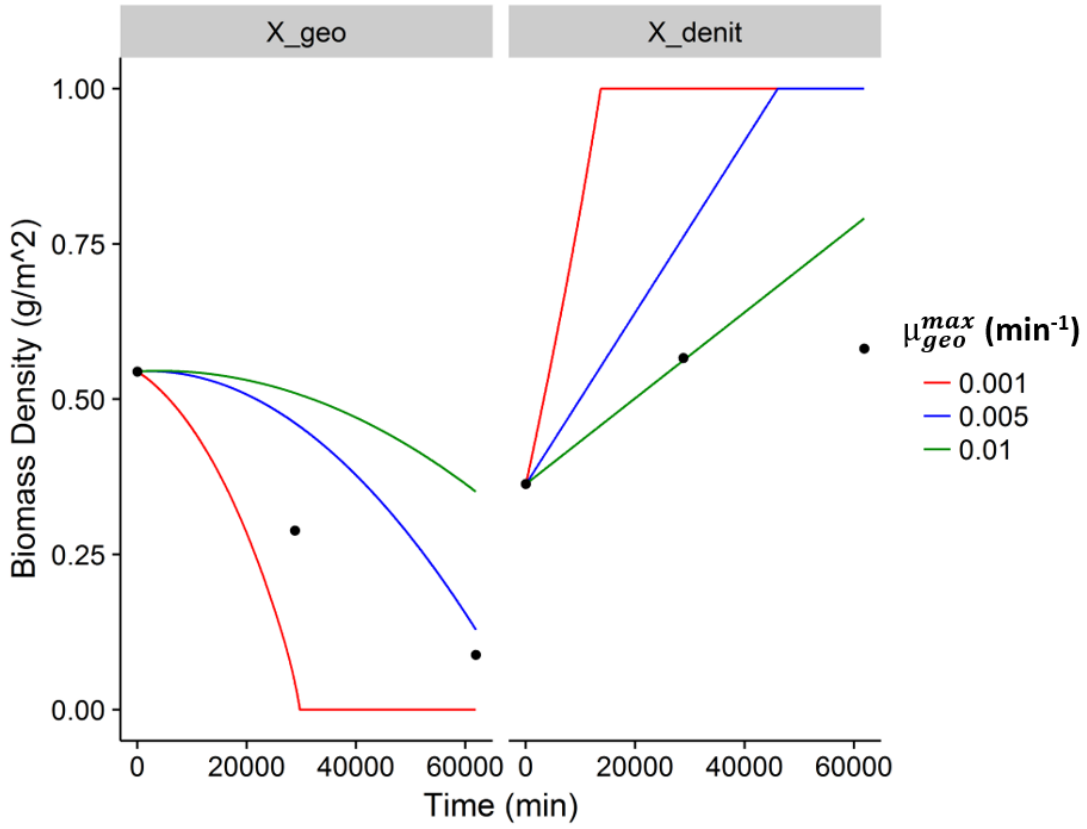

Figure 4.3: Sensitivity of the biomass density to the maximum specific growth rate of anode-respiring bacteria (μ_{geo}^{max}). Points represent observed data.

A multispecies MFC model was developed to simulate the effect of influx of competing electron acceptors into the anode. The model was able to simulate the trend in biomass changes in the anode biofilm. Several key parameters such as the biofilm retention coefficient and the maximum specific growth rate of anode-respiring bacteria were identified as having the most influence on the robustness of these biofilms. In general, the model predicts that ARB that are incapable of using nitrate will be outcompeted by denitrifying bacteria. Since ARB biomass retention was improved when μ_{geo}^{max} was

increased, the most important factor in preserving the community structure of these biofilms is the growth kinetics of the bacteria. The model simulates the general trend in the observed data. The lack of fit to observed data suggests that there are some key phenomena that is not being simulated by the model. This could include activity of nitrate reduction by detached denitrifying bacteria and facultative ARB in suspension, nitrate reduction by facultative ARB in solution (DNRA and denitrification), accurate biofilm detachment models and parameters, mediated electron transfer, etc. This study highlights the importance of detailed kinetic and co-culture studies for estimation of kinetic parameters and understanding the dynamics of competition between different bacteria under varying operational regimes.

CHAPTER 5

CONCLUSIONS

This dissertation made some important contributions that will impact the use of microbial fuel cells for bioremediation and wastewater treatment.

5.1 Nitrite accumulation in biocathodes is due to intracellular competition for electron mediators

Nitrite was observed to be accumulating in a denitrifying biocathode in batch conditions up to 66.4 ± 7.5 % of the initial nitrogen. A model, activated sludge model with an integration of the Nernst-Monod model and indirect coupling of electrons (ASM-NICE), was formulated, calibrated and validated using experimental data. The cause of nitrite accumulation was identified as intracellular competition between nitrate and nitrite reductases for the intracellular reduced electron mediator. The competition was controlled by the affinity of the enzymes (K_{MRedNA} and K_{MredNI}) for the reduced mediator. The calibrated half-saturation constants (K_{MRedNA} and K_{MredNI}) suggested a greater affinity of the nitrate reductase enzyme to the reduced mediator in comparison to the nitrite reductase enzyme. Operationally, longer hydraulic retention times (HRT) might be necessary for achieving complete nitrogen removal.

5.2 An experimental framework for investigating competition in MFCs was created

An important phenomenon to consider when implementing MFCs for wastewater treatment or bioremediation is the potential for presence of alternate electron acceptors

and the competition resulting from their presence. The effect of the presence of such alternate electron acceptors was evaluated using a model contaminant: nitrate. An experimental framework was created that enabled the study of the effect of nitrate on the performance of a MFC as well as the effect on the microbial ecology and activity of the anode-respiring community under a variety of electron donor limiting/non-limiting conditions. An important aspect of the framework is the identification of the critical electron donor concentration ($S_{critical}$) which enabled the change of electron donor availability from limiting to non-limiting. This experimental framework can be directly applied to study the effect of different alternate electron acceptors. The availability of the electron donor was evaluated using the C/N ratio.

5.3 The impact of nitrate on the anode performance and microbial community depended on the C/N ratio

The impact of nitrate depended on the C/N ratio of the influent. The electrochemical performance was significantly affected at low C/N ratios (1.8 and 3.7 mg-C/mg-N) and not affected at high C/N ratios (7.4 mg-C/mg-N). This suggests that the effect of alternate electron acceptors can be mitigated if the ratio of the electron donor/electron acceptor can be optimized to be high. This could be achieved by addition of an external electron donor or by fermentation of primary or secondary sludge. Furthermore, the microbial ecology and performance was either not significantly affected (7.4 mg-C/mg-N-electron donor non-limiting) or recovered upon removal of the alternate electron acceptor after 43 days of perturbation (3.7 mg-C/mg-N) suggesting that as long as the electron donor is not severely limiting (1.8 mg-C/mg-N), the performance and community structure in the anode can be preserved or recovered.

The major response to presence of nitrate in the anode is heterotrophic denitrification

Even though, *Geobacter* spp. have the capability to reduce nitrate to ammonium, the major response of the community was the heterotrophic denitrification of nitrate to N_2 gas. This implies that even though anode-respiring bacteria may have the facultative ability to use an alternate electron acceptor as the electron acceptor, the dynamic changes in the community structure are influenced heavily by the kinetics of reduction of nitrate by the members of the community and more research is required to characterize the kinetics of the various facultative metabolisms in anode-respiring bacteria. This will enable the assessment of risk to the anode performance and community structure posed by alternate electron acceptors that may be introduced into the anode intermittently.

5.4 Microbial growth kinetics and specific detachment rates play a key role in the outcome of competition in MFCs

Modeling of this competition suggested that, apart from the kinetics of alternate electron acceptor utilization, cell detachment from the biofilm plays an important role in the result of the competition. Characterizing this detachment rate for various bacteria and the dependence of this detachment on the concentration of electron acceptor in the bulk solution is critical to completely model the competition.

This research developed a model (ASM-NICE) that effectively simulates nitrite accumulation and helped understand the cause of the accumulation and will help develop strategies to mitigate such accumulations in MFC biocathodes. Furthermore, this research

also contributes an experimental framework to investigate competition in the anode of MFCs. This experimental framework was used to investigate the effect of nitrate and understand the effect of nitrate on the performance and ecology of the anode in MFCs. Furthermore, modeling of this perturbation experiment identified microbial growth kinetics and detachment rates as key phenomena that warrant further investigation.

APPENDICES

APPENDIX A

EFFECT OF DIFFERENT SEQUENCING DATA ANALYSIS STRATEGIES

Sequencing errors can arise when longer regions of the 16S rRNA gene have been sequenced. Using Illumina MiSeq, the maximum number of bps that can be sequences in 1 read is 250 bps (V2 chemistry) and 300 bps (V3 chemistry). In paired-end sequencing, the region of interest is sequences once in the forward direction (5' -> 3') and then again in the reverse direction (3' -> 5'). Hence theoretically, using paired-end sequencing, one could sequence a long region of the 16S rRNA gene using overlapping regions and assembling them in-silico thus lending more specificity to taxonomic classification. However, it has been observed that sequence error rates are high when the forward and reverse reads are not completely overlapping. Furthermore, the V3 chemistry for Illumina sequencing has been observed to have high error rates too.

Sequence errors lead to inflated number of unique sequences and hence cause an issue with distance matrices when sequences are clustered into OTUs. It also leads to an inflated number of OTUs leading to overestimation of diversity and richness. There are two different ways researchers deal with this issue: remove rare sequences (singleton removal) after OTU picking or cluster sequences into OTUs based on their phylotype. The effect of these different strategies on the interpretation of the changes in the community can be significant and needs to be evaluated.

A1 Methods

Three different sequencing analysis strategies were tested: typical mothur pipeline, mothur pipeline with singleton removal and phylotype. The common steps across all three methods are as follows. The raw Fastq files were cleaned using Sickle 1.33 (Joshi and Fass, 2011) with a minimum window quality score of 20. The quality-controlled sequences were analyzed using mothur (Schloss et al., 2009) using the protocol described in Kozich et al (Kozich et al., 2013). The sequences were trimmed to remove primers and barcodes, quality filtered using sickle v1.33 (Joshi and Fass, 2011) with a minimum quality score of 20 and assembled in mothur. The assembled sequences were screened to remove sequences that were less than 425 bps and greater than 470 bps in length. The sequences were aligned to SILVA v123 database. The alignment was screened to remove poorly aligned sequences using vertical = T and trump = . options in mothur. Chimeras were remove using the UCHIME algorithm available through mothur. The sequences were classified using the Naïve Bayesian Classifier (80% confidence threshold) using the RDP training set and consensus taxonomy of OTUs was determined using the 80% cutoff. The main difference between the three different strategies lies in the OTU picking and downstream processing.

A1.1 Mothur Pipeline

In the typical mothur pipeline, the sequences are clustered into OTUs at sequence similarity cutoff of 97% using the average neighbor clustering algorithm. There is no singleton removal performed in this pipeline. Singleton removal or more generally removal of rare sequences involves removing OTUs that have sequences present in very low frequency in the samples. This is not recommended by the typical mothur pipeline

due to the underlying assumption in singleton removal. Singleton removal assumes that these rare sequences are due to sequencing errors and not from microorganisms that are present at very low quantities. Since removing these sequences would mean a loss in information and underestimation of diversity and richness of the community, this method is not recommended by the creators of mothur.

A1.2 Mothur with Singleton Removal

In this analysis strategy, the typical mothur pipeline was followed. After the sequences were clustered into OTUs based on 97% sequence similarity, the OTUs that occurred only once across all samples (singletons) were removed. This is based on the assumption that these OTUs were most likely due to sequencing errors.

A1.3 Phylotyping

In this analysis, the only change is in the OTU clustering procedure. Instead of basing the clustering strategy on sequence similarity cutoff, the sequences are first classified based on their taxonomy at the genus level and then grouped together based on their taxonomy. This method is known to underestimate diversity due to the small number of OTUs that is generated.

A2 Results and Discussion

An important consideration when studying community changes is the effect of microbial ecology analysis pipelines on the interpretation of the data. The interpretation of the change in relative abundances of bacterial classes (Figure A. 1) does not change significantly except for at time point 43 days for C/N ratio of 7.4 mg-C/mg-N, the mothur and phylotype pipeline show a lower relative abundance of *Deltaproteobacteria* compared to Singleton Removal pipeline. This is probably due to the removal of

singletons thus artificially leading to an increase in the relative abundance of *Deltaproteobacteria.*

When diversity indices are calculated for the different pipelines, both the phylotype and singleton removal pipelines show a significantly lower diversity compared to the mothur pipeline. This is to be expected since the number of OTUs in the mothur pipeline is greater than in the phylotype and singleton removal pipelines. Based on this comparison, if the diversity of the community is not under direct investigation, it might be better to use the mothur or phylotype pipeline since these constitute the analyses with least loss of information. Mothur pipeline is preferable and widely accepted. But an important factor to consider is that distance matrices, constructed from this pipeline when regions longer than 250 bp have been sequenced, tend to be very large and not manageable even with high performance computing. Hence it is advisable to stick to V4 sequencing unless there are very clear reasons to sequence a longer region such as discovery of novel sequences or evolutionary analysis.

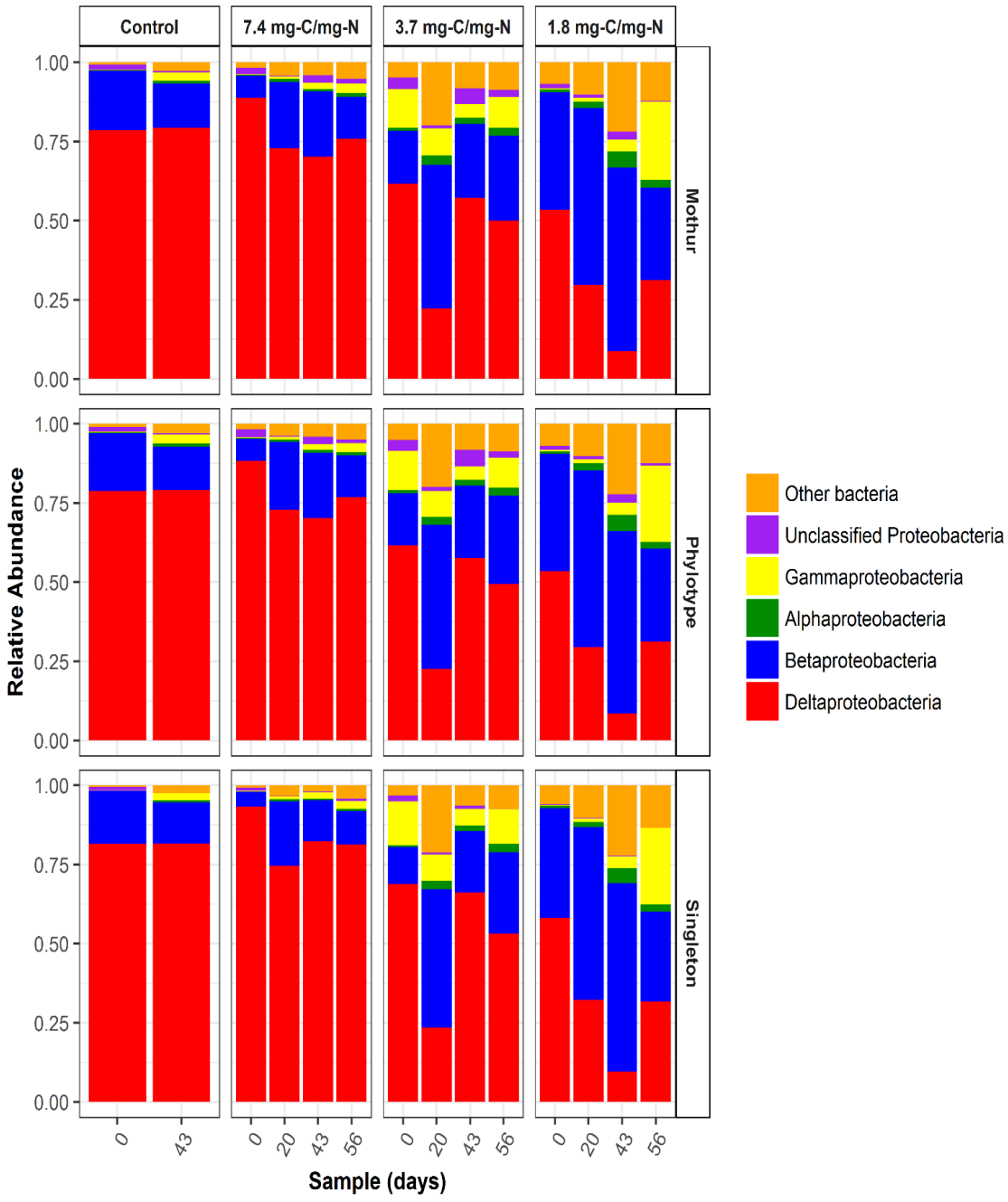

Figure A. 1: Comparison of Different Analysis Pipelines of Relative abundances of bacterial classes at different C/N ratios during different stages of the experiment. The most abundant phylum Proteobacteria has been shown as its classes with the other phyla grouped as Other bacteria.

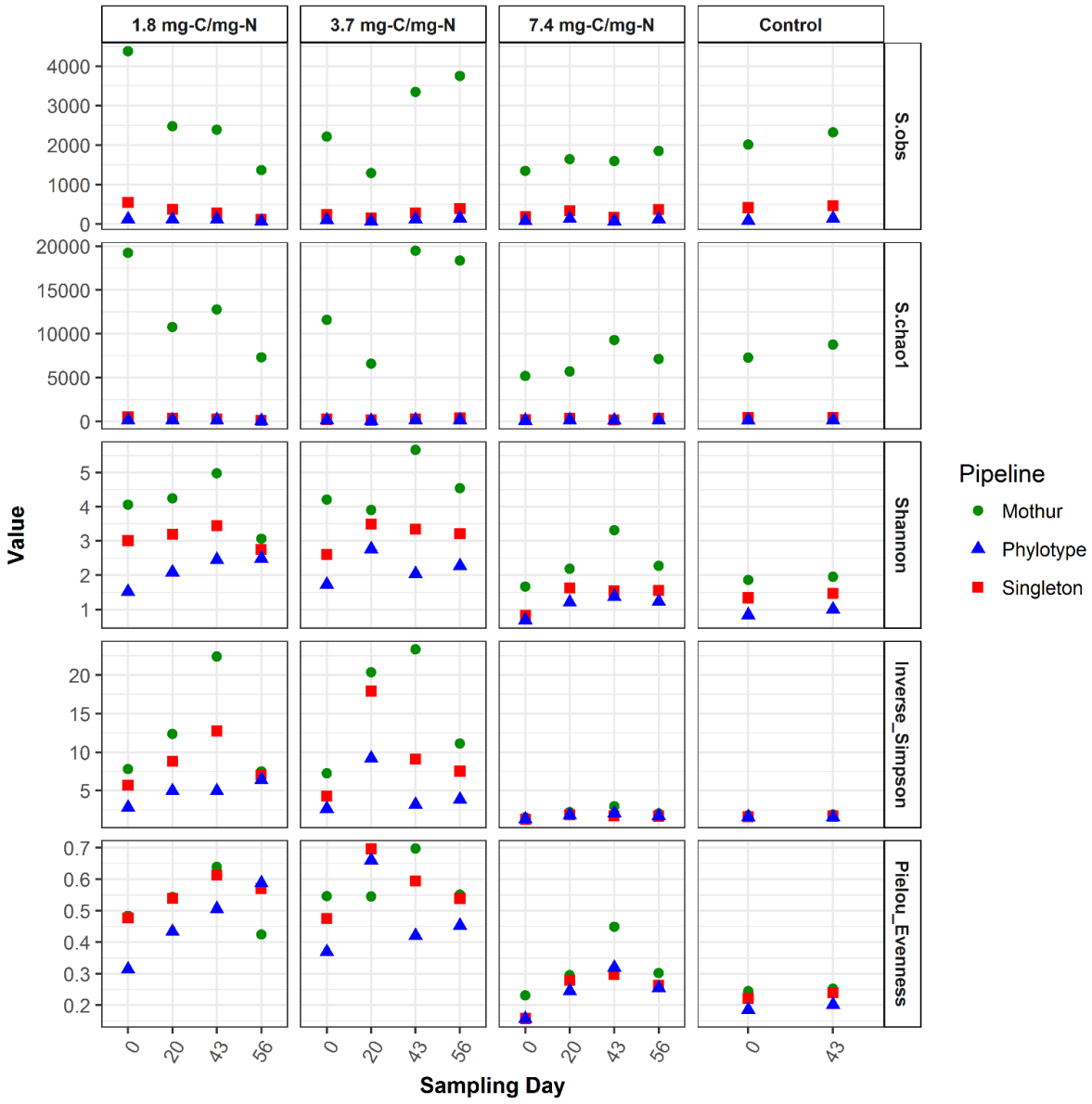

Figure A. 2: Comparison of diversity indices across different pipelines.

APPENDIX B

SUPPLEMENTARY INFORMATION

Table A. 1: RT-qPCR Calibration Results

Target.Name	Run	Intercept	Slope	Efficiency	R^2
16S	1	7.908186	-3.79401	83.47364	0.99919
16S	2	8.61584	-3.70202	86.26131	0.981978
Geo	1	7.554624	-3.99082	78.06347	0.998722
Geo	2	8.501949	-4.04128	76.78526	0.994563
nirK	1	12.45772	-3.02394	114.1381	0.92446
nirK	2	12.92621	-2.93841	118.9372	0.869303
nirS	1	18.27523	-4.99848	58.51148	0.990316
nirS	2	19.3528	-5.09987	57.06644	0.987452

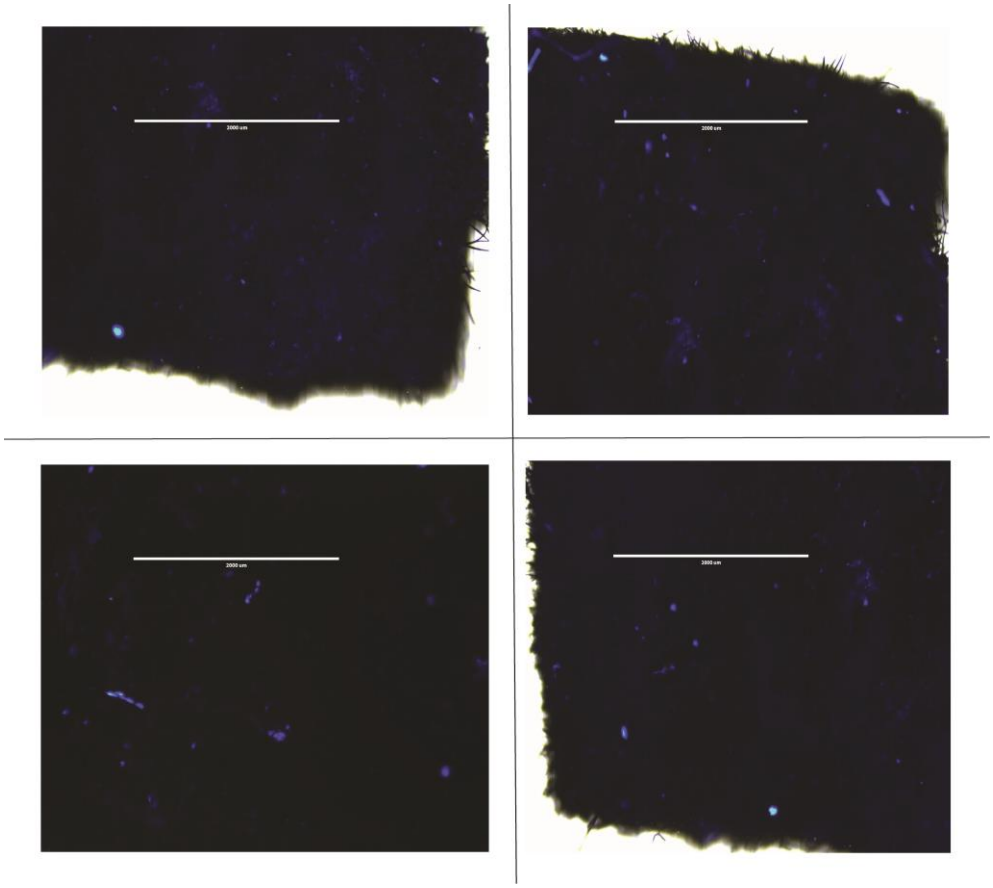

Figure A. 3: Microscopic images of the electrode stained with DAPI. DAPI stains nucleic acids and they appear blue on the black background of the electrode. The scale bar indicates a scale of 2000 µm.

REFERENCES

Aelterman, P., Rabaey, K., The Pham, H., Boon, N., Verstraete, W., 2006. Continuous electricity generation at high voltages and currents using stacked microbial fuel cells. Commun. Agric. Appl. Biol. Sci. 71, 63–6.

Aelterman, P., Versichele, M., Marzorati, M., Boon, N., Verstraete, W., 2008. Loading rate and external resistance control the electricity generation of microbial fuel cells with different three-dimensional anodes. Bioresour. Technol. 99, 8895–8902. doi:10.1016/j.biortech.2008.04.061

Aklujkar, M., Krushkal, J., DiBartolo, G., Lapidus, A., Land, M.L., Lovley, D.R., 2009. The genome sequence of Geobacter metallireducens: features of metabolism, physiology and regulation common and dissimilar to Geobacter sulfurreducens. BMC Microbiol. 9, 109. doi:10.1186/1471-2180-9-109

Albertsen, M., Karst, S.M., Ziegler, A.S., Kirkegaard, R.H., Nielsen, P.H., 2015. Back to Basics - The Influence of DNA Extraction and Primer Choice on Phylogenetic Analysis of Activated Sludge Communities. PLoS One 10, e0132783.

Bae, W., Rittmann, B.E., 1996. Responses of intracellular cofactors to single and dual substrate limitations. Biotechnol. Bioeng. 49, 690–699. doi:10.1002/(SICI)1097-0290(19960320)49:6<690::AID-BIT11>3.0.CO;2-A

Barak, Y., Tal, Y., Rijn, J. Van, 1998. Light-Mediated Nitrite Accumulation during Denitrification by Pseudomonas sp. Strain JR12. Appl. Environ. Microbiol. 64, 813–817.

Bass, R., Etcheverry, L., Bergel, A., 2007. Marine microbial fuel cell : Use of stainless steel electrodes as anode and cathode materials 2–7.

Bellini, M.I., Gutiérrez, L., Tarlera, S., Scavino, A.F., 2013. Isolation and functional analysis of denitrifiers in an aquifer with high potential for denitrification. Syst. Appl. Microbiol. 36, 505–516. doi:10.1016/j.syapm.2013.07.001

Bonanni, P.S., Massazza, D., Busalmen, J.P., 2013. Stepping stones in the electron transport from cells to electrodes in Geobacter sulfurreducens biofilms. Phys. Chem. Chem. Phys. 15, 10300–6. doi:10.1039/c3cp50411e

Bond, D.R., Holmes, D.E., Tender, L.M., Lovley, D.R., 2002. Electrode-Reducing Microorganisms That Harvest Energy from Marine Sediments. Science (80-.). 295, 483–485.

Bond, D.R., Lovley, D.R., 2003. Electricity Production by Geobacter sulfurreducens Attached to Electrodes. Appl. Environ. Microbiol. 69, 1548–1555. doi:10.1128/AEM.69.3.1548-1555.2003

Bond, D.R., Strycharz-Glaven, S.M., Tender, L.M., Torres, C.I., 2012. On electron transport through Geobacter biofilms. ChemSusChem 5, 1099–105. doi:10.1002/cssc.201100748

Bruning-Fann, C.S., Kaneene, J.B., 1993. The effects of nitrate, nitrite and N-nitroso compounds on human health: a review. Vet. Hum. Toxicol. 35, 521–38.

Busalmen, J.P., Esteve-Nuñez, A., Feliu, J.M., 2008. Whole Cell Electrochemistry of Electricity-Producing Microorganisms Evidence an Adaptation for Optimal Exocellular Electron Transport. Environ. Sci. Technol. 42, 2445–2450. doi:10.1021/es702569y

Butler, C.S., Clauwaert, P., Green, S.J., Verstraete, W., Nerenberg, R., 2010. Bioelectrochemical perchlorate reduction in a microbial fuel cell. Environ. Sci. Technol. 44, 4685–91. doi:10.1021/es901758z

Butler, C.S., Nerenberg, R., 2010. Performance and microbial ecology of air-cathode microbial fuel cells with layered electrode assemblies. Appl. Microbiol. Biotechnol. 86, 1399–1408. doi:10.1007/s00253-009-2421-x

Caccavo, F., Lonergan, D.J., Lovley, D.R., Davis, M., Stolz, J.F., McInerney, M.J., 1994. Geobacter sulfurreducens sp. nov., a hydrogen- and acetate-oxidizing dissimilatory metal-reducing microorganism. Appl. Environ. Microbiol. 60, 3752–9.

Castro, C.J., Goodwill, J.E., Rogers, B., Henderson, M., Butler, C.S., 2014. Deployment of the microbial fuel cell latrine in Ghana for decentralized sanitation. J. Water, Sanit. Hygeine Dev. 4, 663–671. doi:10.2166/washdev.2014.020

Chae, K.J., Choi, M., Ajayi, F.F., Park, W., Chang, I.S., Kim, I.S., 2008. Mass Transport through a Proton Exchange Membrane (Nafion) in Microbial Fuel Cells † 169–176.

Channiwala, S.A., Parikh, P.P., 2002. A unified correlation for estimating HHV of solid , liquid and gaseous fuels. Fuel 81, 1051–1063.

Chaudhuri, S.K., Lovley, D.R., 2003. Electricity generation by direct oxidation of glucose in mediatorless microbial fuel cells. Nat. Biotechnol. 21, 1229–32. doi:10.1038/nbt867

Cheng, S., Liu, H., Logan, B.E., 2006. Increased performance of single-chamber microbial fuel cells using an improved cathode structure. Electrochem. commun. 8, 489–494. doi:10.1016/j.elecom.2006.01.010

Cheng, S., Logan, B.E., 2011. Increasing power generation for scaling up single-chamber air cathode microbial fuel cells. Bioresour. Technol. 102, 4468–73. doi:10.1016/j.biortech.2010.12.104

Cherchi, C., Onnis-Hayden, A., El-Shawabkeh, I., Gu, A.Z., 2009. Implication of using different carbon sources for denitrification in wastewater treatments. Water Environ. Res. 81, 788–799. doi:10.2175/106143009X12465435982610

Christophersen, C.T., Morrison, M., Conlon, M.A., 2011. Overestimation of the abundance of sulfate-reducing bacteria in human feces by quantitative PCR targeting the Desulfovibrio 16S rRNA gene. Appl. Environ. Microbiol. 77, 3544–3546. doi:10.1128/AEM.02851-10

Ciudad, G., Rubilar, O., Muñoz, P., Ruiz, G., Chamy, R., Vergara, C., Jeison, D., 2005. Partial nitrification of high ammonia concentration wastewater as a part of a shortcut biological nitrogen removal process. Process Biochem. 40, 1715–1719. doi:10.1016/j.procbio.2004.06.058

Claus, G., Kutzner, H.J., 1985. Physiology and kinetics of autotrophic denitrification by Thiobacillus denitrificans. Appl. Microbiol. Biotechnol. 22. doi:10.1007/BF00252032

Clauwaert, P., Aelterman, P., Pham, T.H., De Schamphelaire, L., Carballa, M., Rabaey, K., Verstraete, W., 2008. Minimizing losses in bio-electrochemical systems: the road to applications. Appl. Microbiol. Biotechnol. 79, 901–913. doi:10.1007/s00253-008-1522-2

Clauwaert, P., Desloover, J., Shea, C., Nerenberg, R., Boon, N., Verstraete, W., 2009. Enhanced nitrogen removal in bio-electrochemical systems by pH control. Biotechnol. Lett. 31, 1537–1543. doi:10.1007/s10529-009-0048-8

Clauwaert, P., Rabaey, K., Aelterman, P., de Schamphelaire, L., Pham, T.H., Boeckx, P., Boon, N., Verstraete, W., 2007a. Biological denitrification in microbial fuel cells. Environ. Sci. Technol. 41, 3354–60.

Clauwaert, P., Van der Ha, D., Boon, N., Verbeken, K., Verhaege, M., Rabaey, K., Verstraete, W., 2007b. Open air biocathode enables effective electricity generation with microbial fuel cells. Environ. Sci. Technol. 41, 7564–9.

Commault, A.S., Lear, G., Packer, M. a, Weld, R.J., 2013. Influence of anode potentials on selection of Geobacter strains in microbial electrolysis cells. Bioresour. Technol. 139, 226–34. doi:10.1016/j.biortech.2013.04.047

Cruz-García, C., Murray, A.E., Klappenbach, J.A., Stewart, V., Tiedje, J.M., 2007. Respiratory nitrate ammonification by *Shewanella oneidensis* MR-1. J. Bacteriol. 189, 656–662. doi:10.1128/JB.01194-06

Deb, K., Pratap, A., Agarwal, S., Meyarivan, T., 2002. A fast and elitist multiobjective genetic algorithm: NSGA-II. IEEE Trans. Evol. Comput. 6, 182–197. doi:10.1109/4235.996017

Desloover, J., Puig, S., Virdis, B., Clauwaert, P., Boeckx, P., Verstraete, W., Boon, N., 2011. Biocathodic nitrous oxide removal in bioelectrochemical systems. Environ. Sci. Technol. 45, 10557–66. doi:10.1021/es202047x

Dewan, A., Beyenal, H., Lewandowski, Z., 2008. Scaling up microbial fuel cells. Environ. Sci. Technol. 42, 7643–8.

Du, Z., Li, H., Gu, T., 2007. A state of the art review on microbial fuel cells: A promising technology for wastewater treatment and bioenergy. Biotechnol. Adv. 25, 464–82. doi:10.1016/j.biotechadv.2007.05.004

Dugan, P.R., Stoner, D.L., Pickrum, H.M., 1992. The Genus Zoogloea, in: Balows, A., Trüper, H.G., Dworkin, M., Harder, W., Schleifer, K.-H. (Eds.), The Prokaryotes: A Handbook on the Biology of Bacteria: Ecophysiology, Isolation, Identification, Applications. Springer New York, New York, NY, pp. 3952–3964. doi:10.1007/978-1-4757-2191-1_58

EPA, 2001. Development and Adoption of Nutrient Criteria into Water Quality Standards.

EPA, 2007. Biological Nutrient Removal: Processes and Costs.

EPRI, 1994. Energy Audit Manual for Water/Wastewater Facilities.

Esteve-Núñez, A., Rothermich, M., Sharma, M., Lovley, D., 2005. Growth of Geobacter sulfurreducens under nutrient-limiting conditions in continuous culture. Environ. Microbiol. 7, 641–648. doi:10.1111/j.1462-2920.2005.00731.x

Fan, A.M., Steinberg, V.E., 1996. Health Implications of Nitrate and Nitrite in Drinking Water: An Update on Methemoglobinemia Occurrence and Reproductive and Developmental Toxicity. Regul. Toxicol. Pharmacol. 23, 35–43. doi:10.1006/rtph.1996.0006

Finkelstein, D.A., Tender, L.M., Zeikus, G.J., 2006. Effect of Electrode Potential on Electrode-Reducing Microbiota. Environ. Sci. Technol. 40, 6990–6995. doi:10.1021/es061146m

Franks, A.E., Nevin, K.P., 2010. Microbial Fuel Cells, A Current Review. Energies 3, 899–919. doi:10.3390/en3050899

Franks, A.E., Nevin, K.P., Jia, H., Izallalen, M., Woodard, T.L., Lovley, D.R., 2009. Novel strategy for three-dimensional real-time imaging of microbial fuel cell communities: monitoring the inhibitory effects of proton accumulation within the anode biofilm. Energy Environ. Sci. 2, 113. doi:10.1039/b816445b

Freguia, S., Rabaey, K., Yuan, Z., Keller, J., 2007. Electron and carbon balances in microbial fuel cells reveal temporary bacterial storage behavior during electricity generation. Environ. Sci. Technol. 41, 2915–2921. doi:10.1021/es062611i

Freguia, S., Rabaey, K., Yuan, Z., Keller, J., 2008a. Syntrophic processes drive the conversion of glucose in microbial fuel cell anodes. Environ. Sci. Technol. Technol. 42, 7937–7943. doi:10.1021/es800482e

Freguia, S., Rabaey, K., Yuan, Z., Keller, J., 2008b. Sequential anode-cathode configuration improves cathodic oxygen reduction and effluent quality of microbial fuel cells. Water Res. 42, 1387–96. doi:10.1016/j.watres.2007.10.007

Füchslin, H.P., Schneider, C., Egli, T., 2012. In glucose-limited continuous culture the minimum substrate concentration for growth, Smin, is crucial in the competition between the enterobacterium Escherichia coli and Chelatobacter heintzii, an environmentally abundant bacterium. ISME J. 6, 777–789. doi:10.1038/ismej.2011.143

Gao, C., Wang, A., Wu, W.-M., Yin, Y., Zhao, Y.-G., 2014. Enrichment of anodic biofilm inoculated with anaerobic or aerobic sludge in single chambered air-cathode microbial fuel cells. Bioresour. Technol. 167, 124–132. doi:10.1016/j.biortech.2014.05.120

Ge, Z., Zhang, F., Grimaud, J., Hurst, J., He, Z., 2013. Long-term investigation of microbial fuel cells treating primary sludge or digested sludge. Bioresour. Technol. 136, 509–514. doi:10.1016/j.biortech.2013.03.016

Gregoire, K.P., Glaven, S.M., Hervey, J., Lin, B., Tender, L.M., 2014. Enrichment of a High-Current Density Denitrifying Microbial Biocathode. J. Electrochem. Soc. 161, H3049–H3057. doi:10.1149/2.0101413jes

Gregory, K.B., Bond, D.R., Lovley, D.R., 2004. Graphite electrodes as electron donors for anaerobic respiration. Environ. Microbiol. 6, 596–604. doi:10.1111/j.1462-2920.2004.00593.x

Gregory, K.B., Lovley, D.R., 2005. Remediation and recovery of uranium from contaminated subsurface environments with electrodes. Environ. Sci. Technol. 39, 8943–7. doi:10.1021/es050457e

Guerrero-Rangel, N., Rodriguez-de la Garza, J.A., Garza-Garcia, Y., Rios-Gonzalez, L.J., Sosa-Santillan, G.J., de la Garza-Rodrguez, I.M., Martinez-Amador, S.Y., Rodriguez-Garza, M.M., Rodriguez-Martinez, J., 2010. Comparative Study of Three Cathodic Electron Acceptors on the Performance of Mediatorless Microbial Fuel Cell. Int. J. Electr. Power Eng. 4, 27–31.

Habermann, W., Pommer, E.H., 1991. Biological Fuel-Cells with Sulfide Storage Capacity. Appl. Microbiol. Biotechnol. 35, 128–133.

He, Z., Angenent, L.T., 2006. Application of Bacterial Biocathodes in Microbial Fuel Cells. Electroanalysis 18, 2009–2015. doi:10.1002/elan.200603628

He, Z., Mansfeld, F., 2009. Exploring the use of electrochemical impedance spectroscopy (EIS) in microbial fuel cell studies. Energy Environ. Sci. 2, 215–219. doi:10.1039/b814914c

He, Z., Minteer, S.D., Angenent, L.T., 2005. Electricity Generation from Artificial Wastewater Using an Upflow Microbial Fuel Cell. Environ. Sci. Technol. 39, 5262–5267. doi:10.1021/es0502876

Heidrich, E.S., Curtis, T.P., Dolfing, J., 2011. Determination of the internal chemical energy of wastewater. Environ. Sci. Technol. 45, 827–832.

Henry, S., Baudoin, E., López-Gutiérrez, J.C., Martin-Laurent, F., Brauman, A., Philippot, L., 2004. Quantification of denitrifying bacteria in soils by nirK gene targeted real-time PCR. J. Microbiol. Methods 59, 327–35. doi:10.1016/j.mimet.2004.07.002

Hernandez, M.E., Newman, D.K., 2001. Extracellular electron transfer. Cell. Mol. Sci. 58, 1562–1571.

Hiatt, W.C., Grady, C.P.L., 2008. An updated process model for carbon oxidation, nitrification, and denitrification. Water Environ. Res. 80, 2145–2156. doi:10.2175/106143008X304776

Himmelheber, D.W., Thomas, S.H., Löffler, F.E., Taillefert, M., Hughes, J.B., 2009. Microbial colonization of an in situ sediment cap and correlation to stratified redox zones. Environ. Sci. Technol. 43, 66–74. doi:10.1021/es801834e

IPCC, Houghton, J.T., Ding, Y., Griggs, D.J., Noguer, M., van der Linden, P.J., Dai, X., Maskell, K., Johnson, C.A., 2001. Climate Change 2001: The Scientific Basis. Cambridge University Press, Cambridge, United Kingdom and New York, NY, USA.

Joshi, N., Fass, J., 2011. Sickle: A sliding-window, adaptive, quality-based trimming tool for FastQ files.

Jung, S., Regan, J.M., 2011. Influence of external resistance on electrogenesis, methanogenesis, and anode prokaryotic communities in microbial fuel cells. Appl. Environ. Microbiol. 77, 564–71. doi:10.1128/AEM.01392-10

Kandeler, E., Deiglmayr, K., Tscherko, D., Bru, D., Philippot, L., 2006. Abundance of narG, nirS, nirK, and nosZ genes of denitrifying bacteria during primary successions of a glacier foreland. Appl. Environ. Microbiol. 72, 5957–62. doi:10.1128/AEM.00439-06

Kashima, H., Regan, J.M., 2015. Facultative nitrate reduction by electrode-respiring Geobacter metallireducens biofilms as a competitive reaction to electrode reduction in a bioelectrochemical system. Environ. Sci. Technol. 49, 3195–3202. doi:10.1021/es504882f

Ki, D., Park, J., Lee, J., Yoo, K., 2008. Microbial diversity and population dynamics of activated sludge microbial communities participating in electricity generation in microbial fuel cells. Water Sci. Technol. 58, 2195–2201. doi:10.2166/wst.2008.577

Kiely, P.D., Call, D.F., Yates, M.D., Regan, J.M., Logan, B.E., 2010. Anodic biofilms in microbial fuel cells harbor low numbers of higher-power-producing bacteria than abundant genera. Appl. Microbiol. Biotechnol. 88, 371–380. doi:10.1007/s00253-010-2757-2

Kiely, P.D., Cusick, R., Call, D.F., Selembo, P.A., Regan, J.M., Logan, B.E., 2011. Anode microbial communities produced by changing from microbial fuel cell to microbial electrolysis cell operation using two different wastewaters. Bioresour. Technol. 102, 388–394. doi:10.1016/j.biortech.2010.05.019

Kiely, P.D., Regan, J.M., Logan, B.E., 2011. The electric picnic: synergistic requirements for exoelectrogenic microbial communities. Curr. Opin. Biotechnol. 22, 378–385. doi:10.1016/j.copbio.2011.03.003

Kim, B.-H., Kim, H.-J., Hyun, M.-S., Park, D.-H., 1999. Direct Electrode Reaction of Fe (III)- Reducing Bacterium *Shewenella putrefaciens*. J. Microbiol. Biotechnol. 9, 127–131.

Kim, G.T., Webster, G., Wimpenny, J.W.T., Kim, B.H., Kim, H.J., Weightman, a J., 2006. Bacterial community structure, compartmentalization and activity in a microbial fuel cell. J. Appl. Microbiol. 101, 698–710. doi:10.1111/j.1365-2672.2006.02923.x

Knowles, R., 1982. Denitrification. Microbiol. Rev. 46, 43–70.

Körner, H., Zumft, W.G., 1989. Expression of denitrification enzymes in response to the dissolved oxygen level and respiratory substrate in continuous culture of Pseudomondas stutzeri. Appl. Environ. Microbiol. 55, 1670–1676.

Kozich, J.J., Westcott, S.L., Baxter, N.T., Highlander, S.K., Schloss, P.D., 2013. Development of a dual-index sequencing strategy and curation pipeline for analyzing amplicon sequence data on the MiSeq Illumina sequencing platform. Appl. Environ. Microbiol. 79, 5112–5120. doi:10.1128/AEM.01043-13

Lee, H.-S., Parameswaran, P., Kato-Marcus, A., Torres, C.I., Rittmann, B.E., 2008. Evaluation of energy-conversion efficiencies in microbial fuel cells (MFCs) utilizing fermentable and non-fermentable substrates. Water Res. 42, 1501–10. doi:10.1016/j.watres.2007.10.036

Lee, H.-S.S., Torres, C.I., Rittmann, B.E., Torres, Ć.I., Rittmann, B.E., 2009. Effects of substrate diffusion and anode potential on kinetic parameters for anode-respiring bacteria. Environ. Sci. Technol. 43, 7571–7577. doi:Doi 10.1021/Es9015519

Lewis, W.M.J., Morris, D.P., 1986. Toxicity of Nitrite to Fish: A Review. Trans. Am. Fish. Soc. 115, 183–195.

Li, W.-W., Yu, H.-Q., He, Z., 2014. Towards sustainable wastewater treatment by using microbial fuel cells-centered technologies. Energy Environ. Sci. 7, 911. doi:10.1039/c3ee43106a

Li, Z., Zhang, X., Lin, J., Han, S., Lei, L., 2010. Azo dye treatment with simultaneous electricity production in an anaerobic-aerobic sequential reactor and microbial fuel cell coupled system. Bioresour. Technol. 101, 4440–5. doi:10.1016/j.biortech.2010.01.114

Liu, H., Cheng, S.A., Logan, B.E., 2005a. Production of electricity from acetate or butyrate using a single-chamber microbial fuel cell. Environ. Sci. Technol. 39, 658–662. doi:10.1021/es048927c

Liu, H., Cheng, S., Logan, B.E., 2005b. Power Generation in Fed-Batch Microbial Fuel Cells as a Function of Ionic Strength , Temperature , and Reactor Configuration. Environ. Sci. Technol. 39, 5488–5493.

Liu, H., Logan, B.E., 2004. Electricity Generation Using an Air-Cathode Single Chamber Microbial Fuel Cell in the Presence and Absence of a Proton Exchange Membrane. Environ. Sci. Technol. 38, 4040–4046. doi:10.1021/es0499344

Liu, H., Ramnarayanan, R., Logan, B.E., 2004. Production of Electricity during Wastewater Treatment Using a Single Chamber Microbial Fuel Cell. Environ. Sci. Technol. 38, 2281–2285. doi:10.1021/es034923g

Logan, B.E., 2008. Microbial Fuel Cells. John Wiley & Sons.

Logan, B.E., 2010. Scaling up microbial fuel cells and other bioelectrochemical systems. Appl. Microbiol. Biotechnol. 85, 1665–1671. doi:10.1007/s00253-009-2378-9

Logan, B.E., Hamelers, B., Rozendal, R., Schröder, U., Keller, J., Freguia, S., Aelterman, P., Verstraete, W., Rabaey, K., 2006. Microbial Fuel Cells: Methodology and Technology. Environ. Sci. Technol. 40, 5181–5192.

Logan, B.E., Regan, J.M., 2006a. Microbial Fuel Cells- Challenges and Applications. Environ. Sci. Technol. 40, 5172–5180.

Logan, B.E., Regan, J.M., 2006b. Electricity-producing bacterial communities in microbial fuel cells. Trends Microbiol. 14, 512–8. doi:10.1016/j.tim.2006.10.003

Lovley, D.R., 2006. Bug juice: harvesting electricity with microorganisms. Nat. Rev. Microbiol. 4, 497–508. doi:10.1038/nrmicro1442

Lovley, D.R., Phillips, E.J.P., 1988. Novel Mode of Microbial Energy Metabolism: Organic Carbon Oxidation Coupled to Dissimilatory Reduction of Iron or Manganese. Appl. Environ. Microbiol. 54, 1472–1480.

Lozupone, C., Knight, R., 2005. UniFrac: a new phylogenetic method for comparing microbial communities. Appl. Environ. Microbiol. 71, 8228–8235. doi:10.1128/AEM.71.12.8228-8235.2005

Malvankar, N.S., Lau, J., Nevin, K.P., Franks, A.E., Tuominen, M.T., Lovley, D.R., 2012. Electrical conductivity in a mixed-species biofilm. Appl. Environ. Microbiol. 78, 5967–71. doi:10.1128/AEM.01803-12

Malvankar, N.S., Vargas, M., Nevin, K.P., Franks, A.E., Leang, C., Kim, B.-C., Inoue, K., Mester, T., Covalla, S.F., Johnson, J.P., Rotello, V.M., Tuominen, M.T., Lovley, D.R., 2011. Tunable metallic-like conductivity in microbial nanowire networks. Nat. Nanotechnol. 6, 573–9. doi:10.1038/nnano.2011.119

Marcus, A.K., Torres, C.I., Rittmann, B.E., 2007. Conduction-Based Modeling of the Biofilm Anode of a Microbial Fuel Cell. Biotechnol. Bioeng. 98, 1171–1182. doi:10.1002/bit

Marsili, E., Rollefson, J.B., Baron, D.B., Hozalski, R.M., Bond, D.R., 2008. Microbial biofilm voltammetry: direct electrochemical characterization of catalytic electrode-attached biofilms. Appl. Environ. Microbiol. 74, 7329–37. doi:10.1128/AEM.00177-08

Martínez Murillo, F., Gugliuzza, T., Senko, J., Basu, P., Stolz, J.F., 1999. A heme-C-containing enzyme complex that exhibits nitrate and nitrite reductase activity from the dissimilatory iron-reducing bacterium *Geobacter metallireducens*. Arch. Microbiol. 172, 313–320. doi:10.1007/s002030050785

Matsuda, S., Liu, H., Hashimoto, K., Nakanishi, S., 2012. Potential and Cell Density Dependences of Extracellular Electron Transfer of Anode-Respiring Geobacter sulfurreducens Cells. Electrochemistry 80, 330–333. doi:10.5796/electrochemistry.80.330

McMurdie, P.J., Holmes, S., 2013. phyloseq: An R Package for Reproducible Interactive Analysis and Graphics of Microbiome Census Data. PLoS One 8. doi:10.1371/journal.pone.0061217

Merkey, B. V, Chopp, D.L., 2014. Modeling the impact of interspecies competition on performance of a microbial fuel cell. Bull. Math. Biol. 76, 1429–53. doi:10.1007/s11538-014-9968-0

Miceli, J.F., Parameswaran, P., Kang, D.-W., Krajmalnik-Brown, R., Torres, C.I., 2012. Enrichment and analysis of anode-respiring bacteria from diverse anaerobic inocula. Environ. Sci. Technol. 46, 10349–55. doi:10.1021/es301902h

Miran, W., Nawaz, M., Kadam, A., Shin, S., Heo, J., Jang, J., Lee, D.S., 2015. Microbial community structure in a dual chamber microbial fuel cell fed with brewery waste for azo dye degradation and electricity generation. Environ. Sci. Pollut. Res. 22, 13477–13485. doi:10.1007/s11356-015-4582-8

Monod, J., 1949. The growth of bacterial cultures. Annu. Rev. Microbiol. 3, 371–394.

Nevin, K.P., Lovley, D.R., 2000. Lack of Production of Electron-Shuttling Compounds or Solubilization of Fe(III) during Reduction of Insoluble Fe(III) Oxide by Geobacter metallireducens. Appl. Environ. Microbiol. 66, 2248–2251. doi:10.1128/AEM.66.5.2248-2251.2000

Newman, D.K., Kolter, R., 2000. A role for excreted quinones in extracellular electron transfer. Nature 405, 94–97. doi:10.1038/35011098

Nguyen, V.K., Hong, S., Park, Y., Jo, K., Lee, T., 2014. Autotrophic denitrification performance and bacterial community at biocathodes of bioelectrochemical systems with either abiotic or biotic anodes. J. Biosci. Bioeng. doi:10.1016/j.jbiosc.2014.06.016

Okamoto, A., Nakamura, R., Nealson, K.H., Hashimoto, K., 2014. Bound Flavin Model Suggests Similar Electron-Transfer Mechanisms in *Shewanella* and *Geobacter*. ChemElectroChem 1, 1808–1812. doi:10.1002/celc.201402151

Oksanen, J., Blanchet, F.G., Friendly, M., Kindt, R., Legendre, P., McGlinn, D., Minchin, P.R., O'Hara, R.B., Simpson, G.L., Solymos, P., Stevens, M.H.H., Szoecs, E., Wagner, H., 2016. vegan: Community Ecology Package.

Pan, Y., Ni, B.-J., Lu, H., Chandran, K., Richardson, D., Yuan, Z., 2015. Evaluating two concepts for the modelling of intermediates accumulation during biological denitrification in wastewater treatment. Water Res. 71, 21–31. doi:10.1016/j.watres.2014.12.029

Pan, Y., Ni, B.J., Yuan, Z., 2013. Modeling electron competition among nitrogen oxides reduction and N 2O accumulation in denitrification. Environ. Sci. Technol. 47, 11083–11091. doi:10.1021/es402348n

Pandit, S., Sengupta, A., Kale, S., Das, D., 2011. Performance of electron acceptors in catholyte of a two-chambered microbial fuel cell using anion exchange membrane. Bioresour. Technol. 102, 2736–2744. doi:10.1016/j.biortech.2010.11.038

Parameswaran, P., Torres, C.I., Lee, H.-S., Krajmalnik-Brown, R., Rittmann, B.E., 2009. Syntrophic interactions among anode respiring bacteria (ARB) and Non-ARB in a biofilm anode: electron balances. Biotechnol. Bioeng. 103, 513–23. doi:10.1002/bit.22267

Park, T.-J., Ding, W., Cheng, S., Brar, M.S., Ma, A.P.Y., Tun, H.M., Leung, F.C., 2014. Microbial community in microbial fuel cell (MFC) medium and effluent enriched with purple photosynthetic bacterium (Rhodopseudomonas sp.). AMB Express 4, 22. doi:10.1186/s13568-014-0022-2

Parot, S., Délia, M.-L., Bergel, A., 2008. Forming electrochemically active biofilms from garden compost under chronoamperometry. Bioresour. Technol. 99, 4809–4816. doi:10.1016/j.biortech.2007.09.047

Pelletier, G.J., Chapra, S.C., Tao, H., 2006. QUAL2Kw – A framework for modeling water quality in streams and rivers using a genetic algorithm for calibration. Environ. Model. Softw. 21, 419–425. doi:10.1016/j.envsoft.2005.07.002

Pham, T.H., Boon, N., Aelterman, P., Clauwaert, P., De Schamphelaire, L., Vanhaecke, L., De Maeyer, K., Höfte, M., Verstraete, W., Rabaey, K., 2008. Metabolites produced by Pseudomonas sp. enable a Gram-positive bacterium to achieve extracellular electron transfer. Appl. Microbiol. Biotechnol. 77, 1119–1129. doi:10.1007/s00253-007-1248-6

Pham, T.H., Rabaey, K., Aelterman, P., Clauwaert, P., De Schamphelaire, L., Boon, N., Verstraete, W., 2006. Microbial Fuel Cells in Relation to Conventional Anaerobic Digestion Technology. Eng. Life Sci. 6, 285–292. doi:10.1002/elsc.200620121

Phung, N.T., Lee, J., Kang, K.H., Chang, I.S., Gadd, G.M., Kim, B.H., 2004. Analysis of microbial diversity in oligotrophic microbial fuel cells using 16S rDNA sequences. FEMS Microbiol. Lett. 233, 77–82. doi:10.1016/j.femsle.2004.01.041

Picioreanu, C., Van Loosdrecht, M.C.M., Katuri, K.P., Scott, K., Head, I.M., 2008. Mathematical model for microbial fuel cells with anodic biofilms and anaerobic digestion. Water Sci. Technol. 57, 965–971. doi:10.2166/wst.2008.095

Picioreanu, C., Xavier, J.B., van Loosdrecht, M.C.M., 2004. Advances in mathematical modeling of biofilm structure. Biofilms 1, 337–349. doi:10.1017/S1479050505001572

Pinto, R.P., Srinivasan, B., Guiot, S.R., Tartakovsky, B., 2011. The effect of real-time external resistance optimization on microbial fuel cell performance. Water Res. 45, 1571–1578. doi:10.1016/j.watres.2010.11.033

Pinto, R.P., Srinivasan, B., Manuel, M.-F., Tartakovsky, B., 2010. A two-population bio-electrochemical model of a microbial fuel cell. Bioresour. Technol. 101, 5256–65. doi:10.1016/j.biortech.2010.01.122

Pocaznoi, D., Calmet, A., Etcheverry, L., Erable, B., Bergel, A., 2012. Stainless steel is a promising electrode material for anodes of microbial fuel cells. Energy Environ. Sci. 5, 9645. doi:10.1039/c2ee22429a

Potter, M.C., 1911. Electrical Effects Accompanying the Decomposition of Organic Compounds. Proc. R. Soc. London. Ser. B, Contain. Pap. a Biol. Character 84, 260–276.

Puig, S., Serra, M., Vilar-Sanz, A., Cabré, M., Bañeras, L., Colprim, J., Balaguer, M.D., 2011. Autotrophic nitrite removal in the cathode of microbial fuel cells. Bioresour. Technol. 102, 4462–7. doi:10.1016/j.biortech.2010.12.100

Rabaey, K., Boon, N., Siciliano, S.D., Verhaege, M., Verstraete, W., 2004. Biofuel Cells Select for Microbial Consortia That Self-Mediate Electron Transfer. Appl. Environ. Microbiol. 70, 5373–5382. doi:10.1128/AEM.70.9.5373

Rabaey, K., Lissens, G., Siciliano, S.D., Verstraete, W., 2003. A microbial fuel cell capable of converting glucose to electricity at high rate and efficiency. Biotechnol. Lett. 25, 1531–1535. doi:10.1023/A:1025484009367

R Core Team, 2015. R: A language and environment for statistical computing. R Foundation for Statistical Computing, Vienna, Austria.

Read, S.T., Dutta, P., Bond, P.L., Keller, J., Rabaey, K., 2010. Initial development and structure of biofilms on microbial fuel cell anodes. BMC Microbiol. 10, 98. doi:10.1186/1471-2180-10-98

Rezaei, F., Richard, T.L., Logan, B.E., 2008. Enzymatic Hydrolysis of Cellulose Coupled With Electricity Generation in a Microbial Fuel Cell. Biotechnol. Bioeng. 101, 1163–1169. doi:10.1002/bit.22015

Rhoads, A., Beyenal, H., Lewandowski, Z., 2005. Microbial Fuel Cell using Anaerobic Respiration as an Anodic Reaction and Biomineralized Manganese as a Cathodic Reactant. Environ. Sci. Technol. 39, 4666–4671. doi:10.1021/es048386r

Rinaldi, A., Mecheri, B., Garavaglia, V., Licoccia, S., Di Nardo, P., Traversa, E., 2008. Engineering materials and biology to boost performance of microbial fuel cells: a critical review. Energy Environ. Sci. 1, 417. doi:10.1039/b806498a

Rismani-Yazdi, H., Christy, A.D., Carver, S.M., Yu, Z., Dehority, B.A., Tuovinen, O.H., 2011. Effect of external resistance on bacterial diversity and metabolism in cellulose-fed microbial fuel cells. Bioresour. Technol. 102, 278–283. doi:10.1016/j.biortech.2010.05.012

Rittmann, B.E., McCarty, P.L., 2001. Environmental Biotechnology: Principles and Applications. New York:McGraw-Hill.

Rotaru, A.-E., Shrestha, P.M., Liu, F., Markovaite, B., Chen, S., Nevin, K.P., Lovley, D.R., 2014. Direct Interspecies Electron Transfer between Geobacter metallireducens and Methanosarcina barkeri. Appl. Environ. Microbiol. 80, 4599–4605. doi:10.1128/AEM.00895-14

Schloss, P.D., Westcott, S.L., Ryabin, T., Hall, J.R., Hartmann, M., Hollister, E.B., Lesniewski, R.A., Oakley, B.B., Parks, D.H., Robinson, C.J., Sahl, J.W., Stres, B., Thallinger, G.G., Van Horn, D.J., Weber, C.F., 2009. Introducing mothur: Open-source, platform-independent, community-supported software for describing and comparing microbial communities. Appl. Environ. Microbiol. 75, 7537–7541. doi:10.1128/AEM.01541-09

Schröder, U., 2007. Anodic electron transfer mechanisms in microbial fuel cells and their energy efficiency. Phys. Chem. Chem. Phys. 9, 2619–29. doi:10.1039/b703627m

Shantaram, A., Beyenal, H., Raajan, R., Veluchamy, A., Lewandowski, Z., 2005. Wireless Sensors Powered by Microbial Fuel Cells. Environ. Sci. Technol. 39, 5037–5042.

Shizas, I., Bagley, D.M., Asce, M., 2005. Experimental Determination of Energy Content of Unknown Organics in Municipal Wastewater Streams 130, 45–53.

Snider, R.M., Strycharz-Glaven, S.M., Tsoi, S.D., Erickson, J.S., Tender, L.M., 2012. Long-range electron transport in Geobacter sulfurreducens biofilms is redox gradient-driven. Proc. Natl. Acad. Sci. U. S. A. 109, 15467–72. doi:10.1073/pnas.1209829109

Soetaert, K., Perzoldt, T., Setzer, W.R., 2010. Solving Differential Equations in R: Package deSolve. J. Stat. Softw. 33, 1–25.

Sogin, M.L., Morrison, H.G., Huber, J.A., Welch, D.M., Huse, S.M., Neal, P.R., Arrieta, J.M., Herndi, G.J., 2006. Microbial Diversity in the Deep Sea and the Underexplored "Rare Biosphere." Proc. Natl. Acad. Sci. 103, 12115–12120. doi:10.1002/9781118010549.ch24

Strand, S.E., McDonnell, A.J., Unz, R.F., 1988. Oxygen and nitrate reduction kinetics of a nonflocculating strain of Zoogloea ramigera. Antonie Van Leeuwenhoek 54, 245–255. doi:10.1007/BF00443583

Strycharz, S.M., Woodard, T.L., Johnson, J.P., Nevin, K.P., Sanford, R.A., Loffler, F.R., Lovley, D.R., 2008. Graphite Electrode as a Sole Electron Donor for Reductive Dechlorination of Tetrachlorethene by *Geobacter lovleyi*. Appl. Environ. Microbiol. 74, 5943–5947. doi:10.1128/AEM.00961-08

Sukkasem, C., Xu, S., Park, S., Boonsawang, P., Liu, H., 2008. Effect of nitrate on the performance of single chamber air cathode microbial fuel cells. Water Res. 42, 4743–4750. doi:10.1016/j.watres.2008.08.029

Sun, Y., Zuo, J., Cui, L., Deng, Q., Dang, Y., 2010. Diversity of microbes and potential exoelectrogenic bacteria on anode surface in microbial fuel cells. J. Gen. Appl. Microbiol. 56, 19–29. doi:10.2323/jgam.56.19

Sydow, A., Krieg, T., Mayer, F., Schrader, J., Holtmann, D., 2014. Electroactive bacteria—molecular mechanisms and genetic tools. Appl. Microbiol. Biotechnol. 98, 8481–8495. doi:10.1007/s00253-014-6005-z

Tchobanoglous, G., Burton, F.L., Stensel, D.H., Metcalf, Eddy, 2003. Wastewater Engineering: Treatment and Reuse, 4th ed. McGraw-Hill.

Tender, L.M., Reimers, C.E., Stecher, H. a, Holmes, D.E., Bond, D.R., Lowy, D. a, Pilobello, K., Fertig, S.J., Lovley, D.R., 2002. Harnessing microbially generated power on the seafloor. Nat. Biotechnol. 20, 821–5. doi:10.1038/nbt716

ter Heijne, A., Hamelers, H.V.M., de Wilde, V., Rozendal, R. a., Buisman, C.J.N., 2006. A Bipolar Membrane Combined with Ferric Iron Reduction as an Efficient Cathode System in Microbial Fuel Cells †. Environ. Sci. Technol. 40, 5200–5205. doi:10.1021/es0608545

Ter Heijne, A., Schaetzle, O., Gimenez, S., Fabregat-Santiago, F., Bisquert, J., Strik, D.P.B.T.B., Barrière, F., Buisman, C.J.N., Hamelers, H.V.M., 2011. Identifying charge and mass transfer resistances of an oxygen reducing biocathode. Energy Environ. Sci. 4, 5035. doi:10.1039/c1ee02131a

Throbäck, I.N., Enwall, K., Jarvis, Å., Hallin, S., 2004. Reassessing PCR primers targeting nirS, nirK and nosZ genes for community surveys of denitrifying bacteria with DGGE. FEMS Microbiol. Ecol. 49, 401–417. doi:10.1016/j.femsec.2004.04.011

Tilman, D., 1977. Resource Competition between Plankton Algae : An Experimental and Theoretical Approach. Ecology 58, 338–348.

Tong, Y., He, Z., 2014. Current-driven nitrate migration out of groundwater by using a bioelectrochemical system. RSC Adv. 4, 10290–10294. doi:10.1039/c3ra47851c

Torres, C.I., Kato Marcus, A., Rittmann, B.E., 2008a. Proton transport inside the biofilm limits electrical current generation by anode-respiring bacteria. Biotechnol. Bioeng. 100, 872–81. doi:10.1002/bit.21821

Torres, C.I., Krajmalnik-Brown, R., Parameswaran, P., Marcus, A.K., Wanger, G., Gorby, Y. a, Rittmann, B.E., 2009. Selecting anode-respiring bacteria based on anode potential: phylogenetic, electrochemical, and microscopic characterization. Environ. Sci. Technol. 43, 9519–24. doi:10.1021/es902165y

Torres, C.I., Marcus, A.K., Lee, H.-S., Parameswaran, P., Krajmalnik-Brown, R., Rittmann, B.E., 2010. A kinetic perspective on extracellular electron transfer by anode-respiring bacteria. FEMS Microbiol. Rev. 34, 3–17. doi:10.1111/j.1574-6976.2009.00191.x

Torres, C.I., Marcus, A.K., Parameswaran, P., Rittmann, B.E., 2008b. Kinetic experiments for evaluating the Nernst-Monod model for anode-respiring bacteria (ARB) in a biofilm anode. Environ. Sci. Technol. 42, 6593–6597. doi:10.1021/es800970w

Torres, C.I., Marcus, A.K., Rittmann, B.E., 2007. Kinetics of consumption of fermentation products by anode-respiring bacteria. Appl. Microbiol. Biotechnol. 77, 689–97. doi:10.1007/s00253-007-1198-z

van den Berg, E.M., Boleij, M., Kuenen, J.G., Kleerebezem, R., van Loosdrecht, M.C.M., 2016. DNRA and Denitrification Coexist over a Broad Range of Acetate/N-NO3− Ratios, in a Chemostat Enrichment Culture. Front. Microbiol. 7, 1842. doi:10.3389/fmicb.2016.01842

van den Berg, E.M., van Dongen, U., Abbas, B., van Loosdrecht, M.C., 2015. Enrichment of DNRA bacteria in a continuous culture. ISME J. 9, 1–9. doi:10.1038/ismej.2015.26

Van Doan, T., Lee, T.K., Shukla, S.K., Tiedje, J.M., Park, J., 2013. Increased nitrous oxide accumulation by bioelectrochemical denitrification under autotrophic conditions: kinetics and expression of denitrification pathway genes. Water Res. 47, 7087–97. doi:10.1016/j.watres.2013.08.041

Van Haandel, A., Kato, M.T., Cavalcanti, P.F.F., Florencio, L., 2006. Anaerobic reactor design concepts for the treatment of domestic wastewater. Rev. Environ. Sci. Bio/Technology 5, 21–38. doi:10.1007/s11157-005-4888-y

van Niekerk, a. M., Jenkins, D., Richard, M.G., 1987. Competitive growth of *Zoogloea ramigera* and type 021N in activated sludge and pure culture - a model for low F:M bulking. J. Water Pollut. Control Fed. 59, 262–273.

van Rijn, J., Tal, Y., Barak, Y., 1996. Influence of Volatile Fatty Acids on Nitrite Accumulation by a Pseudomonas stutzeri Strain Isolated from a Denitrifying Fluidized Bed Reactor. Appl. Environ. Microbiol. 62, 2615–20.

Venkataraman, A., Rosenbaum, M. a., Perkins, S.D., Werner, J.J., Angenent, L.T., 2011. Metabolite-based mutualism between Pseudomonas aeruginosa PA14 and Enterobacter aerogenes enhances current generation in bioelectrochemical systems. Energy Environ. Sci. 4, 4550. doi:10.1039/c1ee01377g

Virdis, B., Rabaey, K., Rozendal, R. a, Yuan, Z., Keller, J., 2010. Simultaneous nitrification, denitrification and carbon removal in microbial fuel cells. Water Res. 44, 2970–80. doi:10.1016/j.watres.2010.02.022

Virdis, B., Rabaey, K., Yuan, Z., Keller, J., 2008. Microbial fuel cells for simultaneous carbon and nitrogen removal. Water Res. 42, 3013–24. doi:10.1016/j.watres.2008.03.017

Wagner, R.C., Call, D.F., Logan, B.E., 2010. Optimal set anode potentials vary in bioelectrochemical systems. Environ. Sci. Technol. 44, 6036–41. doi:10.1021/es101013e

Wagner, R.C., Regan, J.M., Oh, S.-E., Zuo, Y., Logan, B.E., 2009. Hydrogen and methane production from swine wastewater using microbial electrolysis cells. Water Res. 43, 1480–1488. doi:10.1016/j.watres.2008.12.037

Wang, A., Liu, W., Cheng, S., Xing, D., Zhou, J., Logan, B.E., 2009. Source of methane and methods to control its formation in single chamber microbial electrolysis cells. Int. J. Hydrogen Energy 34, 3653–3658. doi:10.1016/j.ijhydene.2009.03.005

Wang, X., Feng, Y., Ren, N., Wang, H., Lee, H., Li, N., Zhao, Q., 2009. Accelerated start-up of two-chambered microbial fuel cells: Effect of anodic positive poised potential. Electrochim. Acta 54, 1109–1114. doi:10.1016/j.electacta.2008.07.085

Wen, Q., Wu, Y., Zhao, L., Sun, Q., Kong, F., 2010. Electricity generation and brewery wastewater treatment from sequential anode-cathode microbial fuel cell. J. Zhejiang Univ. B (Biomed Biotechnol) 11, 87–93. doi:10.1631/jzus.B0900272

White, H.K., Reimers, C.E., Cordes, E.E., Dilly, G.F., Girguis, P.R., 2009. Quantitative population dynamics of microbial communities in plankton-fed microbial fuel cells. ISME J. 3, 635–646. doi:10.1038/ismej.2009.12

Wickham, H., 2009. ggplot2: Elegant graphics for data analysis. Springer, New York.

Wickham, H., Francois, R., 2016. dplyr: A Grammar of Data Manipulation.

Yan, H., Saito, T., Regan, J.M., 2012. Nitrogen removal in a single-chamber microbial fuel cell with nitrifying biofilm enriched at the air cathode. Water Res. 46, 2215–2224. doi:10.1016/j.watres.2012.01.050

Yoon, S., Sanford, R.A., Löffler, F.E., 2015. Nitrite Control over Dissimilatory Nitrate/Nitrite Reduction Pathways in Shewanella loihica Strain PV-4. Appl. Environ. Microbiol. 81, 3510–3517. doi:10.1128/AEM.00688-15

Zhang, F., Ge, Z., Grimaud, J., Hurst, J., He, Z., 2013. Long-Term Performance of Liter-Scale Microbial Fuel Cells Treating Primary Effluent Installed in a Municipal Wastewater Treatment Facility. Environ. Sci. Technol. 47, 4941–4948.

Zhang, Y., Angelidaki, I., 2013. A new method for in situ nitrate removal from groundwater using submerged microbial desalination-denitrification cell (SMDDC). Water Res. 47, 1827–1836. doi:10.1016/j.watres.2013.01.005

Zhou, M., Wang, H., Hassett, D.J., Gu, T., 2013. Recent advances in microbial fuel cells (MFCs) and microbial electrolysis cells (MECs) for wastewater treatment, bioenergy and bioproducts. J. Chem. Technol. Biotechnol. 88, 508–518. doi:10.1002/jctb.4004

Zhou, Y., Oehmen, A., Lim, M., Vadivelu, V., Ng, W.J., 2011. The role of nitrite and free nitrous acid (FNA) in wastewater treatment plants. Water Res. 45, 4672–82. doi:10.1016/j.watres.2011.06.025

Zinder, S.H., Anguish, T., Cardwell, S.C., 1984. Selective inhibition by 2-bromoethanesulfonate of methanogenesis from acetate in a thermophilic anaerobic digestor. Appl. Environ. Microbiol. 47, 1343–5.